Constraining Physics Beyond the Standard Model in Post-Higgs Era

A thesis submitted in partial fulfillment of
the requirements for the degree of

Doctor of Philosophy

by

Tanmoy Mondal

(Roll No. 11330016)

Under the guidance of

Dr. Partha Konar

Associate Professor

Theoretical Physics Division

Physical Research Laboratory, Ahmedabad, India.

DEPARTMENT OF PHYSICS

INDIAN INSTITUTE OF TECHNOLOGY GANDHINAGAR

2016

to

my parents

&

teachers

Declaration

I declare that this written submission represents my ideas in my own words and where others' ideas or words have been included, I have adequately cited and referenced the original sources. I also declare that I have adhered to all principles of academic honesty and integrity and have not misrepresented or fabricated or falsified any idea/data/fact/source in my submission. I understand that any violation of the above will be cause for disciplinary action by the Institute and can also evoke penal action from the sources which have thus not been properly cited or from whom proper permission has not been taken when needed.

(Signature)

(Name: Tanmoy Mondal)

(Roll No: 11330016)

Date:

CERTIFICATE

It is certified that the work contained in the thesis titled **“Constraining Physics Beyond the Standard Model in Post-Higgs Era ”** by **Tanmoy Mondal** (11330016), has been carried out under my supervision and that this work has not been submitted elsewhere for a degree.

I have read this dissertation and that, in my opinion, it is fully adequate in scope and quality as a dissertation for the degree of Doctor of Philosophy.

Dr. Partha Konar
Associate Professor
Indian Institute of Technology Gandhinagar
Ahmedabad – 382424, India

Publications

Publications included in the thesis

1. Joydeep Chakrabortty, Partha Konar and **Tanmoy Mondal**:
   Constraining a class of B-L extended models from vacuum stability and perturbativity,
   Phys.Rev. D **89**, 056014 (2014)

2. Joydeep Chakrabortty, Partha Konar and **Tanmoy Mondal**:
   Copositive Criteria and Boundedness of the Scalar Potential
   Phys.Rev. D **89**, 095008 (2014)

3. Kaushik Bhattacharya, Joydeep Chakrabortty, Suratna Das and **Tanmoy Mondal**:
   Higgs vacuum stability and inflationary dynamics after BICEP2 and PLANCK dust polarisation
   JCAP 1412 (2014) 12, 001

4. Gulab Bambhaniya, Subrata Khan, Partha Konar and **Tanmoy Mondal**:
   Constraints on a seesaw model leading to Quasi-Degenerate neutrinos and signatures at the LHC
   Phys.Rev. D **91**, 095007 (2015)

5. Ujjal Dey, Partha Konar and **Tanmoy Mondal**:
   Unitarity constraints and Charge Breaking minima in left right symmetric model
   Phys.Rev. D **92**, 096005 (2015)

Publications not included in thesis

- Tanushree Basak and **Tanmoy Mondal**:
  Constraining Minimal $U(1)_{B-L}$ model from Dark Matter Observations
  Phys.Rev. D **89** 063527, (2014)

- Tanushree Basak and **Tanmoy Mondal**:
  Class of Higgs-portal Dark Matter models in the light of gamma-ray excess from Galactic center
  Phys.Lett. B 744 (2015) 208-212

- Gulab Bambhaniya, Srubabati Goswami, Subrata Khan, Partha Konar and **Tanmoy Mondal**:
  Looking for hints of a reconstructible seesaw model at the Large Hadron Collider
  Phys.Rev. D **91** 075007, (2015)

Acknowledgements

This thesis would not have come to reality without the help, support and guidance of many people. I would like to express my gratitude towards all of them in this opportunity.

First and foremost I wish to express my sincere thanks to my supervisor, Dr. Partha Konar. It was a great experience to work under his supervision. His continuous support and constant encouragement regarding thesis related study made my research possible. He has been the epitome of friend, philosopher and guide through my years at PRL.

I take this opportunity to thank thank Prof. Srubabati Goswami for her advices at different stages of my thesis. It was a great experience to collaborate with her. I thank my collaborator Prof. Joydeep Chakrabortty for his support starting from the very beginning of my research carrier. It was a pleasure to work with Dr. Tanushree Basak, Dr. Gulab Bambhaniya and Dr. Subrata Khan.

I convey my sincere thanks to my Doctoral Studies Committee, Prof. Saurabh Rindani and Prof. Srubabati Goswami for evaluating my work in a regular basis. Their valuable comments help me to improve scientific outcomes. Also I am grateful to them for the examination of this thesis.

I thank Abhaya Kumar Swain and Gulab Bambhaniya for innumerable discussions sessions regarding thesis related and non thesis related discussions. I thank my office-mates Abhaya, Gulab, Monojit, Ujjal, Lata and Akanksha for the time with laughter, mutual encouragement and support. Also I am grateful to Ujjal and Gulab for the proofreading of this thesis.

I thank former area chairman Prof. S. Mohanty and current area chairman, Prof. H. Mishra for providing necessary facilities to carry out research work. The Theoretical Physics (THE-PH) division provided me a nice research environment which I always enjoyed. I express my gratitude to all the past and present members of the division: Dr. D. Angom, Dr. N. Mahajan, Dr. R. Rangarajan, Dr. N Singh, Dr. B. Sahoo, Prof. A. Joshipura, Prof. J. Bhatt, Razaahmed Z Maniar, Bhagyashree, Khushbu and Sujata Krishna.

It would have been impossible to pass the five years without the joyful company Abhaya, Alok, Anirban, Arun, Chithrabhanu, Gaurava, Girish, Guruprasad, Ikshu, Kuldeep, Manu, Sanjay and Shraddha.

I convey my sincere thanks to my seniors and juniors for an enjoyable hostel environment. I enjoyed very much the philosophical discussions with Amrendra and mythological discussions with Upendra, Monojit and Wagheesh.

Thanks to my M.Sc friends at IIT Madras, special thanks to Anirban, Debasis, *Dipankar, Madhumita, Nabadyuti Subhajit, Sayani and Ushasi. I express my gratitude to Prof. M. Pattabiraman, our M.Sc supervisor for his advices regarding PhD.*

I spend a lot of time Googling and without it the thesis would have been impossible. I am grateful to 9gag[*], *PHD(Piles Higher and Deeper)*[†], *WBH(Wait-But-Why)* [‡], *xkcd*[§] *and Vsauce*[¶] *for helping me to keep calm and do research.*

I am grateful to Indian Institute of Technology, Gandhinagar (IIT Gn) for my registration.

I thank entire family of PRL for all the research facilities and for providing and excellent hostel facility at Thaltej.

Last, but not the least, I would like to thank my family; without their love and support it would have been impossible to reach here.

(Tanmoy)

[*] www.9gag.com

[†] www.phdcomics.com

[‡] www.waitbutwhy.com

[§] http://xkcd.com/

[¶] https://www.youtube.com/user/Vsauce

Abstract

In the history of elementary particle physics, the discovery of the Higgs boson at the Large Hadron Collider (LHC) in July 4, 2012 is an important breakthrough which completes the Standard Model (SM) of particle physics. Nevertheless, there exist experimental observations which cannot be explained by the SM, like the neutrino oscillations, dark matter, baryon asymmetry etc. With these experimental shortcomings it is evident that there exist some beyond the Standard Model (BSM) physics. There are several ways to extend the SM to explain some of the experimental phenomena which is still to be observed in the state-of-the-art experiment like LHC. But the recent Higgs discovery can shed some light in the uncharted territory of theoretical physics. We are living at a minima of the Higgs potential where the Higgs field acquires a vacuum expectation value (vev) which is intertwined with the Higgs boson mass (m_H) measured at the LHC. The stability of the minimum is ensured by the condition that the Higgs quartic coupling should be positive. But recent observation of m_H at the LHC indicates that the SM minima does not remain stable upto the Planck scale. This also indicates that there must be some new physics phenomena which will stabilize the minimum. Hence the stability analysis of the BSM scenarios is necessary to constrain parameters of the model. There are other constraints like perturbativity and unitarity of scattering amplitudes of longitudinal gauge boson modes which will also restrict the parameter space.

The BSM models that include many scalar fields posses scalar potential with many quartic couplings. Due to the complicated structures of such scalar potentials it is indeed difficult to adjudge the stability of the vacuum. Thus one needs to formulate a proper prescription for computing the vacuum stability criteria. We have used the idea of copositive matrices to deduce the conditions that guarantee the boundedness of the scalar potential. We have discussed the basic idea behind the copositivity and then used that to determine the vacuum stability criteria for the Left-Right symmetric models with doublet, and triplet scalars and Type-II seesaw. As this idea is based on the strong mathematical arguments it helps to compute simple and unique stability criteria embracing the maximum

allowed parameter space.

We study the $B-L$ gauge extension of the Standard Model which contains a singlet scalar and three right-handed neutrinos. The vacuum expectation value of the singlet scalar breaks the $U(1)_{B-L}$ symmetry. The $B-L$ symmetry breaks when the complex singlet scalar acquires a *vev*. We studied two different cases of $B-L$ breaking scale: TeV scale and $\sim 10^{10}$ GeV. The TeV scale breaking scenario can have signatures at the LHC and we have constrained parameter space of this model. The high scale breaking scenario provides a constrained parameter space where both the issues of vacuum stability and high-scale inflation can be successfully accommodated.

The Left-Right symmetric model (LRSM) is theoretically well motivated and also contains rich phenomenology. We used idea of copositivity to calculate vacuum stability conditions for two variants of the LRSM. We incorporate the unitarity conditions in LRSM which can translate into giving a stronger constraint on the model parameters together with the criteria derived from vacuum stability and perturbativity. In this light, we demonstrate the bounds on the masses of the physical scalars present in the model and find the scenario where multiple scalar modes are in the reach of Large Hadron Collider.

We have also studied a variant of TeV scale seesaw model in which three additional heavy right handed neutrinos are added to the standard model to generate the quasi-degenerate light neutrinos. This model is theoretically interesting since it can be fully rebuilt from the experimental data of neutrino oscillations except for an unknown factor in the Dirac Yukawa coupling. We study the constrains on this coupling coming from meta-stability of electro-weak vacuum. Even stronger bound comes from the lepton flavor violating decays on this model, especially in a heavy neutrino mass scenario which is within the collider reach. Bestowed with these constrained parameters, we explore the production and discovery potential coming from these heavy neutrinos at the 14 TeV run of Large Hadron Collider. Signatures with tri-lepton final state together with backgrounds are considered in a realistic simulation.

Keywords: Vacuum Stability, Copositivity, Extended Scalar Sector, Beyond the Standard Model, Z' Model, B-L symmetry, Left-Right symmetry, TeV scale seesaw, Quasi-degenerate neutrinos, Collider Phenomenology

Contents

List of Figures

List of Tables

List of Abbreviations

SM	Standard Model
BSM	Beyond the Standard Model
QCD	Quantum ChromoDynamics
GWS	Glashow-Weinberg-Salam
EW	Electro-Weak
EWSB	Electro-Weak Symmetry Breaking
LHC	Large Hadron Collider
ATLAS	A Toroidal LHC ApparatuS
CMS	Compact Muon Solenoid
LQT	Lee-Quigg-Thacker
LH	Left Handed
RH	Right Handed
LRSM	Left Right Symmetric Model
MLRSM	Minimal LRSM
LRT	LR Model with Triplet Scalars
LRD	LR Model with Doublet Scalars
vev	Vacuum Expectation Value
COP	Copositivity
$B-L$	Baryon number minus Lepton number
GUT	Grand Unified Theory
RGE	Renormalization Group Equation
CMBR	Cosmic Microwave Background Radiation
2HDM	Two Higgs Doublet Model
LFV	Lepton Flavor Violation
VBF	Vector Boson Fusion
QD	Quasi Degenerate

Chapter 1

Introduction

Ever since the ancient times, people are interested to know how Nature works. Today, the best theory as we understand Nature is the Standard Model (SM) of particle physics along with the theory of General Relativity. Dynamics and interactions of the fundamental particles and their interactions (except gravitational) are contained in the SM of particle physics. The theory is backed by huge amount of experimental evidences and by far is the most precise theory ever constructed. The elegance of the construction relies on symmetry principles. Almost all the elementary particles remain massless if absolute symmetry holds. As we observe that several of these elementary particles are in fact massive, we have to have a mechanism to generate mass. In this chapter we will briefly describe the Standard Model and also the Higgs mechanism which is responsible for giving masses to most of the elementary particles along with a few force carriers.

1.1 The Standard Model of Particle Physics

The Standard Model is a quantum field theoretical description of three of the four fundamental forces, viz., strong, electro-magnetic and weak interactions. Quantum chromodynamics (QCD) is the theory of strong interactions governed by the non-Abelian gauge group $SU(3)_c$ [1]. The theory of electromagnetic and weak interaction (from now on electro-weak theory) is called Glashow-Weinberg-Salam(GWS) model [2–4], named after the developers of the model. The full

Fields	Names	Spin	$SU(3)_c$	$SU(2)_L$	$U(1)_Y$
$Q_L^i = \begin{pmatrix} u_L^i \\ d_L^i \end{pmatrix}$	quarks	$\frac{1}{2}$	3	2	$\frac{1}{3}$
u_R^i		$\frac{1}{2}$	3	1	$\frac{4}{3}$
d_R^i		$\frac{1}{2}$	3	1	$-\frac{2}{3}$
$L_L^i = \begin{pmatrix} \nu_L^i \\ e_L^i \end{pmatrix}$	leptons	$\frac{1}{2}$	1	2	-1
e_R^i		$\frac{1}{2}$	1	1	-2
G	gauge fields	1	8	1	0
$W^\pm, W^3$		1	1	3	0
B		1	1	1	0
Φ	Higgs field	0	1	2	1

Table 1.1: The fundamental fields of the SM are tabulated here with their representations under SM gauge groups. The subscript L/R represents left/right chiral† fermions. Also note that the gauge bosons lie in the adjoint representation of the respective symmetry group. Here superscript i $(= 1, 2, 3)$ stands for the generation index .

symmetry group of the SM is

$$\mathcal{G}_{SM} = SU(3)_c \otimes SU(2)_L \otimes U(1)_Y, \tag{1.1}$$

where all the symmetries are gauged. The gauge group $SU(2)_L \otimes U(1)_Y$ corresponds to the GWS model. All the elementary particles are fermions (half integer spin) and the force carrier particles are bosons (integer spin). The fermions are assigned intrinsic quantum numbers depending on how they behave under a particular symmetry. In Table 1.1 we have summarized the field content of the SM and also tabulated dimensions of representations under different gauge groups. The last column represent the intrinsic quantum number under the $U(1)_Y$ group. There exist three generations of fermions and labelled by the index i $(= 1, 2, 3)$ which is called the generation index. A particular interaction is governed by a gauge group and the mediators of that interaction are called the gauge bosons which lie in the adjoint representations of the respective symmetry group. Mediators of the strong force are called *gluons* and denoted by G. The gauge bosons

†A particle is right-handed if the direction of its spin is the same as the direction of its momentum. It is left-handed if the directions of spin and momentum are opposite. Chirality is the Lorentz invariant generalization of this handedness to massive particles and is analogous to handedness for massless particles.

$W^{\pm}$ mediate the charged current weak interaction, whereas the neutral part W^3 and B mix with each other and produce two vector bosons, Z and the photon (γ). The neutral weak interaction mediator is the Z boson and γ is responsible for the electromagnetic force. The mixing between the W^3 and B will be discussed later in this chapter. The only scalar field in the SM is the Higgs field introduced to generate mass via the Higgs mechanism which we will discuss in detail. Now we focus on all the three different sectors (gauge, fermionic and scalar) in short.

1.1.1 Gauge Sector

This sector contains only the spin-1 fields. Gluons are denoted by G^{α}_{μ} where $\alpha = 1, 2, \cdots, 8$ labels the component of the adjoint representation of the $SU(3)_c$ group. The $SU(2)_L$ gauge bosons are denoted as W^a_μ where $a = 1, 2, 3$. The vector boson associated with the $U(1)$ gauge group is B_μ.

The gauge invariant SM Lagrangian containing all these gauge fields can be written as

$$\mathcal{L}_{\text{Gauge}} = -\frac{1}{4} G^{\alpha}_{\mu\nu} G^{\mu\nu\alpha} - \frac{1}{4} W^a_{\mu\nu} W^{\mu\nu a} - \frac{1}{4} B_{\mu\nu} B^{\mu\nu}, \tag{1.2}$$

where the field strengths are defined by

$$\begin{aligned} G^{\alpha}_{\mu\nu} &= \partial_\mu G^{\alpha}_{\nu} - \partial_\nu G^{\alpha}_{\mu} - g_3 f^{\alpha\beta\gamma} G^{\beta}_{\mu} G^{\gamma}_{\nu}, & (1.3)\\ W^a_{\mu\nu} &= \partial_\mu W^a_\nu - \partial_\nu W^a_\mu - g_2 \epsilon^{abc} W^b_\mu W^c_\nu, & (1.4)\\ B_{\mu\nu} &= \partial_\mu B_\nu - \partial_\nu B_\mu. & (1.5) \end{aligned}$$

Here g_2 and g_3 which define strengths of the interactions are the coupling constants of the $SU(2)_L$ and $SU(3)_c$ gauge groups respectively. The factors $f^{\alpha\beta\gamma}$ and ϵ^{abc} are called structure constants which relates the commutation relation between the generators of the associated Lie algebra. Note that due to gauge invariance we cannot write mass a term like $m^2 W_\mu W^\mu$ and all the gauge bosons are massless here. We will discuss later how some of the gauge bosons will become massive.

1.1.2 Fermion Sector

The gauge invariant fermion Lagrangian can be written as

$$\mathcal{L}_{\text{fermion}} = \sum_f i\,\overline{\psi_f}\,\not{D}\psi_f, \tag{1.6}$$

where $\not{D} = \gamma^\mu D_\mu$ with D_μ being the covariant derivative. The exact form of the covariant derivative is

$$D_\mu \equiv \partial_\mu + i\,g_3\,\frac{\lambda^a}{2}\,G^a_\mu + i\,g_2\,\frac{\sigma^a}{2}\,W^a_\mu + i\,g_1\,Y\,B_\mu\,, \tag{1.7}$$

where λ^a $(a = 1, 2, \cdots, 8)$ are the Gell-Mann matrices and σ^a $(a = 1, 2$ & $3)$ are the usual Pauli matrices. These matrices are the generators of $SU(3)_c$ and $SU(2)_L$ gauge groups respectively. The $U(1)$ gauge coupling strength is g_1. Again it is not possible to write a mass term of the form $m_f\,\overline{f}\,f$ as it will violate gauge invariance.

1.1.3 Scalar Sector

The SM contains a single spin-zero field namely the Higgs field, a complex scalar field which is a doublet under the $SU(2)_L$. In component notation it can be represented as

$$\Phi = \begin{pmatrix} \phi^+ \\ \phi^0 \end{pmatrix}. \tag{1.8}$$

The Lagrangian associated with the scalar field reads as

$$\mathcal{L}_{\text{scalar}} = (D_\mu\Phi)^\dagger\,(D^\mu\Phi) - V(\Phi), \tag{1.9}$$

where $V(\Phi)$ is the scalar potential which has the form

$$V(\Phi) = -\mu^2\Phi^\dagger\Phi + \lambda(\Phi^\dagger\Phi)^2. \tag{1.10}$$

Since the Higgs field is singlet under the $SU(3)_c$ gauge group, the covariant derivative in Eq. 1.9 takes the following form

$$D_\mu \equiv \partial_\mu + i\, g_2 \frac{\sigma^a}{2} W^a_\mu + i\, g_1 \frac{\mathbb{I}}{2} B_\mu, \tag{1.11}$$

where $\mathbb{I}$ is the identity matrix. Interactions of the Higgs boson with other gauge bosons originate from the scalar kinetic term in Eq. 1.9. The fermions also interact with the Higgs boson through the Yukawa interaction of the form,

$$\mathcal{L}_{\text{Yukawa}} = \overline{Q_L}\, Y_u\, u_R\, \Phi + \overline{Q_L}\, Y_d\, d_R\, \tilde{\Phi} + \overline{L_L}\, Y_e\, e_R\, \Phi + h.c., \tag{1.12}$$

where $\tilde{\Phi} = i\sigma_2 \Phi^*$ and we have suppressed all the generation indices. The matrices Y_u, Y_d and Y_e are the Yukawa matrices which encode the respective Yukawa couplings.

Now we discuss how this Higgs boson is responsible for generating masses for elementary fermions.

1.1.4 Spontaneous Symmetry Breaking

If the SM gauge group remains exact then all the gauge bosons and fermions remain massless. But in Nature we observe massive fermions and massive electroweak gauge bosons, which demands breaking of the underlying symmetry to a lower symmetry group. Also we know that the electromagnetic gauge invariance is unbroken and the mediator of this interaction, the photon (γ) remains massless. So it is obvious that the symmetry breaking pattern is

$$SU(2)_L \otimes U(1)_Y \xrightarrow{\langle\Phi\rangle} U(1)_{em}. \tag{1.13}$$

Let us now briefly discuss how this symmetry breaking happens. It is easy to check that the Higgs potential in Eq. 1.10 is invariant under the $SU(2)_L \otimes U(1)_Y$ gauge group. However for the parameter μ^2, $\lambda > 0$, the potential has a minimum at

$$\Phi_{\rm min} = \langle \Phi \rangle = \frac{1}{\sqrt{2}} \begin{pmatrix} 0 \\ v \end{pmatrix} \qquad \text{with} \qquad v = \frac{\mu}{\sqrt{\lambda}}. \tag{1.14}$$

Now at $\Phi_{\rm min}$, only a particular combination of $SU(2)_L$ and $U(1)_Y$ generators remains unbroken, i.e.,

$$\left(\sigma_3 + \frac{Y}{2}\right) \langle \Phi \rangle = 0. \tag{1.15}$$

Thus the electromagnetic charge is linear combination: $Q = T_{3L} + \frac{Y}{2}$, where T_{3L} is the 3^{rd} component of the isospin generators (which is basically σ_3).

Masses of elementary particles

At the minimum of the Higgs potential we can now calculate the interactions of the Higgs boson with other gauge bosons by using the following form (in the unitary gauge),

$$\Phi = \frac{1}{\sqrt{2}} \begin{pmatrix} 0 \\ v + H(x) \end{pmatrix}, \tag{1.16}$$

where $H(x)$ is a small perturbation around the minimum which will be the Higgs boson field. Substituting this in the scalar potential Eq. 1.10 we have the following relations:

$$m_H^2 = 2\lambda v^2, \; v^2 = \frac{\mu^2}{\lambda}. \tag{1.17}$$

Now as we know $m_H \simeq 125$ GeV, the scalar potential is fixed with parameters[‡]

$$\mu^2 \sim (88\text{GeV})^2 \qquad\qquad \lambda \sim 0.13. \tag{1.18}$$

Similarly, using Eq. 1.16 in the kinetic part of the scalar Lagrangian Eq. 1.9 we can easily find that the gauge boson mass eigenstates are $W_\mu^{\pm}$[§], Z_μ and A_μ

[‡]The value of vacuum expectation value v is known from independent observation of gauge boson masses using the Eq.1.22 we will discuss shortly.

where,

$$W^{\pm} = \frac{1}{\sqrt{2}}\left(W^1_\mu \mp i\, W^2_\mu\right), \tag{1.19}$$

$$\begin{pmatrix} Z_\mu \\ A_\mu \end{pmatrix} = \begin{pmatrix} \cos\theta_w & -\sin\theta_w \\ \sin\theta_w & \cos\theta_w \end{pmatrix} \begin{pmatrix} W^3_\mu \\ B_\mu \end{pmatrix}, \tag{1.20}$$

where the weak mixing angle θ_w is called the 'Weinberg angle' and is defined as,

$$\cos\theta_w = \frac{g_2}{\sqrt{g_1^2 + g_2^2}}. \tag{1.21}$$

The corresponding mass eigenvalues are,

$$\begin{aligned} m^{\pm}_W &= \frac{1}{2}\, v\, g_2, \\ m_Z &= \frac{1}{2}\, v\, \sqrt{g_1^2 + g_2^2} = \frac{m_W}{\cos\theta_w}, \\ m_A &= 0. \end{aligned} \tag{1.22}$$

Thus the gauge bosons become massive except the photon owing to spontaneous breaking of the gauge symmetry. The fermion masses originate by the Yukawa couplings by substituting for Φ (from Eq. 1.16) in Eq. 1.12. The corresponding Lagrangian now takes the form,

$$\mathcal{L}^{\text{mass}}_{\text{Yukawa}} = \overline{u_L}\, M_u\, u_R + \overline{d_L}\, M_d\, d_R + \overline{e_L}\, M_e\, e_R + h.c., \tag{1.23}$$

where we have used $M_f = \frac{1}{\sqrt{2}} Y_f\, v$. Again we have suppressed the generation indices and the matrices M_u, M_d and M_e are the mass matrices.

The mathematical framework of the SM model, alluded to above, took its final form in the early 70's. Discovery of the neutral current (1973), the W and Z bosons (1983), the b quark(1977), the t quark(1995) and ν_τ proved the correctness of this model. Recently the discovery of the Higgs boson at the Large Hadron

[§] W^1_μ and W^2_μ are degenerate mass eigenstates and $W^{\pm}_\mu$ combination is a charge eigenstate with mass eigenvalue same as that of W^1_μ or W^2_μ .

Collider both by ATLAS [5] and CMS [6] collaborations have put the Standard Model (SM) on a firm footing. However there are a few outstanding issues which the SM cannot explain. In the next section we will sketch some of the problems that need to be addressed for our complete understanding of the Nature.

1.1.5 Issues with the SM

In spite of being a very successful theory to explain most of the experimental data, we are certain that the SM is not the complete theory and we need to go beyond the SM paradigm. Here we will briefly describe some of the puzzles that cannot be addressed in the SM.

Neutrino Oscillation and Seesaw

Convincing indications of BSM physics have emerged from the phenomenon of neutrino oscillation observed in terrestrial experiments. Neutrino oscillation is a quantum mechanical phenomenon in which one flavor of neutrino is converted to another. These results have conclusively established that neutrinos have non-zero mass and flavor mixing. But in the SM neutrinos are massless due to absence of right handed neutrinos. In principle it is possible to write down Majorana mass terms with left handed(LH) particles alone. But in the SM the LH neutrinos are doublet under $SU(2)_L$ and the gauge invariant Majorana mass term is possible if there exists a scalar which is a triplet under $SU(2)_L$. Such a scalar is certainly not present in the SM. Thus neutrino oscillation implies that we need to look beyond the SM.

Seesaw mechanism is a generic mechanism to generate neutrino masses and it naturally explains the smallness of these masses. The origin of seesaw is the dimension-5 effective operator $\frac{c_5}{M}LLHH$, where L(H) being the SM lepton(Higgs) doublet and c_5 is a dimensionless effective coupling. To achieve this effective operator, we need to introduce heavy field which violates lepton number by two units. M is the mass of the heavy particle.

Dark Matter

Roughly 25 percent of the universe is made up of material that we cannot directly observe. But there are several observations which indirectly confirm the existence of non-luminous non-relativistic matter. One of the famous observations comes from the galaxy rotation curve, which is almost flat for spiral galaxies. This phenomena cannot be explained exclusively by luminous matter. Also the precise measurement of temperature fluctuation in the spectrum of Cosmic Microwave Background Radiation(CMBR) confirms that there must exist non-baryonic matter with energy density roughly five times more than that of visible baryonic matter. Moreover, gravitational lensing observations from the Bullet cluster confirm the existence of dark matter. Dark matter can be made of non baryonic and electrically neutral colorless elementary particle. The Neutrinos in the SM can be the dark matter but since rest mass of neutrinos are very small compare to neutrino decoupling temperature ($\sim$ 1 MeV) they can only be hot dark matter which can not explain the structure formation. Hence we need to go beyond the SM to explain all the the astrophysical observations.

Baryonic Asymmetry

Baryon asymmetry refers to the observation that there is matter in the Universe but not much antimatter. We know that the galaxies do not contain antimatter because if they did, we should have observed gamma rays that would be produced when large amount of antimatter annihilate with matter. So at an early time, there must have been a phenomenon which generated a little bit more matter than antimatter. The asymmetry is quantified using the asymmetry parameter

$$\eta_b = \frac{n_{\text{baryon}} - n_{\text{anti-baryon}}}{n_{\text{photon}}}, \tag{1.24}$$

where n defines the number density. From cosmological measurements such as made by the Planck Collaboration we get the asymmetry as $\eta_b \sim 6 \times 10^{-10}$. The following conditions must be satisfied in order to have baryon asymmetry:

1. Baryon number violation.

2. Violation of both Charge conjugation symmetry, C, and Charge conjugation times Parity, CP symmetry.

3. The Universe is out of thermal equilibrium.

These are called Shakharov's conditions. The amount of CP violation present in the SM is not enough to the generate desired amount of asymmetry.

Hierarchy Problem

The hierarchy problem is a long standing theoretical puzzle which impels one to go for BSM scenarios. We know that all couplings and parameters are modified by higher order effects. When the mass of a fermion receives radiative corrections the correction term is proportional to the mass of the fermion. In the limit $m_f \to 0$, we have an additional symmetry, viz.,the chiral symmetry. But this is not true for a scalar field and the mass correction is quadratically dependent on the highest scale available in the theory (which is the Planck scale $M_{Pl} \sim 10^{19}$ GeV if there exists no new physics between the electro-weak scale and the Planck scale). We have already observed a Higgs boson with mass $\sim$ 125 GeV and we know that quantum correction to this mass scale is

$$m_h^2 = m^2 + \delta\, m^2 \simeq (125 \text{ GeV})^2\,, \tag{1.25}$$

but

$$\delta\, m^2 \propto \kappa M_{Pl}^2 \sim 10^{38}\,(\text{ GeV})^2\,. \tag{1.26}$$

Hence the correction term must cancel upto 34 decimal places which is unnatural. The problem can be rephrased as *"Why is the Planck scale (M_{Pl}) so different from the electro-weak scale?"*. In the Standard Model we do not have any solution to this problem. The most popular solution for the hierarchy problem is Supersymmetry. Extra Dimensional models can also evade this hierarchy problem.

All these unsolved problems clearly direct us to extensions of the SM of particle physics.

1.2 Beyond the Standard Model

Any extension of the SM is called beyond the SM (BSM) scenario. These models can possess extra symmetry or may contain new particles which are not present in the SM. Many BSM models possess extra scalar fields along with the SM Higgs and thus the extended scalar potential contains many quartic couplings. While some of these couplings can be related directly to masses of (neutral or charged) heavy scalars, other couplings only generate mass splitting among these heavy scalars. These quartic couplings can be constrained by imposing vacuum stability, perturbativity and unitarity of scattering amplitudes of longitudinal gauge boson modes. Vacuum stability gives a lower limit, whereas perturbativity and unitarity constrain the couplings from above. Unitarity constraint was first analyzed by Lee, Quigg and Thacker (LQT) [7] for the SM where they examined two-body scattering amplitudes involving the Higgs boson and also longitudinal gauge bosons ($V_L \equiv W_L^{\pm}, Z_L$). Since we are interested in the high energy behavior of the scattering amplitudes, it is possible to use unphysical scalars instead of V_Ls owing to the famous equivalence theorem. Unitarity has been used to constrain models which contain an extended scalar sector like two Higgs doublet model (2HDM) or Type-II seesaw model [8].

Since neutrino oscillation is one of the strongly established BSM effects so far, it is very important to study models which can explain the generation of neutrino mass naturally. Moreover, with the ongoing LHC experiment it is possible to explore these models up to a few TeV. But the vast parameter space of these models makes it a challenging task to explore the models at colliders like the LHC, and it is very important to constrain these models theoretically to predict precise signals. With this view we consider various models which can naturally generate neutrino masses and can be probed at the LHC in near future.

The first model we consider is the $U(1)_{B-L}$ model which is the minimal gauge extension of the Standard Model. The model can explain neutrino mass generation via the seesaw mechanism and can also provide a viable dark matter candidate. Since the $(B-L)$ breaking scale can be as low as a few TeV it is very important to study this model as it can be probed at the LHC in the near future. This model was studied in [9] with different values of the SM Higgs boson mass. The effect of different parameters on the vacuum stability was not discussed there. We have studied this model in great detail with the observed mass of the Higgs boson. We have also discussed the effect of other parameters of the model in vacuum stability analysis [10, 11].

Another class of models are the Left-Right symmetric models (LRSMs) [12–15] which are very appealing as BSM scenarios. These models resolve the origin of Parity violation in weak interactions; spontaneous breaking of Parity occurs at the higher energies beyond which Parity is an exact symmetry. LRSM predicts the presence of heavy right handed neutrinos and thus explains light neutrino mass generation via the seesaw mechanism. Moreover LRSM can be realized as a low energy effective theory of non-supersymmetric Grand Unified Theories(GUTs) [16]. We analyze vacuum stability aspects of these models in [10, 17]

Finally demonstrate how vacuum metastability can constrain TeV scale phenomenological seesaw models which are likely to be constrained by LHC in the next run. In this model the stability issue affects the Dirac Yukawa coupling as opposed to the scalar quartic couplings. Thus the production rate and phenomenology of heavy neutrinos are directly affected by metastability of the EW vacuum. Our results are discussed in [18].

We try to constrain parameters of the new physics models using theoretical constraints like vacuum stability, unitarity and perturbativity which we describe in the next chapter.

1.3 Thesis Overview

The thesis is organised as follows: In the next chapter (Chapter 2) we describe the methodology of our analysis. There we discuss how vacuum stability can be used to constrain parameters of BSM scenarios. To calculate vacuum stability criteria we have used the notion of copositivity which is widely used in the theory of linear systems. We describe how copositivity can be used to find vacuum stability criteria. We also touch upon the subject of unitarity of scattering matrices. Equipped with the tools we then move to the various BSM scenarios which are well motivated and can be observed in the LHC in near future. In Chapter 3 we consider a minimal gauge extension of the SM namely the $U(1)_{B-L}$ model. We describe the model and present how vacuum stability can constrain the model. Next we consider another phenomenologically interesting model, the left-right symmetric model. We have depicted the model in Chapter 4 and also discussed impact of vacuum stability and unitarity on this model. In Chapter 5 we consider a TeV scale seesaw model which contains right handed neutrinos along with the SM particles. The Yukawa coupling of this model can be restricted severely if we consider metastability of the electro-weak vacuum. Finally we summarize in Chapter 6.

Chapter 2

Methodology

In this chapter, we briefly discuss the methods we have used to calculate various theoretical constraints on a BSM scenario. In the scalar sector the main theoretical constraints are coming from vacuum stability, unitarity of scattering amplitudes and perturbativity of quartic couplings. The condition of perturbativity is straight-forward : *All scalar quartic couplings should be* $\leq 4\pi$. Calculation of vacuum stability criteria and unitarity conditions is discussed in detail in this chapter.

2.1 Vacuum Stability

In the previous chapter we briefly discussed the Standard Model which contains a Higgs boson. Symmetry breaking occurs when the Higgs field acquires a vacuum expectation value (vev). The scalar Lagrangian and the scalar potential are written in Eq. 1.9 and in Eq. 1.10 respectively.

In the unitary gauge *, the scalar doublet (Φ) can be written as

$$\Phi = \frac{1}{\sqrt{2}} \begin{pmatrix} 0 \\ \varphi \end{pmatrix}. \tag{2.1}$$

Then the scalar potential expressed in Eq. 1.10 becomes function of the real scalar

*Gauge choice is necessary to deal with redundant degrees of freedom of a scalar field (here, the Higgs field). In unitarity gauge number of scalar degrees of freedom becomes minimal.

field φ,

$$V_\varphi = -\frac{1}{2}\mu^2\varphi^2 + \frac{1}{4}\lambda\varphi^4. \tag{2.2}$$

After the φ develops a vev, we can write $\varphi = v + H$ and consequently all particles in the SM get masses (except neutrinos and photons). The mass of the Higgs particle H can be written as

$$m_H^2 = 2\lambda v^2,\ v^2 = \frac{\mu^2}{\lambda}. \tag{2.3}$$

Quantum loop corrections make the mass parameter and the quartic coupling dependent on the energy scale Λ,

$$V_{\text{eff}} = -\frac{1}{2}\mu(\Lambda)^2\varphi^2 + \frac{1}{4}\lambda(\Lambda)\varphi^4. \tag{2.4}$$

Here the scale Λ can be taken to be the field value φ. While discussing about vacuum stability [†] we are concerned with large field values and can safely neglect the quadratic term in the potential. The coupling λ varies with the energy scale Λ which is governed by the renormalization group equation (RGE),

$$\Lambda\frac{d}{d\Lambda}\lambda = \beta_\lambda, \tag{2.5}$$

and at one loop β_λ is given by [19]

$$\beta_\lambda = \frac{1}{(4\pi)^2}\left[24\lambda^2 - 6y_t^4 + \frac{3}{8}\left(2g_2^4 + \left(g_2^2 + g_1^2\right)^2\right) + \left(-9g_2^2 - 3g_1^2 + 12y_t^2\right)\lambda\right]. \tag{2.6}$$

In the previous equation $g_1\,(g_2)$ is the $U(1)_Y\,(SU(2)_L)$ gauge coupling and y_t is the top quark Yukawa coupling. When λ becomes negative at a particular energy scale the potential turns out to be unbounded from below which indicates that the vacuum stability criterion for the SM is $\lambda > 0$.

As we can see from Eq. 2.6 the running of the quartic coupling depends on the top-quark Yukawa coupling and also on the gauge couplings[‡]. The top-

[†] Vacuum is stable if the potential is bounded from below.

[‡] The SU(3) gauge coupling g_3 does not affect the scalar quartic coupling directly at one-loop. However it affects indirectly through the top-quark Yukawa coupling.

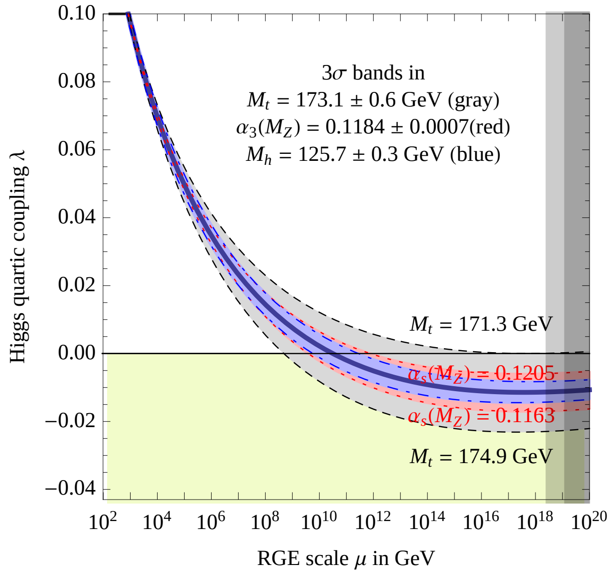

Figure 2.1: Running of the quartic coupling as a function of energy scale using the state-of-the-art three loop beta functions for all the couplings. Effect of y_t and g_3 is also shown here. Note that the scale μ is the same as the scale Λ we have defined. This figure is taken from [20].

quark coupling and the strong coupling constant affect the running of the quartic coupling and is depicted in the Fig. 2.1. Depending on the value of the top-quark mass and the strong coupling constant the quartic coupling λ becomes negative at energy scale 10^{8-11} GeV which makes the SM vacuum unstable.

Thus it indicates that some new physics might be there before the SM vacuum stability gets ruptured i.e., below the scale where λ becomes negative. The physics beyond the SM is expected to take care of stability of the vacuum of the full scalar potential. In the literature the stability of the vacua was discussed in several scenarios beyond Standard Model. These models are extended by an extra gauge symmetry and (or) addition of new particles. Quantum corrections of the quartic couplings depend on the spin of the particles that belong to the particular model. The fermion loop contributions contain a relative minus sign relative to that for the bosonic fields. Thus the Yukawa couplings tend to spoil the stability unlike the gauge and other scalar self couplings.

In a theory involving multiple scalar fields the structure of the potential is complicated. The vacuum stability criteria depend on some combinations of the scalar quartic couplings. Now we will discuss different methods to calculate the stability conditions which will ensure that the scalar potential remains bounded from below provided the stability criteria are satisfied.

2.2 Positivity of Quadratic Equation

Let us consider a theory which contains two scalar fields ϕ_A and ϕ_B, then the most general potential involving both the scalar fields can be written as :

$$V_0 = A|\phi_A|^4 + B|\phi_A|^2|\phi_B|^2 + C|\phi_B|^4. \tag{2.7}$$

Here, we have neglected the quadratic terms, since we are interested in high energy behavior of the couplings. We can rewrite the above equation (Eq. 2.7) as follows:

$$\begin{aligned} V_0 &= \left(\sqrt{A}\,|\phi_A|^2 - \sqrt{C}\,|\phi_B|^2\right)^2 + (B + 2\sqrt{AC})\,|\phi_A|^2|\phi_B|^2, \\ &= \lambda_{11}x^2 + 2\lambda_{12}xy + \lambda_{22}y^2. \end{aligned} \tag{2.8}$$

To ensure that the potential is bounded from below, it is evident that the necessary and sufficient conditions are (cf. Eq. 2.8)

$$\lambda_{11} \geq 0, \quad \lambda_{22} \geq 0 \;\text{ and }\; 2\lambda_{12} + 2\sqrt{\lambda_{11}\,\lambda_{22}} \geq 0. \tag{2.9}$$

It is possible that a BSM scenario can involve more than two scalars and using the aforementioned conditions iteratively we can calculate stability conditions for those models. We explain this in detail afterwards in Section 2.4.1.

2.3 Copositivity of Symmetric Matrix

Apart from using the positivity of quadratic forms we can use matrix properties such as copositivity (COP) to adjudge stability criteria. The notion of copositivity was first introduced by Motzkin in 1952 [21] in the context of linear algebra and thereafter it has been explored in the literatures of mathematics, see e.g., some of the widely accepted references [22, 23]. It has been noted that the positive definite matrices are subset of the copositive (conditionally positive) matrices and are included within that. Some of the references, extremely useful for our analysis, in which copositive criteria have been discussed are [24–26] and more recently [27].

Definition : *Let $\mathcal{S}_n$ be a set of symmetric matrices of order n, and $\Re_n$ be the real coordinate vector space. Any matrix $\Lambda \in \mathcal{S}_n$ is defined to be copositive iff the quadratic form $x^T \Lambda x \geq 0$ for all non-negative vectors (x), i.e., $x \in \Re_n^+$, the non-negative orthant*[§] *of $\Re_n$.*

Analytic criteria for copositivity are extremely complicated and lengthy for larger order matrices with negative off-diagonal elements. The general COP conditions up to order four matrices are available which we will briefly discuss in the next few sections. Also we should keep in mind that if some of the off-diagonal elements of a higher order (≥ 4) matrix are non-negative then copositivity can be addressed using the knowledge of COP criteria for rather lower order matrices.

2.3.1 Copositivity Conditions of Order Two Matrices

Let us consider a quadratic form,

$$\mathcal{F}(x, y) = \lambda_{11} x^2 + \lambda_{22} y^2 + 2\lambda_{12} xy. \tag{2.10}$$

We can easily convert the above equation to a matrix equation

$$\mathcal{F}(x, y) = X^T\, \mathcal{S}_2\, X, \qquad \text{where } X = \begin{pmatrix} x \\ y \end{pmatrix}, \tag{2.11}$$

where $\mathcal{S}_2$ is a symmetric matrix of order two [¶]:

$$\mathcal{S}_2 = \begin{pmatrix} \lambda_{11} & \lambda_{12} \\ & \lambda_{22} \end{pmatrix}. \tag{2.12}$$

[§] An orthant can be understood as the n-dimensional Euclidean space, generalization of a quadrant or an octant in two or three dimensions respectively.

[¶] As for symmetric matrices $(\Lambda)_{ij} = (\Lambda)_{ji}$, we are not writing the full matrix. The upper-triangular matrix with the diagonal elements are sufficient to represent the full matrix. Through out the thesis we have used this notation to represent the symmetric matrices.

This matrix is copositive if and only if

$$\lambda_{11} \geq 0, \quad \lambda_{22} \geq 0, \quad \text{and} \quad \lambda_{12} + \sqrt{\lambda_{11}\lambda_{22}} \geq 0. \tag{2.13}$$

These conditions are the same as the criteria that we have described in the Section 2.2. However, for larger matrices (order three or more) there will be no one-to-one correspondence between conditions derived using the method of positivity of quadratic form and COP conditions. This is due to the fact that we can use the method of positivity taking two fields at a time in any order.

2.3.2 Order three matrix

Now we will consider a symmetric matrix of order three:

$$\mathcal{S}_3 = \begin{pmatrix} \lambda_{11} & \lambda_{12} & \lambda_{13} \\ & \lambda_{22} & \lambda_{23} \\ & & \lambda_{33} \end{pmatrix}. \tag{2.14}$$

This matrix is copositive if and only if,

$$\begin{aligned} &\lambda_{11} \geq 0, \quad \lambda_{22} \geq 0, \quad \lambda_{33} \geq 0, \\ &\lambda_{12} + \sqrt{\lambda_{11}\lambda_{22}} \geq 0, \quad \lambda_{23} + \sqrt{\lambda_{22}\lambda_{33}} \geq 0, \quad \lambda_{13} + \sqrt{\lambda_{11}\lambda_{33}} \geq 0, \\ &\sqrt{\lambda_{11}\lambda_{22}\lambda_{33}} + \lambda_{12}\sqrt{\lambda_{33}} + \lambda_{23}\sqrt{\lambda_{11}} + \lambda_{13}\sqrt{\lambda_{22}} \\ &+\sqrt{2(\lambda_{12} + \sqrt{\lambda_{11}\lambda_{22}})(\lambda_{23} + \sqrt{\lambda_{22}\lambda_{33}})(\lambda_{13} + \sqrt{\lambda_{11}\lambda_{33}})} \ \ \geq 0. \end{aligned} \tag{2.15}$$

2.3.3 Order four matrix

Let us consider a symmetric matrix of order four:

$$\mathcal{S}_4 = \begin{pmatrix} \lambda_{11} & \lambda_{12} & \lambda_{13} & \lambda_{14} \\ & \lambda_{22} & \lambda_{23} & \lambda_{24} \\ & & \lambda_{33} & \lambda_{34} \\ & & & \lambda_{44} \end{pmatrix}. \tag{2.16}$$

To determine whether this matrix is copositive or not we need to adjudge eight different cases depending on the sign distributions of the off-diagonal elements. But in all the cases one generic condition that all the diagonal elements are positive, must be satisfied. From here onwards $\{i, j, k, l\}$ are any permutation of $\{1, 2, 3, 4\}$.

Case I: If all the off-diagonal elements of $\mathcal{S}_4$ are positive then this is copositive if and only if $\lambda_{ii} \geq 0 \; \forall \, i$.

Case II: If $\lambda_{ij} \leq 0$ and other off-diagonal elements are positive then $\mathcal{S}_4$ is copositive if and only if $(\lambda_{ii}\lambda_{jj} - \lambda_{ij}^2) \geq 0$.

Case III: If $\lambda_{ij}, \lambda_{lk} \leq 0$ and other off-diagonal elements are positive then the matrix is copositive if and only if $(\lambda_{ii}\lambda_{jj} - \lambda_{ij}^2) \geq 0$, $(\lambda_{ll}\lambda_{kk} - \lambda_{lk}^2) \geq 0$.

Case IV: If $\lambda_{ij}, \lambda_{ik} \leq 0$ then we must have $\left(\lambda_{ii}\lambda_{jk} - \lambda_{ij}\lambda_{ik} + \sqrt{(\lambda_{ii}\lambda_{jj} - \lambda_{ij}^2)(\lambda_{ii}\lambda_{kk} - \lambda_{ik}^2)}\;\right) \geq 0$ to make this matrix copositive.

Case V: If $\lambda_{ij}, \lambda_{jk}, \lambda_{ik} \leq 0$ while the other off-diagonal elements are positive then $\mathcal{S}_4$ is copositive if and only if the following order three matrix is copositive:

$$\begin{pmatrix} \lambda_{ii} & \lambda_{ij} & \lambda_{ik} \\ & \lambda_{jj} & \lambda_{jk} \\ & & \lambda_{kk} \end{pmatrix}.$$

Case VI: If $\lambda_{ij}, \lambda_{ik}, \lambda_{il} \leq 0$ and other off-diagonal elements are positive then the following matrix:

$$\begin{pmatrix} \lambda_{ii}\lambda_{jj} - \lambda_{ij}^2 & \lambda_{ii}\lambda_{jk} - \lambda_{ij}\lambda_{ik} & \lambda_{ii}\lambda_{jl} - \lambda_{ij}\lambda_{il} \\ & \lambda_{ii}\lambda_{kk} - \lambda_{ik}^2 & \lambda_{ii}\lambda_{kl} - \lambda_{ik}\lambda_{il} \\ & & \lambda_{ii}\lambda_{ll} - \lambda_{il}^2 \end{pmatrix}$$

must be copositive in order to make $\mathcal{S}_4$ copositive.

Case VII: If $\lambda_{ij}, \lambda_{jk}, \lambda_{kl} \leq 0$ and other off-diagonal elements are positive then we need to construct a matrix of order three which has to be copositive and that will imply $\mathcal{S}_4$ is copositive. Let us consider a matrix $\mathcal{S}_3^{'}$:

$$\begin{pmatrix} \lambda_{kk}\big(\lambda_{jj}\lambda_{ik}^2 - 2\lambda_{ij}\lambda_{ik}\lambda_{jk} + \lambda_{ii}\lambda_{jk}^2\big) & \lambda_{kk}(\lambda_{jj}\lambda_{ik} - \lambda_{ij}\lambda_{jk}) & \lambda_{kk}(\lambda_{ik}\lambda_{jl} - \lambda_{jk}\lambda_{il}) \\ & \lambda_{jj}\lambda_{kk} - \lambda_{jk}^2 & \lambda_{kk}\lambda_{jl} - \lambda_{jk}\lambda_{kl} \\ & & \lambda_{kk}\lambda_{ll} - \lambda_{kl}^2 \end{pmatrix}.$$

Thus $\mathcal{S}_4$ matrix will be copositive if and only if $\mathcal{S}_3^{'}$ is copositive.

Case VIII: If $\lambda_{ij}, \lambda_{jk}, \lambda_{kl}, \lambda_{il} \leq 0$ and other off-diagonal elements are positive then similar to the Case VII one needs to reconstruct a matrix of order three which has to be copositive in order to make $\mathcal{S}_4$ copositive. That matrix of order three should be $\mathcal{S}_3^{''}$:

$$\begin{pmatrix} \lambda_{ll}(\lambda_{ii}\lambda_{jl}^2 - 2\lambda_{ij}\lambda_{il}\lambda_{jl} + \lambda_{jj}\lambda_{il}^2) & \lambda_{ll}(\lambda_{ii}\lambda_{jl} - \lambda_{ij}\lambda_{il}) & \lambda_{ll}(\lambda_{ik}\lambda_{jl} - \lambda_{il}\lambda_{jk}) \\ & \lambda_{ii}\lambda_{ll} - \lambda_{il}^2 & \lambda_{ll}\lambda_{ik} - \lambda_{il}\lambda_{kl} \\ & & \lambda_{kk}\lambda_{ll} - \lambda_{kl}^2 \end{pmatrix}.$$

To derive analytic criteria for copositivity of a higher order matrix, one can make use of the rank reduction theorem as discussed in [24] and use the reduced rank criteria successively. Using this rank reduction theorem, copositivity criteria for order five matrices have also been computed in [28]. In our analysis higher order (more than four) matrices contain many non-negative off-diagonal elements. Thus the knowledge of copositivity of order four matrix is sufficient to deal with all our example models.

2.3.4 Copositivity Using Principal Sub-matrices

Since analytic form of copositive criteria for the most generic symmetric matrices of larger order is not straight forward and not available till date, one can suitably explore the alternative algorithm exploiting the copositivity conditions recursively. There are few approaches available in this direction and they are in principle available to incorporate numerically. We have discussed one such proposition[‖] and shown how they can be incorporated and tested in a numerical code. For that purpose, we note the theorem in [25, 26] where it was shown that the necessary and sufficient conditions for the copositivity can be expressed as, Λ *is copositive iff every principal sub-matrix* Λ' *of* Λ *does not posses any positive eigenvector associated with a negative eigenvalue.* This procedure is useful while we are dealing with a matrix numerically.

While adjudging the validity of a model up to a certain scale we need to perform the renormalization group evolutions of the quartic couplings belonging to the scalar potential. There this matrix can be constructed out of these quartic couplings at each scale and one can check the copositivity using this method. Now we will provide a brief algorithm encoded in MATHEMATICA for this approach.

Algorithm to examine copositivity of any given order n matrix

Here we have demonstrated an algorithm for a matrix of order n. Let us first define a matrix of order n and some initializations:

```
mats= {{a11,a12,...,a1n},{a21,a22,...,a2n},....,{an1,an2,...,ann}};
degree = Length[mats]; Print[degree];
mat[1, 1] = mats;
For[ii = 1, ii <= degree, ii++, {n[ii] = 1}];
matdummy[1, 1] = degree + 1;
mategsystm[1, 1] = Eigensystem[mat[1, 1]];
counter = 0;
```

Number of principal sub-matrices of matrix of order n is $(2^n - 1)$. It is very easy to identify the principal sub-matrices of order n and order *one* of a particular matrix. It will have n-numbers of principal sub-matrices of order *one* and they

‖Yet another prescription given in [29] puts conditions on determinant and adjugate matrix to find whether a matrix of order n is copositive or not.

are the just diagonal elements of the original matrix. The matrix itself is the principal sub-matrix of order n.

```
For[ibig = 2, ibig <= degree,  ibig++, {
  For[ismall = 1, ismall <= Binomial[degree, ibig - 2], ismall++, {
    For[i[ibig] = 1, i[ibig] < matdummy[ibig - 1, ismall], i[ibig]++, {
      mat[ibig, n[ibig]++] =
      Drop[mat[ibig - 1, ismall], {i[ibig]}, {i[ibig]}];
      matdummy[ibig, n[ibig] - 1] = i[ibig];
      mategsystm[ibig, n[ibig] - 1] =
      Eigensystem[mat[ibig, n[ibig] - 1]];
      }]
    }]
  }]
```

Now one needs to calculate all the eigenvalues and identify the negative ones. Then one has to check whether the eigenvector associated with the negative eigenvalue is negative or not. If the eigenvector is positive then the matrix of order n is *not* Copositive.

```
For[pp = 1, pp <= degree , pp++, {
  For[oo = 1, oo <= Binomial[degree, pp - 1], oo++, {
     For[ii = 1, ii <= degree + 1 - pp, ii++, {
        If[N[Extract[mategsystm[pp, oo], {1, ii}]] < 0, {
          vector[pp, oo] = N[Extract[mategsystm[pp, oo], {2, ii}]];
          If[MemberQ[vector[pp, oo], _?Positive] !=
                                MemberQ[vector[pp, oo], _?Negative],
             Print["Error!!!!! ----->\tEigenvalue= ",
                            N[Extract[mategsystm[pp, oo], {1, ii}]],
                    "\tEigenvector:\t", vector[pp, oo]]; counter++]
           }]
        }];
     }];
  }]
```

Thus finally determine whether the matrix is copositive or not:

```
If[counter != 0, Print["\n The Matrix is NOT copositive."],
                           Print["\n The Matrix is copositive."]];
```

Numerical example with an order four symmetric matrix

```
mats= {{1,-0.72,-0.59,0.6},  {-0.72,1,0.21,-0.46},  {-0.59,0.21,1,0.6},
               {0.6,-0.46,0.6,-1} } ;
```

Principal sub-matrices of order *three*

$$\begin{pmatrix} 1 & 0.21 & -0.46 \\ 0.21 & 1 & 0.6 \\ -0.46 & 0.6 & -1 \end{pmatrix}, \begin{pmatrix} 1 & -0.72 & -0.59 \\ -0.72 & 1 & 0.21 \\ -0.59 & 0.21 & 1 \end{pmatrix},$$

$$\begin{pmatrix} 1 & -0.59 & 0.6 \\ -0.59 & 1 & 0.6 \\ 0.6 & 0.6 & -1 \end{pmatrix}, \begin{pmatrix} 1 & -0.72 & 0.6 \\ -0.72 & 1 & -0.46 \\ 0.6 & -0.46 & -1 \end{pmatrix}.$$

Eigensystems associated with negative eigenvalues {eigenvectors}

```
-1.27588    {0.214546,-0.26745,0.939383}
-1.39819    {-0.300393,-0.300393,0.905278}
-1.19908    {-0.221234,0.129747,0.966551}
```

Principal sub-matrices of order *two*

$$\begin{pmatrix} 1 & 0.6 \\ 0.6 & -1 \end{pmatrix}, \begin{pmatrix} 1 & -0.46 \\ -0.46 & -1 \end{pmatrix}, \begin{pmatrix} 1 & 0.6 \\ 0.6 & -1 \end{pmatrix},$$

$$\begin{pmatrix} 1 & 0.21 \\ 0.21 & 1 \end{pmatrix}, \begin{pmatrix} 1 & -0.59 \\ -0.59 & 1 \end{pmatrix}, \begin{pmatrix} 1 & -0.72 \\ -0.72 & 1 \end{pmatrix}.$$

Eigensystems associated with negative eigenvalues {eigenvectors}

```
-1.16619    {0.266934,-0.963715}
-1.10073    {-0.213904,-0.976855}
-1.16619    {0.266934,-0.963715}
```

Principal sub-matrices of order *one*

$$(1), (1), (1), (-1).$$

Eigensystems associated with negative eigenvalues {eigenvectors}

```
-1    {1.}

   The  matrix is NOT copositive.
```

2.4 Basis Dependency of the Copositive Conditions

Here we would like to make an important note related to the *basis dependency* of the copositivity of a symmetric matrix. In general it is indeed possible to switch on some norm preserving rotation and that might change the structure of the quadratic form in new basis. This choice can even be made such that the matrix out of the transformed quadratic form is no longer copositive. But this is not counter-intuitive since any arbitrary norm preserving rotation can import the elements of $\Re_n^-$ and the transformed matrix might be non-copositive. Moreover, this is not the reason of worry in our case. As soon as we mention that this quadratic form is a part of our Lagrangian, arbitrary rotations are prohibited. From the symmetry principle we can allow only those rotations which leave the Lagrangian invariant. This simply says that the all allowed rotations will leave the quadratic form intact in any new basis. From the point of copositivity the quadratic form is the fundamental one, i.e., if the matrix corresponding to a quadratic form is copositive then any other matrices written in any other basis out of that quadratic form will be copositive.

Another important property of copositivity is its *invariance under the operation of permutation and scaling*. So, if Λ be a copositive matrix then after combined operation, the new matrix $PD\Lambda DP^T$ is also copositive given that P be a permutation matrix and D is a diagonal matrix with non-negative elements.

We will use this property in our analysis to ensure a single set of copositivity conditions independent to the order of the basis elements.

2.4.1 Vacuum Stability and Copositivity

So far we have sketched the mathematical foundation and the criteria of copositivity of symmetric matrices of finite order. Now we intend to implement this idea to adjudge the stability of the scalar potential. We will see how the copositivity guarantees the boundedness (≥ 0) of the quadratic form. Since part of the scalar potential that contains the quartic couplings plays the crucial role while deciding the vacuum stability of the corresponding potential, we shall concentrate on those terms only. We would like to note that this part of the scalar potential is treated as the quadratic form while the basis are bi-linear in fields. We construct symmetric matrices in terms of monomial basis so that the quadratic form $x^T \Lambda x \geq 0$ as expressed in the copositivity definition can be achieved. Hence one can directly apply the copositivity conditions for these Λ matrices whose elements are made of quartic couplings. Thus by implementing the mathematical idea of copositivity we can guarantee the boundedness of the potential along the all field directions. This construction also allows us to find the largest parameter space over which the vacuum is stable.

An Example With New Physics

To consolidate the claim, now we will present an example where we have shown how copositivity can help to find the largest parameter space. We revisit the Type–II seesaw model discussed in [30], and adopt the same scalar potential for having a straightforward comparison of vacuum stability conditions. Scalar sector of this models consists of a doublet scalar (Φ) and a triplet scalar (Δ) with weak hypercharge $+1$ and $+2$ respectively. Structures of these scalars can be written in the following form:

$$\Phi = \begin{pmatrix} \phi^+ \\ \phi^0 \end{pmatrix} \quad , \quad \Delta = \begin{pmatrix} \delta^+/\sqrt{2} & \delta^{++} \\ \delta^0 & -\delta^+/\sqrt{2} \end{pmatrix} .$$

Scalar potential for Type–II seesaw can be written as [30]:

$$\begin{aligned} V^{Q}_{Type-II}(\Phi,\Delta) &= \frac{\lambda}{4}\left(\Phi^\dagger\Phi\right)^2 + \lambda_1\left(\Phi^\dagger\,\Phi\right)\left(\mathrm{Tr}[\Delta^\dagger\Delta]\right) + \lambda_2\left(\mathrm{Tr}[\Delta^\dagger\Delta]\right)^2 \\ &+\lambda_3\mathrm{Tr}[\left(\Delta^\dagger\Delta\right)^2] + \lambda_4\left(\Phi^\dagger\,\Delta\,\Delta^\dagger\Phi\right). \end{aligned}$$

The neutral components of the scalars acquire *vevs* as follows:

$$\langle\Phi\rangle = \begin{pmatrix} 0 \\ v \end{pmatrix} \quad , \quad \langle\Delta\rangle = \begin{pmatrix} 0 & 0 \\ v_\Delta & 0 \end{pmatrix}.$$

leading to spontaneous breaking of the symmetry. To establish the multi-field conditions, Arhrib *et.al.* used the same method discussed in 2.2.

As our first example we have chosen a simpler 3-field direction that contains the field directions $\phi^0\,,\phi^+$ and δ^+ and corresponding potential term is

$$\begin{aligned} {}^{3F}V_{10}(\phi^0\,,\,\phi^+\,,\,\delta^+) &= (\lambda_2+\frac{\lambda_3}{2})\delta^{+4} + \frac{\lambda}{4}\,\phi^{04} + \frac{\lambda}{4}\,\phi^{+4} + \frac{\lambda}{2}\phi^{+2}\phi^{02} \\ &+(\lambda_1+\frac{\lambda_4}{2})\delta^{+2}\,\phi^{+2} + (\lambda_1+\frac{\lambda_4}{2})\delta^{+2}\,\phi^{02}. \end{aligned} \tag{2.17}$$

The notation ${}^{3F}V_{10}$ stands for the 10^{th} 3-Field potential direction as described in our article [17].

Using the method suggested in [30] and discussed in 2.2 one can calculate the necessary stability conditions as

$$\begin{aligned} &\lambda > 0 \quad \& \quad \lambda_2 + \frac{\lambda_3}{2} > 0 \quad \& \quad 2\lambda_1 + \lambda_4 + \sqrt{2\lambda(2\lambda_2+\lambda_3)} > 0 \quad \& \\ &\left(2\lambda_1+\lambda_4 > 0 \;\;||\;\; 2\lambda(2\lambda_2+\lambda_3) > (2\lambda_1+\lambda_4)^2\right). \end{aligned} \tag{2.18}$$

These expressions exactly match with criteria given in [30]. For the same potential, the independent COP criteria**

$$\begin{gathered} \lambda \geq 0, \qquad \lambda_2 + \tfrac{\lambda_3}{2} \geq 0, \\ \kappa_1 = \kappa_3 = \frac{\lambda_1+\frac{\lambda_4}{2}}{2} + \sqrt{\tfrac{\lambda}{4}\left(\lambda_2+\tfrac{\lambda_3}{2}\right)} \geq 0, \\ \kappa_2 = \tfrac{\lambda}{4} + \sqrt{\tfrac{\lambda}{4}\cdot\tfrac{\lambda}{4}} = \tfrac{\lambda}{2} \geq 0, \end{gathered}$$

**The fourth term in Eq. 2.19 can be simplified and written in terms of other conditions.

$$\sqrt{\left(\frac{\lambda}{4}\right)\left(\frac{\lambda}{4}\right)\left(\lambda_2+\frac{\lambda_3}{2}\right)} \; + \; \frac{\lambda}{4}\sqrt{\lambda_2+\frac{\lambda_3}{2}}+\frac{\lambda_1+\frac{\lambda_4}{2}}{2}\sqrt{\frac{\lambda}{4}}$$
$$+ \; \frac{\lambda_1+\frac{\lambda_4}{2}}{2}\sqrt{\frac{\lambda}{4}}+\sqrt{2(\kappa_1)(\kappa_2)(\kappa_3)} \geq 0, \quad (2.19)$$

can be noted in compact form as

$$\lambda > 0 \quad \& \quad \lambda_2+\frac{\lambda_3}{2} > 0 \quad \& \quad 2\lambda_1+\lambda_4+\sqrt{2\lambda(2\lambda_2+\lambda_3)} > 0. \qquad (2.20)$$

Here both the methods give the same allowed parameter space since the additional part in eqn. 2.18 does not put any new constraint.

In a second example we consider two 3-field directions (ϕ^0, δ^+, δ^0) and (ϕ^+, δ^+, δ^{++}). Corresponding stability conditions are more complicated:

- For 3-field direction (ϕ^0, δ^+, δ^0)

$$\begin{aligned}\lambda \; > \; & 0 \wedge \lambda_2+\lambda_3 > 0 \; \wedge 2\lambda_2+\lambda_3 > 0 \; \wedge \sqrt{\lambda(\lambda_2+\lambda_3)}+\lambda_1+\lambda_4 > 0 \wedge \\ & \Bigg(\Bigg\{ 2\lambda(2\lambda_2+\lambda_3) > (2\lambda_1+\lambda_4)^2 \wedge \\ & \Bigg[\Bigg(\sqrt{2}\sqrt{\lambda_3(\lambda_2+\lambda_3)((2\lambda_1+\lambda_4)^2-2\lambda(2\lambda_2+\lambda_3))}+2\lambda_2\lambda_4 > 2\lambda_1\lambda_3 \wedge \\ & \lambda_3 < 0\Bigg) \vee \Bigg(\frac{(2\lambda_2+\lambda_3)((2\lambda_1+\lambda_4)(2\lambda_1+3\lambda_4)-4\lambda(\lambda_2+\lambda_3))}{2\lambda_1+\lambda_4} > 0 \wedge \\ & 2\lambda_1+\lambda_4 < 0\Bigg)\Bigg]\Bigg\} \vee 2\lambda_1+\lambda_4 > 0\Bigg). \end{aligned} \qquad (2.21)$$

- For 3-field direction (ϕ^+, δ^+, δ^{++})

$$\begin{aligned}\lambda \; > \; & 0 \wedge 2\lambda_2+\lambda_3 > 0 \wedge \lambda_2+\lambda_3 > 0 \; \wedge \sqrt{\lambda(4\lambda_2+2\lambda_3)}+2\lambda_1+\lambda_4 > 0 \wedge \\ & \Bigg(\Bigg\{\lambda(\lambda_2+\lambda_3) > (\lambda_1+\lambda_4)^2 \vee \\ & \Bigg[\Bigg(\sqrt{2}\sqrt{\lambda_3(\lambda_2+\lambda_3)\Big((\lambda_1+\lambda_4)^2-(\lambda_2+\lambda_3)\Big)} > \lambda_4(\lambda_2+\lambda_3) \wedge \lambda_3 < 0\Bigg) \\ & \vee(2\lambda_1\lambda_2+3\lambda_1\lambda_3+\lambda_3\lambda_4 > \frac{2\lambda(\lambda_2+\lambda_3)^2}{\lambda_1+\lambda_4} \wedge \lambda_1+\lambda_4 < 0)\Bigg]\Bigg\} \vee \lambda_1+\lambda_4 > 0\Bigg). \end{aligned} \qquad (2.22)$$

These two equations are same as the Eqs. B.27 and B.33 of Ref. [30]. Looking throughout the parameter space we have verified that these different looking conditions in fact cover *the same parameter space*. Instead of two apparently different looking conditions, *invariance of copositivity ensures a single set of stability conditions for both the directions* ${}^{3F}V_2$ and ${}^{3F}V_3$ as follows

$$\begin{aligned} {}^{3F}V_2(\phi^0\,,\,\delta^+\,,\,\delta^0) &= (\lambda_2+\lambda_3)\delta^{04} + (\lambda_2+\frac{\lambda_3}{2})\delta^{+4} + \frac{\lambda}{4}\,\phi^{04} + 2(\lambda_2+\lambda_3)\delta^{02}\delta^{+2} \\ &+ (\lambda_1+\lambda_4)\phi^{02}\delta^{02} + (\lambda_1+\frac{\lambda_4}{2})\delta^{+2}\,\phi^{02}. \end{aligned} \tag{2.23}$$

$$\begin{aligned} {}^{3F}V_3(\phi^+\,,\,\delta^+\,,\,\delta^{++}) &= (\lambda_2+\frac{\lambda_3}{2})\delta^{+4} + (\lambda_2+\lambda_3)\delta^{++4} + \frac{\lambda}{4}\,\phi^{+4} + 2(\lambda_2+\lambda_3)\delta^{+2}\delta^{++2} \\ &+ (\lambda_1+\lambda_4)\phi^{+2}\delta^{++2} + (\lambda_1+\frac{\lambda_4}{2})\delta^{+2}\,\phi^{02}. \end{aligned} \tag{2.24}$$

In matrix form both can be represented in basis ($\phi^{02} \Leftrightarrow \phi^{+2}, \delta^{+2}, \delta^{02} \Leftrightarrow \delta^{++2}$):

$$\begin{pmatrix} \frac{\lambda}{4} & \frac{\lambda_1+\lambda_4}{2} & \frac{\lambda_1+\frac{\lambda_4}{2}}{2} \\ & \lambda_2+\lambda_3 & \lambda_2+\lambda_3 \\ & & \lambda_2+\frac{\lambda_3}{2} \end{pmatrix}.$$

<u>Copositivity condition</u>:

$$\begin{aligned} &\lambda \geq 0, \qquad \lambda_2+\lambda_3 \geq 0, \qquad \lambda_2+\frac{\lambda_3}{2} \geq 0, \\ &\kappa_1 = \lambda_2+\lambda_3+\sqrt{(\lambda_2+\frac{\lambda_3}{2})\left(\lambda_2+\frac{\lambda_3}{2}\right)} \geq 0, \\ &\kappa_2 = \frac{\lambda_1+\frac{\lambda_4}{2}}{2}+\sqrt{\frac{\lambda}{4}(\lambda_2+\lambda_3)} \geq 0, \\ &\kappa_3 = \frac{\lambda_1+\lambda_4}{2}+\sqrt{\frac{\lambda}{4}(\lambda_2+\lambda_3)} \geq 0, \end{aligned}$$

$$\begin{aligned} \sqrt{\frac{\lambda}{4}\,(\lambda_2+\lambda_3)\,(\lambda_2+\frac{\lambda_3}{2})} \;+\; &\frac{\lambda_1+\lambda_4}{2}\sqrt{\lambda_2+\frac{\lambda_3}{2}}+\frac{\lambda_1+\frac{\lambda_4}{2}}{2}\sqrt{\lambda_2+\lambda_3} \\ &+(\lambda_2+\lambda_3)\sqrt{\frac{\lambda}{4}}+\sqrt{2\,(\kappa_1)(\kappa_2)(\kappa_3)} \geq 0. \end{aligned}$$

This is ensured by the following property of copositivity: invariance under permutations. Note that the basis are different in each case, however, that is not a problem since we are only interested to find the conditions for stability in these situations, and as expected the basis dependency does not matter at all. The stability conditions calculated using copositivity ensure the boundedness of the potential with mathematical confirmations. Moreover it *ensures the minimum allowed conditions resulting into more parameter space* compared to the conditions obtained from the successive squaring method. This was also verified numerically that the COP conditions correspond to ${}^{3F}V_2$ (or, ${}^{3F}V_3$) indeed allow more parameter space.

We would like to end this section pointing out the limitation of copositivity in the application to vacuum stability analysis. Restrictions arise due to the fact they the basis vectors x of the quadratic form $x^T \Lambda\, x$ should be non-negative vectors. Hence if there exist a term like $\lambda_{1234}\phi_1\phi_2\phi_3\phi_4$ in the potential, we have to construct basis vectors like $\phi_1\phi_2$. Since ϕ_i's are complex scalar field the term $\phi_1\phi_2$ may not be non-negative vectors for all values of the fields ϕ_1 and ϕ_2. In this case only a fraction of the full parameter space can be analyzed using copositivity.

2.5 Unitarity of scattering amplitudes

To find the upper bound of scalar masses of any theory we can rely on the perturbative unitarity of the scattering amplitude. Any scattering amplitude can be written as an infinite sum of partial waves, in the form,

$$\mathcal{M}(\theta) = 16\pi \sum_{l=0}^{\infty} a_l\,(2l+1)\,P_l(\cos\theta), \tag{2.25}$$

where a_l is the scattering amplitude of order l, θ is the scattering angle and $P_l(\cos\theta)$ is l^{th}-order Legendre polynomial. In SM, by analyzing the two-body scattering between longitudinal gauge bosons and Higgs it was shown in the pioneering paper by LQT [7] that unitarity of S-matrix constrains the zeroth partial wave amplitude as, $|a_0| \leq 1$ which in turn restricts the Higgs quartic coupling and therefore constrains the Higgs mass from the above. The unitarity

Charge(q)	0	1	2	3	4
Number of possible 2-particle states	$\frac{n(n+1)}{2} + s^2 + d^2$	$s(n+d)$	$nd + \frac{s(s+1)}{2}$	sd	$\frac{d(d+1)}{2}$

Table 2.1: Number of all possible q-charged 2-particle states constructed from n neutral, s singly charged and d doubly charged fields.

constraint can be recast as,

$$|\mathcal{M}| \leq 8\pi, \tag{2.26}$$

where $\mathcal{M}$ is the full tree level matrix element. This method can be extended to the scenario where extra scalar fields are present [8, 31–33]. Thus in the present scenario, we also consider the appropriate two-body channels. By virtue of equivalence theorem, in the high energy limit, one can use the unphysical scalars instead of original longitudinal components of the gauge bosons. Thus the relevant $2 \to 2$ scatterings will get contributions from the quartic couplings; the contribution from trilinear couplings can safely be ignored due to the fact that the diagrams resulting from the trilinear couplings will have an E^2-suppression coming from the intermediate propagators. So we need to find the matrix elements for relevant $2 \to 2$ processes. Accordingly an S-matrix can be constructed by taking different two-particle states as rows and columns and each entry of that matrix will give the scattering amplitude between the corresponding 2-particle state in the row and the 2-particle state in the column. Clearly, the unitarity constraints (eq. 2.26) manifest themselves as bounds on the eigenvalues of this matrix.

The 2-particle states are made of the component fields of the scalar particles of any BSM theory. As an example, let us consider that a model contains neutral, singly charged and doubly charged states. Using them we constructed all possible q-charged 2-particle states, where q can be anything from zero to four. If one has (n)-neutral, (s)-singly charged and (d)-doubly charged fields then the number of all possible 2-particle states are tabulated in the table 2.1.

An Example

Let us consider a doublet scalar field:

$$\Phi = \begin{pmatrix} \phi^{+} \\ \phi_r^0 + i\,\phi_i^0 \end{pmatrix}.$$

Then all possible 2-particle states are as follows:

$$\begin{aligned} \text{Neutral basis} \;\; &: \;\; \phi_r^0\,\phi_r^0\;,\;\phi_r^0\,\phi_i^0\;,\;\phi_i^0\,\phi_i^0\;,\;\phi^+\,\phi^- \\ \text{Singly charged basis} \;\; &: \;\; \phi^+\,\phi_r^0\;,\;\phi^+\,\phi_i^0 \qquad\qquad \text{Doubly charged basis} : \phi^+\,\phi^+ \end{aligned}$$

We have used this method to explicitly compute the unitarity bounds for the Left-Right symmetric model with triplet scalars as discussed in Chapter 4 and also full calculation can be found in the appendix C. For the case of gauged $U(1)_{B-L}$ model, unitarity have been studied extensively in [34].

2.6 Conclusion

The vacuum stability is an important issue that must be addressed for any beyond standard model scenario. Thus one needs to carefully examine the vacuum stability criteria that lead to the boundedness of the full scalar potential.

The straight forward way to calculate the stability criteria is by using the positivity of the quadratic form. However this calculation is very complicated when multiple scalar fields are involved and often contains combinatorial ambiguity.

We have adopted another technique which is well discussed in the context of Linear Algebra, namely *copositivity of symmetric matrix*. Here we have discussed two approaches to check the copositivity – using the explicit structure of that matrix and other one using the principal sub-matrices. We have first discussed how to reconstruct the symmetric matrices using the quartic couplings and then compute the copositivity criteria to deduce the vacuum stability conditions. We have then used this method for complicated models like Left-Right symmetry to compute the stability criteria for these models for different field directions. Apart from this analytical but in some sense restricted procedure we also discuss an alternative method to check whether a matrix is copositive or not using principal sub-matrix formalism. For the principal sub-matrix approach we have provided a general algorithm to check the copositivity of a symmetric matrix of finite order and also provide explicit numerical example.

Also we have discussed how perturbative unitarity of the scattering amplitudes can constrain quartic couplings. These constraints can easily be translated into the upper bound of the masses of the physical scalars present in any BSM scenario. We obtain these constraints by evaluating the zeroth order partial wave amplitude of various $2 \to 2$ scatterings.

Chapter 3

$B - L$ Extended Standard Model

In this chapter we discuss the minimal $U(1)_{B-L}$ extension of the SM [9, 35]. It has been noted in [36] that an extra $U(1)$ gauge symmetry along with the SM can provide solutions to some of the unaddressed issues in the SM. These extra Abelian symmetry groups can, in general, originate from different high scale GUTs, like $SO(10), E(6)$. These larger groups contain $U(1)_{B-L}$ as a part of the intermediate gauge symmetries.

The gauge group under consideration is $SU(3)_C \otimes SU(2)_L \otimes U(1)_Y \otimes U(1)_{B-L}$. This minimal model contains an extra complex singlet scalar field S and the $B-L$ symmetry is broken once S acquires a vacuum expectation value (*vev*) [9, 35, 37]. Thus, the *vev* determines the breaking scale of the $B-L$ symmetry and also the mass of the extra neutral gauge boson Z_{B-L}.

Now we briefly discuss the scalar, gauge and fermion sector of this model.

3.1 Scalar sector

The scalar sector consists of a Higgs doublet Φ as in the SM and a complex singlet scalar S. The scalar kinetic energy term reads as:

$$\mathscr{L}_s = (D^\mu \Phi)^\dagger (D_\mu \Phi) + (D^\mu S)^\dagger (D_\mu S) - V(\Phi, S), \tag{3.1}$$

where the potential $V(\Phi, S)$ is given as:

$$V(\Phi, S) = -m^2\Phi^\dagger\Phi - \mu^2 \mid S \mid^2 + \lambda_1(\Phi^\dagger\Phi)^2 + \lambda_2 \mid S \mid^4 + \lambda_3\, \Phi^\dagger\Phi \mid S \mid^2 . \quad (3.2)$$

After the scalars acquire *vevs*, these fields then be expressed as:

$$\Phi \equiv \begin{pmatrix} 0 \\ \frac{1}{\sqrt{2}}(v+\phi) \end{pmatrix}, \qquad S \equiv \frac{1}{\sqrt{2}}(v_{B-L} + s)\,, \quad (3.3)$$

where, the EW symmetry breaking *vev* v and the $B-L$ breaking *vev* v_{B-L} are real and positive.

Now minimizing the scalar potential we find the following relations:

$$\begin{aligned} -m^2 + 2\lambda_1 v^2 + \lambda_3\, v\, v_{\text{B-L}}^2 &= 0, \\ -\mu^2 + 4\lambda_2 v_{\text{B-L}}^2 + \lambda_3\, v^2\, v_{\text{B-L}} &= 0. \end{aligned} \quad (3.4)$$

Using the minimization equations it is easy to find the scalar mass matrix, which takes the following form:

$$\mathcal{M} = \begin{pmatrix} \lambda_1 v^2 & \frac{\lambda_3 v_{B-L} v}{2} \\ \frac{\lambda_3 v_{B-L} v}{2} & \lambda_2 v_{B-L}^2 \end{pmatrix} = \begin{pmatrix} \mathcal{M}_{11} & \mathcal{M}_{12} \\ \mathcal{M}_{21} & \mathcal{M}_{22} \end{pmatrix}. \quad (3.5)$$

After diagonalizing this mass matrix we construct two physical scalar states, light h and heavy H, having masses M_h and M_H respectively:

$$M_{H,h}^2 = \frac{1}{2}\left[\mathcal{M}_{11} + \mathcal{M}_{22} \pm \sqrt{(\mathcal{M}_{11} - \mathcal{M}_{22})^2 + 4\mathcal{M}_{12}^2}\right]. \quad (3.6)$$

The mass eigenstates $(h,\, H)$ are linear combinations of ϕ and s, and written as

$$\begin{pmatrix} h \\ H \end{pmatrix} = \begin{pmatrix} \cos\alpha & -\sin\alpha \\ \sin\alpha & \cos\alpha \end{pmatrix} \begin{pmatrix} \phi \\ s \end{pmatrix}. \quad (3.7)$$

Here we assume that the lightest mass eigenstate h is the SM-like Higgs boson. The scalar mixing angle α can be expressed in terms of the elements of the mass matrix Eq. 3.5,

$$\tan(2\alpha) = \frac{2\mathcal{M}_{12}}{\mathcal{M}_{11} - \mathcal{M}_{22}} = \frac{\lambda_3\, v\, v_{_{B-L}}}{\lambda_1 v^2 - \lambda_2 v_{_{B-L}}^2}. \tag{3.8}$$

Using eqs. 3.6 and 3.8 the quartic coupling constants λ_1, λ_2, and λ_3 can be recast in the following forms:

$$\begin{aligned}
\lambda_1 &= \frac{1}{4v^2}\Big\{ \left(M_H^2 + M_h^2\right) - \cos 2\alpha \left(M_H^2 - M_h^2\right) \Big\}, \\
\lambda_2 &= \frac{1}{4v_{_{B-L}}^2}\Big\{ \left(M_H^2 + M_h^2\right) + \cos 2\alpha \left(M_H^2 - M_h^2\right) \Big\}, \\
\lambda_3 &= \frac{1}{2\, v\, v_{_{B-L}}}\Big\{ \sin 2\alpha \left(M_H^2 - M_h^2\right) \Big\}.
\end{aligned} \tag{3.9}$$

It can be noted from Eq. 3.9 that we would get a duplicate set of solutions with inverted sign of both α and λ_3. Also when the mixing angle α vanishes the quartic coupling λ_1 becomes purely the SM quartic coupling and λ_2 is determined solely by the additional scalar state. By setting λ_3 to zero, vanishing mixing angle also ensures that there is no mixing between the SM Higgs doublet and the additional singlet.

3.2 Gauge Sector

The model contains another $U(1)$ symmetry along with the SM gauge symmetry and this $U(1)_{B-L}$ symmetry is broken by the additional complex singlet scalar S. Due to the presence of an extra $U(1)_{B-L}$ gauge symmetry, there is an additional gauge kinetic Lagrangian term which reads,

$$\mathscr{L}_{B-L}^{KE} = -\frac{1}{4} F'^{\mu\nu} F'_{\mu\nu}\,, \tag{3.10}$$

where,

$$F'_{\mu\nu} = \partial_\mu B'_\nu - \partial_\nu B'_\mu\,, \tag{3.11}$$

The covariant derivative for the $SU(2)_L \otimes U(1)_Y \otimes U(1)_{B-L}$ sector in this

Particle	Q	u_R	d_R	L	e_R	Φ	S	$N_{R^{1,2}}$	N_{R^3}
$SU(2)_L$	2	1	1	2	1	2	1	1	1
$U(1)_Y$	1/3	4/3	-2/3	-1	-2	1	0	0	0
$U(1)_{B-L}$	1/3	1/3	1/3	-1	-1	0	2	-1	-1

Table 3.1: Particle content of the minimal $U(1)_{B-L}$ model and their representations (for $SU(2)_L$) and internal quantum numbers (for $U(1)_{Y/B-L}$)

model is modified as*

$$D_\mu \equiv \partial_\mu + ig_2\, T^a\, W_\mu{}^a + ig_1\, Y\, B_\mu + i(\widetilde{g}\, Y + g_{_{B-L}}\, Y_{B-L})\, B'_\mu\,. \tag{3.12}$$

Here $\widetilde{g}$ is a free parameter which quantifies mixing between the $U(1)$ gauge groups. If we set $\widetilde{g}$ to zero, then the model is called pure $B-L$ model.

We will now use this covariant derivative in the kinetic term of the scalar Lagrangian in Eq. 3.1 to calculate the masses of gauge bosons. The SM gauge bosons B_μ and W^3_μ will mix with the new gauge boson B'_μ and after symmetry breaking there will be two massive physical fields Z and Z_{B-L} and one massless photon field A. Assuming there is no mixing at tree level, i.e., $\widetilde{g}=0$ at EW scale, the physical gauge boson masses are given as

$$M_Z^2 = \frac{1}{4}\left(g_{_1}^2 + g_{_2}^2\right) v^2, \tag{3.13}$$

$$M^2_{Z_{B-L}} = 4g^2_{_{B-L}} v^2_{_{B-L}}. \tag{3.14}$$

We will use this expressions in our analysis. Explicit expressions for masses of neutral gauge bosons and the mixing matrix can be found in [40].

3.3 Fermion Sector

Along with the Standard Model particles, three right-handed neutrinos (ν_R) with $Q_{B-L} = -1$ have to be introduced in this model for the sake of anomaly cancel-

*In principle it is also possible to write another term in the Eq. 3.10, $\frac{\kappa}{2} F^{\mu\nu} F'_{\mu\nu}$ which is the kinetic mixing term. This term is allowed by gauge invariance only for Abelian gauge groups. It is possible to diagonalize the kinetic terms by a GL(2,R) transformation [38,39] and we arrive at the covariant derivative stated here.

lation. The relevant Yukawa interactions can be written as

$$-\mathcal{L}_Y = y^l_{ij}\overline{l_{iL}}\,\widetilde{\Phi}\,\nu_{jR} + y^h_{ij}\,\overline{(\nu_R)^c_i}\,\nu_{jR}\,S + h.c. \tag{3.15}$$

where $\widetilde{\Phi} = i\sigma_2\Phi^*$ with σ_2 being the second Pauli matrix. the second term of the above equation is the Majorana mass term for RH neutrinos. We see from the Eq. 3.15 that conservation of $B-L$ charge requires the singlet scalar field, S, to have $Q_{B-L} = -2$. When the SM Higgs and the singlet scalar S acquire *vev*s the neutrino mass matrix takes the form

$$M_\nu = \begin{pmatrix} 0 & m_D \\ m_D^T & m_R \end{pmatrix}, \tag{3.16}$$

where $m_D = y^l\frac{v}{\sqrt{2}}$ and $m_R = \sqrt{2}\ y^h v_{_{B-L}}$. The light (m_{ν_l}) and heavy (m_{ν_h}) neutrino masses are

$$m_{\nu_l} = -m_D^T m_R^{-1} m_D, \tag{3.17}$$

$$m_{\nu_h} = m_R. \tag{3.18}$$

In this model, the heavy neutrino mass m_R is also generated through the Yukawa terms unlike the gauge invariant Majorana mass term in type-I seesaw. It can be noted that for $m_R \sim \mathcal{O}(\text{TeV})$, y^l needs to be very small to generate light neutrino masses $\sim \mathcal{O}(\text{eV})$. But y^h can be large $\sim \mathcal{O}(1)$ as $v_{_{B-L}}$ is around the TeV scale.

In Table 3.3 we summarize the particle content of the $U(1)_{B-L}$ model along with their representation (for $SU(2)_L$) and internal quantum numbers (for $U(1)_{Y/B-L}$).

3.4 Vacuum Stability of TeV scale $B-L$ symmetry

In the previous section we argued that successful light neutrino mass generation does not constrain y^h. But as the heavy neutrino is also coupled to the SM-like Higgs, y^h affects the vacuum stability of the scalar potential in this model and gets constrained. The gauge coupling $g_{_{B-L}}$ and the *vev* of the $B-L$ breaking scale (v_{B-L}) are also free parameters. In this section we discuss how these parameters are constrained from vacuum stability of the scalar potential and also from perturbativity of the couplings.

It is clear from the structure of the potential (Eq. 3.2) that the vacuum stability conditions are different from that for the SM due to the presence of an extra singlet scalar. If all the quartic couplings are positive, the potential will be trivially bounded from below, i.e., the vacuum is stable and these stability conditions read simply as $\lambda_{1,2,3} > 0$. But it is indeed possible to allow λ_3 to be negative and the vacuum still can be made stable. Thus vacuum stability conditions beyond the trivial ones allow a larger parameter space and need to be accommodated in these conditions. We find the non-trivial vacuum stability criteria using the proposal dictated in [30], as[†]

$$\begin{aligned} 4\lambda_1\lambda_2 - \lambda_3^2 > 0, \\ \lambda_1 > 0, \quad \lambda_2 > 0. \end{aligned} \tag{3.19}$$

Together with these we have also incorporated perturbativity constraints on quartic couplings by demanding an upper limit, i.e., $|\lambda_i| < 1$ $(i = 1, 2, 3)$. Noting that from Eqs. 3.6 and 3.8 that the physical Higgs field is an admixture of two scalar fields ϕ and s, in our study the scalar mixing angle α is considered to be a free parameter instead of the quartic couplings $\lambda_i (i = 1, 2, 3)$. This model consists of two different scales, the EW scale and the $B-L$ symmetry breaking scale. Thus two RGEs are invoked for the analysis. As we have two Abelian couplings in this model, there might be mixing between them [41, 42]. To simplify the situation, without hampering any other conclusions, we impose no mixing between the Z_{B-L} and Z gauge bosons at the tree-level. This follows from the condition $\widetilde{g}(Q_{EW}) = 0$ as already discussed in the previous section. As a consequence, the $B-L$ breaking *vev* $v_{_{B-L}}$ relates to the new Z_{B-L} boson mass as in Eq. 3.14. For demonstration, we have picked the value of this additional gauge coupling at the breaking scale as, $g_{_{B-L}} = 0.1$. For simplicity, we further assume that heavy

[†]Note that in the positive λ_3 region stability criteria are trivially satisfied *i.e.* all λ_i's are positive. In Fig.3.1 we have shown this region to compare with the negative λ_3 region.

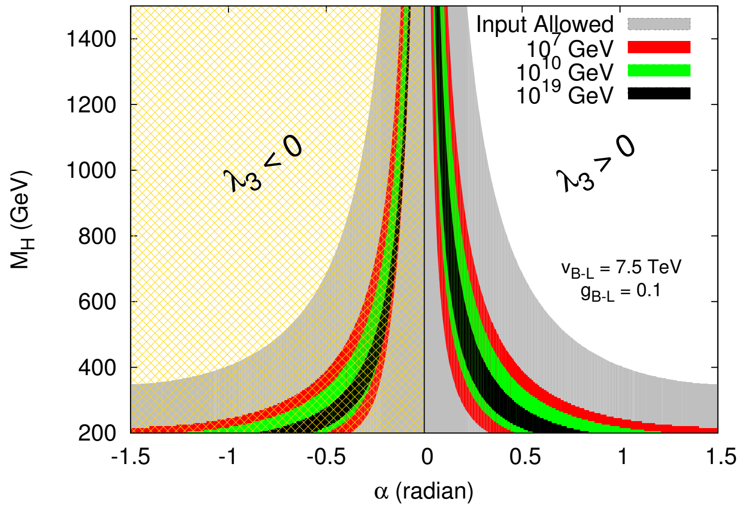

Figure 3.1: The allowed parameter space in heavy Higgs mass (M_H) and scalar mixing angle (α) plane, consistent with vacuum stability and perturbativity bounds are shown here. The gray region is the domain of allowed input parameters. The red, green, and black sub-parameter spaces show the domain of M_H and α for which this $B-L$ theory is valid till 10^7, 10^{10} and 10^{19} GeV respectively. The Majorana neutrino mass is fixed at 200 GeV and $B-L$ breaking *vev* ($v_{_{B-L}}$) is set at 7.5 TeV. The $U(1)_{B-L}$ gauge coupling is taken to be 0.1. The shaded region satisfy $\lambda_3 < 0$ (as well as $\alpha < 0$ from Eq. 3.9). Thus the non-trivial vacuum stability conditions are being satisfied in this region.

neutrinos are degenerate $m^{1,2,3}_{\nu_h} \equiv m_{\nu_h} \simeq 200$ GeV, which is within the allowed values. We have used the central value of the light Higgs mass (M_h) as 125 GeV, top quark mass as 173.2 GeV and strong coupling constant α_s as 0.1184. Thus the remaining free parameters in our study are M_H, α and $v_{_{B-L}}$. We have explored the correlated constraints on these parameters from vacuum stability and perturbativity.

The set of RGEs of different couplings that we have used in our analysis are listed in appendix A.2 [9]. The parameter space consistent with vacuum stability in the heavy Higgs mass (M_H) and scalar mixing angle (α) plane is depicted in Fig. 3.1. All the couplings are perturbative through out their evolutions. The grey region is the domain of allowed input parameters. The red, green, and black sub-parameter spaces show the domain of M_H and α for which this $B-L$ theory is valid till 10^7, 10^{10} and 10^{19} GeV respectively. In this figure, for a particular heavy scalar mass each allowed domain is restricted at some minimum (maximum) value of α due to the vacuum stability (perturbativity) of the quartic couplings. The other parameters, like the Majorana neutrino mass is fixed at 200 GeV and $B-L$ breaking *vev* (v_{B-L}) is set at 7.5 TeV. The $U(1)_{B-L}$ gauge coupling is taken to be 0.1 which implies $M_{Z_{B-L}}$=1.5 TeV, consistent with the present experimental bound [43]. The yellow shaded region contains the set of allowed parameters for $\lambda_3 < 0$ (i.e. for $\alpha < 0$ from Eq. 3.9). Though the pattern of the allowed parameter space in the positive λ_3 region is very similar to that of the negative λ_3 region, it is not exactly symmetric. The upper boundaries of each color in the Fig. 3.1 matches exactly for both positive and negative α region. This is not surprising because the outer boundary is determined by the perturbativity of the couplings and thus not affected by the vacuum stability conditions which are different for different signs of λ_3. However, the lower boundaries are the outcome of the demand to satisfy the criteria of vacuum stability. Allowed parameters in the yellow shaded region (which represents $\lambda_3 < 0$) in the Fig. 3.1 reflects the non-trivial vacuum stability condition in Eq. 3.19, which sequentially plays a role in determining the lower boundaries in the allowed parameters. Thus expectedly in the positive α region (i.e. $\lambda_3 > 0$ region) the allowed parameter space is larger than that for negative α (i.e. $\lambda_3 < 0$). Also, note that $\alpha = 0$ leads to the decoupling limit when the heavy scalar will not affect the vacuum stability. It can easily be inferred from Fig. 3.1 that the parameter space shrinks as the validity of the model is demanded towards the Planck scale .

To study the effect of vacuum stability on different parameters, we plot the region in the $M_H - \alpha$ plane which corresponds to parameters consistent with vacuum stability and where all the couplings are perturbative till the Planck Scale. In Fig. 3.2(a) the Majorana neutrino Yukawa coupling y^h is varied keeping v_{B-L} and g_{B-L} fixed. As y^h increases, the allowed parameter space shrinks since the Yukawa coupling affects the quartic couplings negatively in their RG evolutions. Thus larger Yukawa couplings spoil the vacuum stability. Fig. 3.2(b) shows the dependence on $B-L$ breaking *vev* for fixed g_{B-L} and y^h. v_{B-L} determines the scale of new physics beyond the Standard Model, i.e., from where the RGEs are being modified due to the presence of new particles. Larger v_{B-L} implies that the new set of RGEs come to play later. In the $B-L$ extended model, λ_3 is inversely

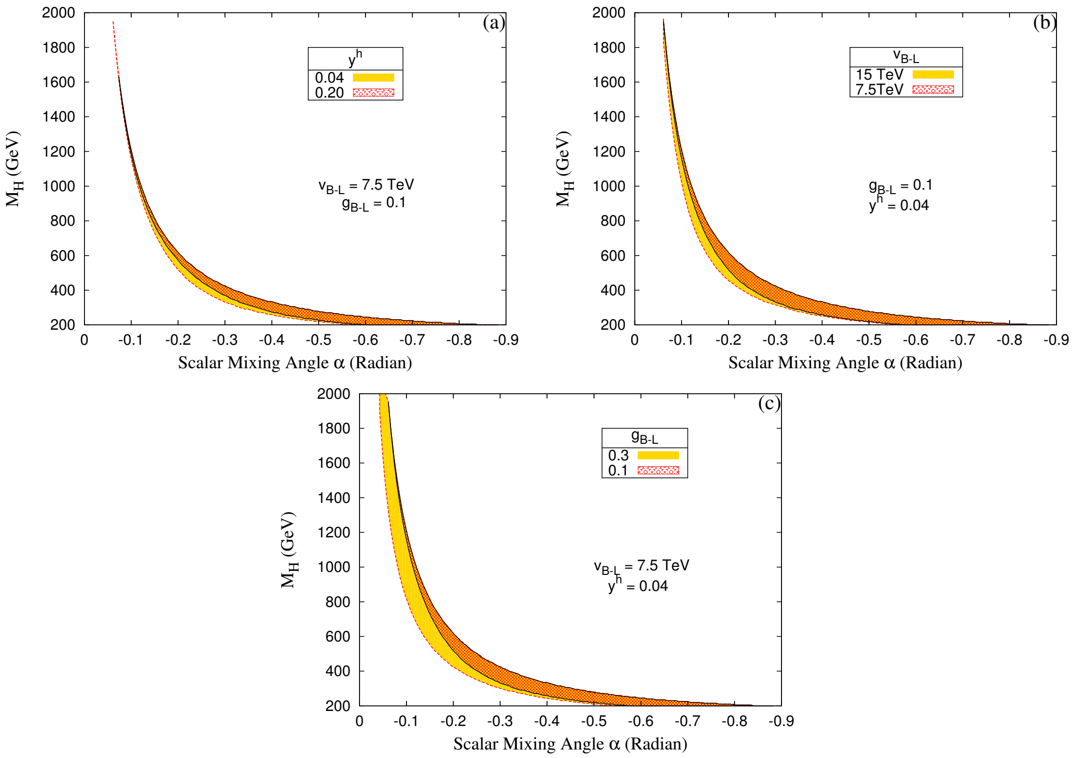

Figure 3.2: Allowed parameter space in $M_H - \alpha$ plane, with α varies between $[0, -\pi/2]$, consistent with vacuum stability, perturbativity bounds up to Planck scale. Figure (a): Majorana neutrino Yukawa coupling y^h is varied keeping $v_{_{B-L}}$ and $g_{_{B-L}}$ fixed. Figure (b): Two different set of $B-L$ breaking *vev*, $v_{_{B-L}}$ are chosen keeping $g_{_{B-L}}$ and y^h fixed. Figure (c): In this plot $g_{_{B-L}}$ varies where $v_{_{B-L}}$ and y^h are kept constant.

proportional to $v_{_{B-L}}$ at the EW scale (see Eq. 3.9). Thus for the same set of values of M_H and α, λ_3 is smaller for larger $v_{_{B-L}}$ at 15 TeV. The RGE of λ_3 is such that for our choice of parameters it grows with mass scale. Thus there is a possibility of generating large λ_3 such that vacuum stability and perturbativity conditions are not valid at some higher scale. This plot therefore shows that it is possible to have larger allowed parameter space for larger $v_{_{B-L}}$. Finally in Fig. 3.2(c), $g_{_{B-L}}$ varies where $v_{_{B-L}}$ and Y^h are kept constant. As the larger values of the gauge couplings affect the RGEs of the quartic couplings positively, the vacuum stability is improved. Thus with the larger value of gauge coupling the larger parameter space is allowed. But the $U(1)$ coupling increases with the mass scale. Hence the couplings with much larger values at low scale might be non-perturbative in the high scale. In our analysis, when $v_{_{B-L}}$ is at 7.5 TeV, any value of $g_{_{B-L}}$ more than 0.34 are disallowed as the coupling becomes non-perturbative before Planck scale.

3.5 High scale $B - L$ symmetry and vacuum stability

In the previous section we have shown that a TeV scale $B - L$ gauged symmetry can restore vacuum stability of the scalar potential. However, the $B - L$ breaking scale is not necessary to be in TeV scale and in principle high scale breaking of the symmetry is allowed. In this section we discuss about high scale breaking of $B - L$ symmetry and its implication towards vacuum stability.

Theoretical motivation for this model comes from the fact that it can yield high-scale inflation successfully [11, 44, 45]. The $B - L$ symmetry breaking scalar can accommodate the inflaton field. Also, couplings between the scalar of the $U(1)_{B-L}$ and the SM particles help to reheat the Universe at the end of the inflation.

As has been proposed in [46], presence of a heavy scalar, besides the SM particles, eventually leads to a threshold correction to the SM Higgs quartic coupling and helps to stabilize the electroweak vacuum as long as the mass of the heavy scalar lies below the instability scale of electroweak vacuum which is around 10^{10} GeV.

Threshold Correction

To show how the threshold correction due to the presence of a heavy scalar modifies the evolution of the Higgs quartic coupling λ_1 at a lower scale [46], let us consider the scalar potential after $U(1)_{B-L}$ symmetry breaking. At lower energy scales, when the heavy scalar S has reached its minimum, its equation of motion yields (using Euler-Lagrange equation)

$$S^\dagger S = \frac{1}{2} v_{B-L}^2 - \frac{\lambda_3}{2\lambda_2} \Phi^\dagger \Phi. \tag{3.20}$$

Below the mass scale of the heavy scalar, one can thus integrate out the heavy field S using the above equation of motion and the potential becomes

$$V(\Phi)|_{\text{eff}} = \left(\lambda_1 - \frac{\lambda_3^2}{4\lambda_2}\right)(\Phi^\dagger\Phi)^2 - m^2(\Phi^\dagger\Phi). \tag{3.21}$$

After that the dynamics of this theory is effectively governed by the SM particles where the SM scalar potential is written as

$$V(\Phi)|_{\text{SM}} \equiv \lambda_\Phi(\Phi^\dagger\Phi)^2 - m^2(\Phi^\dagger\Phi), \qquad \lambda_\Phi(m_s) = \left[\lambda_1 - \frac{\lambda_3^2}{4\lambda_2}\right]_{m_s}. \tag{3.22}$$

Here λ_Φ is the SM Higgs quartic coupling related to the electroweak symmetry breaking scale and the SM Higgs mass only. This shows that the matching condition (at the scale $Q = m_s$) of the Higgs quartic coupling gives a tree-level shift, $\delta_\lambda = \frac{\lambda_3^2}{4\lambda_2}$, as we go from λ_1 just above m_s to λ_Φ just below m_s.

This is a pure tree-level effect by which the heavy scalar of the extended theory affects the stability bound of the low energy effective theory even when these two theories are effectively decoupled. The Higgs quartic coupling λ_Φ of the low energy effective theory receives a positive shift at the mass scale of the inflaton which thus helps to avoid the instability which might have occurred above m_s scale.

Inflation in the $B-L$ model

In this model under consideration the real part $s(t, \mathbf{x})$ of the $U(1)_{B-L}$ breaking scalar field, S, apart from the *vev*, can be written as a background field $s_0(t)$ which plays the role of an inflaton and fluctuations $\delta s(t, \mathbf{x})$ which give rise to the primordial perturbations during inflation. Such a scenario has previously been considered in [45]. Before going into the details and particularities of our inflationary set up, we first briefly discuss what we know from the simplest single-field inflationary model in the light of recent BICEP2 as well as PLANCK observations. The amplitude of the two-point correlation function or the power spectrum of primordial scalar perturbations are measured through the two-point correlation of the temperature fluctuations in the CMBR. PLANCK has measured this value as [47]

$$\mathcal{P}_{\mathcal{R}} \sim 2.215 \times 10^{-9}. \tag{3.23}$$

The ratio of the tensor ($\mathcal{P}_T$) and the scalar ($\mathcal{P}_{\mathcal{R}}$) power spectrum is represented by

$$r = \frac{\mathcal{P}_T}{\mathcal{P}_{\mathcal{R}}}\,, \tag{3.24}$$

where r is conventionally called the tensor-to-scalar ratio. This ratio r has recently been measured by the BICEP2 experiment to be $0.20^{+0.07}_{-0.05}$ [48]. But after the release of PLANCK's recent dust data [49] the observation of BICEP2 has been put under serious scrutiny. Though for the time being, before PLANCK and BICEP2 combine their observations, the upper-limit on r set by PLANCK [49] still survives, i.e.,

$$r < 0.11 \quad (95\%\,\mathrm{CL}). \tag{3.25}$$

In single-field scenarios, the tensor power spectrum turns out to be a sole function of the Hubble parameter H during inflation,

$$\mathcal{P}_T = \frac{2}{\pi^2}\frac{H^2}{M_{\mathrm{Pl}}^2}, \tag{3.26}$$

where $M_{\mathrm{Pl}} \sim 2.4 \times 10^{18}$ GeV is the reduced Planck mass. As the Hubble parameter during inflation is related to the inflaton potential V_s by

$$H^2 = \frac{V_s}{3M_{\mathrm{Pl}}^2}, \tag{3.27}$$

knowing $\mathcal{P}_{\mathcal{R}}$ and r one can determine both the Hubble parameter during inflation

$$H \sim \sqrt{r} \times 10^{-4} M_{\mathrm{Pl}}, \tag{3.28}$$

and the scale of inflation $V_s^{1/4}$

$$V_s^{\frac{1}{4}} \sim \left(\frac{r}{0.01}\right)^{\frac{1}{4}} \times 10^{16}\,\mathrm{GeV}. \tag{3.29}$$

Furthermore, in a single-field model the scalar power spectrum turns out to be

$$\mathcal{P}_{\mathcal{R}} = \frac{H^2}{(2\pi)^2}\left(\frac{H^2}{\dot{s}_0^2}\right), \tag{3.30}$$

where the over-dot represents derivative with respect to cosmic time t and this yields the tensor-to-scalar ratio as

$$r = \frac{8}{M_{\mathrm{Pl}}^2}\left(\frac{\dot{s}_0}{H}\right)^2 = \frac{8}{M_{\mathrm{Pl}}^2}\left(\frac{ds_0}{dN}\right)^2, \tag{3.31}$$

where N is the number of e-foldings during inflation. This indicates that the excursion of the inflaton field during inflation would be

$$\frac{\Delta s_0}{M_{\mathrm{Pl}}} = \int_{N_{\mathrm{end}}}^{N_{\mathrm{CMB}}} dN \sqrt{\frac{r}{8}}\,, \tag{3.32}$$

where N_{end} and N_{CMB} are the number of e-foldings at the end of inflation and when the largest observable mode in the CMBR leave the horizon before inflation ends, respectively. Assuming that r would not change much during inflation, and $\Delta N \approx 65$ to solve the issues with Big Bang scenario, we have

$$\frac{\Delta s_0}{M_{\mathrm{Pl}}} = \sqrt{530 \times r}. \tag{3.33}$$

Hence, for $r \geq \mathcal{O}(10^{-2})$ the field excursion during inflation would be super-Planckian (large-field inflationary models), and for $r < \mathcal{O}(10^{-2})$ it would be sub-Planckian (small-field inflationary models).

In the present model the inflaton potential can be written as [45]

$$V(s_0) = \frac{1}{4}\lambda_2(s_0^2 - v_{B-L}^2)^2 + a\lambda_2 \log\left(\frac{s_0}{v_{B-L}}\right) s_0^4\,, \tag{3.34}$$

where we have

$$a \equiv \frac{1}{16\pi^2\lambda_2}\left(20\lambda_2^2 + 2\lambda_3^2 + 2\lambda_2\left(\sum_i (Y_i^{N_R})^2 - 24g_{B-L}^2\right) + 96g_{B-L}^4 - \sum_i (Y_i^{N_R})^4\right). \tag{3.35}$$

The above potential contains the radiative correction added to the tree-level one. Here $Y_i^{N_R}$ stand for the right handed neutrino Yukawa couplings. The value of 'a' determines whether the $U(1)_{B-L}$ symmetry is broken through the tree-level potential or the radiatively generated logarithmic term. As the value of 'a' mostly depends on the value of g_{B-L} and $Y_i^{N_R}$, it can either be positive or negative depending upon the values of the couplings at inflationary scale. At tree level one can then identify the mass term of the inflaton as

$$m_s = \sqrt{\lambda_2} v_{B-L}\,. \tag{3.36}$$

In large-field inflationary models one would naturally expect the quartic term with radiative corrections to dominate over the mass term in the inflaton potential and the form of the potential responsible for inflation would be

$$V_s(s_0) \approx \frac{1}{4}\lambda_2 s_0^4 + a\lambda_2 \log\left(\frac{s_0}{v_{B-L}}\right) s_0^4. \tag{3.37}$$

The flatness of the potential is determined by the slow-roll parameters

$$\epsilon_V = \frac{1}{2}M_{\rm Pl}^2\left(\frac{V_s'}{V_s}\right)^2, \quad \eta_V = M_{\rm Pl}^2\left(\frac{V_s''}{V_s}\right), \quad \xi_V^2 = M_{\rm Pl}^4\left(\frac{V_s'V_s'''}{V_s^2}\right), \tag{3.38}$$

where a prime denotes derivative with respect to the field s_0. These slow-roll parameters remain small ($\epsilon_V, \eta_V \ll 1$) during inflation till ϵ_V becomes ~ 1, which marks the end of inflation. In a single-field scenario the tensor-to-scalar ratio r and the scalar spectral index n_s (which is a measure of the tilt of the scalar power spectrum) are related to the slow-roll parameters by

$$r \approx 16\epsilon_V, \qquad n_s \approx 1 - 6\epsilon_V + 2\eta_V, \tag{3.39}$$

which are measured in CMBR observations. PLANCK measures the scalar spectral index as $n_s = 0.9603 \pm 0.0073$ [50]. The evolution of the scalar spectral index can also be determined in terms of the slow-roll parameters as:

$$\frac{dn_s}{d\ln k} \approx 16\epsilon_V\eta_V - 24\epsilon_V^2 - 2\xi_V^2. \tag{3.40}$$

If one assumes that the quartic self-interacting term without the radiative correction in the inflaton potential drives inflation, the tensor-to-scalar ratio and the scalar spectral index turn out to be

$$\begin{aligned} r &= \frac{128M_{\rm Pl}^2}{s_0^2}, \\ n_s &= 1 - \frac{24M_{\rm Pl}^2}{s_0^2}. \end{aligned} \tag{3.41}$$

The number of e-foldings can be computed as

$$N_k = \frac{1}{M_{\rm Pl}^2}\int_{s_{0_{\rm end}}}^{s_{0_k}} \frac{V_s ds_0}{V_s'}, \tag{3.42}$$

where s_{0_k} is the field value at the co-moving scale k and $s_{0_{\rm end}}$ is the field value at the end of inflation. This yields

$$N_{k_*} \approx \frac{s_{0_{k*}}^2}{8M_{\rm Pl}^2}, \tag{3.43}$$

where k_* denotes the pivot scale and it has been considered that $s_{0_{\rm end}} \ll s_{0_{k_*}}$. Hence, if the mode corresponding to the pivot scale would have left the horizon around 65 e-foldings before inflation ends, then the above expression helps to determine the field value during that time, which turns out to be $s_{0_{k_*}} \sim 23M_{\rm Pl}$. The tensor-to-scalar ratio and the scalar spectral index at scale k can be expressed in terms of the e-foldings as

$$\begin{aligned} r_k &= \frac{16}{N_k}, \\ n_{s_k} &= 1 - \frac{3}{N_k}. \end{aligned} \tag{3.44}$$

The number of e-folds when the pivot scale crosses the horizon during inflation can also be written as

$$N_* \simeq 65 + 2\ln\left(\frac{V_s(s_{0_*})^{1/4}}{10^{14}\,\mathrm{GeV}}\right) - \ln\left(\frac{T_f}{10^{10}\,\mathrm{GeV}}\right), \tag{3.45}$$

where T_f is the temperature at the end of inflation and can be considered as the reheating temperature T_{RH}. If the pivot scale set by PLANCK, i.e., $k_* = 0.002$ Mpc^{-1}, crosses the horizon during inflation when $N_* \sim 65$ then it generates large tensor-to-scalar ratio as $r_* \sim 0.25$ which is also large enough even for BICEP2 observations. This corresponds to the field excursion during inflation to be $\Delta s \sim 12\, M_{\mathrm{Pl}}$. Hence, our aim would be to generate lower values of r while keeping the scenario consistent with the observations of n_s and $\mathcal{P}_{\mathcal{R}}$ by PLANCK. It has been pointed out in [51] that the radiative corrections to the quartic potential play an important role to lower the tensor-to-scalar ratio. Hence, for our inflationary scenario we consider the inflaton potential including radiative correction for inflation. When inflation is driven by this quartic potential, we find

$$\begin{aligned}
V_s &= \frac{1}{4}\lambda_2 s_0^4\left[1 + 4a\ln\left(\frac{s_0}{v_s}\right)\right], \\
V_s' &= \lambda_2 s_0^3\left[1 + a + 4a\ln\left(\frac{s_0}{v_s}\right)\right], \\
V_s'' &= 3\lambda_2 s_0^2\left[1 + \frac{7}{3}a + 4a\ln\left(\frac{s_0}{v_s}\right)\right], \\
V_s''' &= 6\lambda_2 s_0\left[1 + \frac{13}{3}a + 4a\ln\left(\frac{s_0}{v_s}\right)\right].
\end{aligned} \tag{3.46}$$

These give the slow-roll parameters as

$$\epsilon_V = \frac{8M_{\mathrm{Pl}}^2}{s_0^2}\left[\frac{u^2}{(u-1)^2}\right], \quad \eta_V = \frac{12M_{\mathrm{Pl}}^2}{s_0^2}\left[\frac{u+4/3}{u-1}\right], \quad \xi_V^2 = \frac{96M_{\mathrm{Pl}}^4}{s_0^4}\left[\frac{u(u+10/3)}{(u-1)^2}\right], \tag{3.47}$$

where we have defined $u = (1 + a + 4a\ln s_0/v_{B-L})/a$. Hence, the tensor-to-scalar ratio, the scalar spectral index and the running of the scalar spectral index can be written as:

$$\begin{aligned} r &= \frac{128M_{\rm Pl}^2}{s_0^2}\frac{u^2}{(u-1)^2}, \\ n_s &= 1-\frac{8M_{\rm Pl}^2}{s_0^2}\frac{3u^2-u+4}{(u-1)^2}, \\ \frac{dn_s}{d\ln k} &= -\frac{64M_{\rm Pl}^4}{s_0^4}\left[\frac{u(3u^3-4u^2+15u+10)}{(u-1)^4}\right], \end{aligned} \tag{3.48}$$

respectively. If we consider the radiative correction to the scalar potential, as given in Eq. (3.46), to be negligible (which implies $a \to 0$, i.e., $u \to \infty$), the standard expressions for r and n_s for quartic coupling can be recovered. Furthermore, the scalar power spectrum given in Eq. (3.30), can be represented as

$$\mathcal{P}_{\mathcal{R}} = \frac{1}{24\pi^2\epsilon_V}\left(\frac{V_s}{M_{\rm Pl}^4}\right) = \frac{1}{12\pi^2M_{\rm Pl}^6}\left(\frac{V_s^3}{V_s'^2}\right), \tag{3.49}$$

where we have used the Hubble slow-roll parameter $\epsilon = \frac{1}{2M_{\rm Pl}^2}\frac{\dot{s}_0^2}{H^2}$ and the Friedmann equation during inflation given in Eq. (3.27) with $\epsilon \approx \epsilon_V$. The power spectrum for the inflaton potential including radiative correction turns out to be

$$\mathcal{P}_{\mathcal{R}} = \frac{\lambda_2}{768\pi^2}\left(\frac{s_0}{M_{\rm Pl}}\right)^6\frac{a(u-1)^3}{u^2}. \tag{3.50}$$

Now, this scenario can be realized in two cases. In the limit $u \gg 1$, one can have $|a| \ll 1$, then the radiative corrections become negligible. In such a case the standard results for ϕ^4 potential should be retrieved. The other branch known as hilltop solution is important when $u \approx 1$ leading to $a \sim -\left(4\ln(s_0/v_{B-L})\right)^{-1}$.

We also require to determine the reheat temperature in order to compute the number of e-foldings which corresponds to the pivot scale as given in Eq. (3.45). We notice that, apart from the self-interaction term, the inflaton field is also coupled to the SM Higgs field via the mixing term λ_3 which allows it to decay into a pair of SM Higgs during inflation. The decay rate of such an interaction is given as [45]:

$$\Gamma_S(s_0 \to SS) = \frac{\lambda_3^2 v_{B-L}^2}{32\pi m_s}. \tag{3.51}$$

This decay of inflaton field into SM Higgs would make inflaton unstable for larger values of λ_3. Thus one requires to restrain the decay width of the inflaton during inflation. This requirement can be met if one demands that $\Gamma_S < m_s$ which yields

$$\lambda_3 < \sqrt{32\pi\lambda_2}. \tag{3.52}$$

From Eq. (3.51) we can also roughly estimate the order of reheating temperature $T_{\rm RH}$ if the reheating phase is dominated by the Higgs decay. If during the reheating phase the inflaton and its decay products are just in equilibrium then $\Gamma_S \sim H$ where H is the Hubble parameter during the radiation dominated reheating phase. This condition yields

$$\frac{\lambda_3^2 v_{B-L}^2}{32\pi m_s} = \sqrt{\frac{\pi^2}{90}g_*}\,\frac{T_{\rm RH}^2}{M_{\rm Pl}}, \tag{3.53}$$

where $g_* \sim 100$.

Now, let us determine the parameters for a large-field inflationary scenario and take $s_{0_{k_*}} \sim 23 M_{\rm Pl}$. Putting the central value of scalar spectral index as $n_s = 0.9603$, we find two solutions (u_*) for u at the pivot scale: -0.333 and -11.001. The first solution indicates a hilltop branch inflation, whereas the second one gives rise to a ϕ^4-branch inflation. Let us now analyze the parameters for these two scenarios :

- **Hilltop inflation :** If one sets the *vev* that breaks $U(1)_{B-L}$, i.e., the scale of inflation as 10^{16} GeV, then for $u_* = -0.333$ one finds $a_* \sim -0.028$. This indicates the field value at the end of inflation would be $s_{0_{\rm end}} \sim 0.71\,M_{\rm Pl}$ when $\epsilon_V \approx 1$. This value of u_* yields the tensor-to-scalar ratio as $r_* = 0.015$ and the inflaton quartic coupling, from the observation of the scalar power amplitude by PLANCK, as $\lambda_2 \sim 1.89\times10^{-13}$. This yields the tree-level mass of the inflaton as $m_s \sim 4.3\times10^9$ GeV. The evolution of the spectral index in such a scenario would be $\frac{dn_s}{d\ln k}|_{k_*} \sim 1.07\times10^{-4}$. In this scenario the inflaton-Higgs coupling can be of the order of 10^{-6}, which yields the reheating temperature as $T_{\rm RH} \sim 1.29 \times 10^{13}$ GeV. This reheating temperature and the energy-scale of inflation yield the e-folding at which pivot scale would have exited the horizon as $N_* \sim 67$.

- ϕ^4**−branch inflation :** If one sets the scale of inflation to be 10^{16} GeV like the hilltop case, one gets $a_* \sim -0.022$ for $u_* = -11.001$. This indicates that the field value at the end of inflation, when $\epsilon_V \approx 1$, would be $s_{0_{\rm end}} \sim 2.6\, M_{\rm Pl}$. This u_* yields the tensor-to-scalar ratio as $r_* = 0.203$ and the inflaton quartic coupling, from the observation of the scalar power amplitude, as $\lambda_2 \sim 3.6 \times 10^{-13}$. This provides the tree-level mass of the inflaton as $m_s \sim 6.0 \times 10^9$ GeV. The running of the spectral index in such a scenario would be $\frac{dn_s}{d\ln k}|_{k_*} \sim -5.6 \times 10^{-4}$. In this scenario the inflaton-Higgs coupling can be of the order of 10^{-6}, which yields the reheating temperature as $T_{\rm RH} \sim 1.09 \times 10^{13}$ GeV. This reheating temperature and the energy-scale of inflation generate the e-folding at which pivot scale would have left the horizon as $N_* \sim 67$.

Vacuum Stability

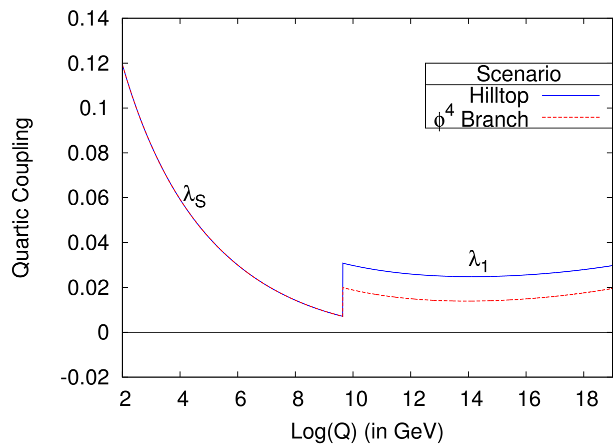

Figure 3.3: This plot shows the running of the SM quartic coupling as a function of energy scale. The discrete jump at scale very near to $\sim 10^{10}$ GeV is because of the presence of the inflaton having mass $\sim 10^{10}$ GeV.

In the previous subsection, we have shown that to achieve successful inflation the inflaton quartic coupling have to be fine tuned. Fine-tuning of inflaton quartic coupling evidently brings down the mass scale of the inflaton field which turns out to be below the instability scale of the electroweak vacuum. Following [46], one can integrate out the heavy inflaton field below its mass scale which then adds a tree-level threshold correction to the low energy effective Higgs quartic coupling λ_Φ given by

$$\lambda_1 = \lambda_\Phi + \frac{\lambda_3^2}{4\lambda_2}.$$

Hence, below the inflaton mass scale the stability condition ($\lambda_\Phi > 0$) for the SM Higgs quartic coupling would get shifted upwards $\lambda_1 > \delta\lambda \equiv \frac{\lambda_3^2}{4\lambda_2}$. The other two quartic couplings λ_2 and λ_3 would start evolving at energies above this mass scale. The relevant RGEs are written in appendix A.2. To illustrate the threshold effect, the running of Higgs quartic coupling has been shown in Fig. 3.3. Here we have taken the heavy scalar mass $m_s = 8\times 10^8$ GeV before which λ_Φ runs according to SM β-functions. Beyond that point new loop effects due to the extended theory start to affect its running and the discrete jump in the Higgs quartic coupling at m_s is due to the threshold effect.

Apart from the SM fermions this model also contains three right handed neutrinos, ν_{R_i}, which appear in the Lagrangian as in Eq. 3.15. The second term in the above Lagrangian gives rise to the coupling of the inflaton to heavy right handed neutrinos and also masses for ν_R. It is important to note that when the $(B-L)$ symmetry is broken at the TeV scale the masses of the right handed neutrinos are less compared to the present scenario. In the case of TeV scale breaking the Yukawa couplings (Y^{ν_L}) giving rise to the Dirac mass of light neutrinos have to be vanishingly small unless some special textures are considered. Thus in such cases, impact of Y^{ν_L} in the evolutions of the quartic and other necessary couplings is negligible. But in the present case the right handed neutrino masses are very heavy $\sim 10^{11-13}$ GeV, due to high $U(1)_{B-L}$ breaking scale. Thus the light neutrino masses are still light $\sim \mathcal{O}(\text{eV})$ even with $Y^{\nu_L} \sim \mathcal{O}(1)$. Hence unlike the cases where $U(1)_{B-L}$ symmetry is broken at TeV scale, one cannot ignore the contributions of light neutrino Yukawa couplings Y^{ν_L} in the RGEs in our scenario (see appendix A.2).

Looking at the threshold correction, which is essential for electroweak vacuum stability, it may seem that $\lambda_3 < 0$ can still be retained as a possible condition.

But in our analysis this opportunity of achieving a larger parameter space for λ_3 is restricted as here λ_2 is very small $\sim 10^{-14}$ due to inflationary constraints. The absolute value of λ_3 can never be too large as it affects the running of λ_2 by driving its value to a much larger value which might not be able to explain inflationary dynamics. Thus λ_3 is constrained from above by the requirement of inflation. The smallness of $|\lambda_3|$ ensures that the two scalars present in the theory are basically decoupled from each other as the mixing angle between then becomes too small.

3.6 Conclusion

We analyzed the structure of the scalar potentials of SM$\otimes U(1)_{B-L}$ model. We found that the addition of new scalars help to stabilize the scalar potential. Using one-loop RGEs we constrained the parameter space of this model. Effect of different parameters like new gauge coupling g_{B-L}, RH neutrino Yukawa and $B - L$ breaking *vev* have been discussed.

Another scenario of SM$\otimes U(1)_{B-L}$ has been discussed where the $B - L$ gauge symmetry is broken at very high scale beyond the SM instability scale. In this case the presence of a heavy scalar yields a threshold correction to the Higgs quartic coupling, if one integrates out this heavy scalar below its mass scale. Hence if the mass of this heavy scalar lies below the electroweak instability scale ($\sim 10^{10}$ GeV), the threshold correction eventually helps avoid the instability of the vacuum by correctly uplifting the value of the SM Higgs quartic coupling at this mass scale.

In summary, it is meaningful to mention that more precise knowledge of the SM parameters, like Higgs mass, top quark mass and strong coupling will constrain the parameters (couplings, masses, scales) of new physics and that might direct us towards the correct theory for beyond standard model physics.

Chapter 4

Left-Right Symmetric Model

The Standard Model of particle physics does not treat left-handed and right-handed particles in the same way. The left handed quarks and leptons transform as doublets under the $SU(2)_L$ gauge group, whereas the right-handed fields are singlets under the same gauge group. This is due to the chiral structure of the weak interaction. On the other hand SM cannot explain non-conservation of Parity in weak interaction which was first observed by Madame Wu in beta decay of ^{60}Co [52].

Left-Right symmetric model (LRSM) unravel the aforementioned issues of the SM. In addition, there are several features which appear naturally in LRSM but remained unexplained in the SM. Some of these are:

- Generation of tiny non zero neutrino masses via seesaw mechanism.
- Physical interpretation of the hypercharge quantum number (Y) in terms of Baryon number (B) and Lepton number (L).
- Possibility to realize gauge coupling unification in the non-supersymmetric GUTs where LRSMs appear as low energy effective theories [16]

The matter field contents now are symmetric and represented as left and right handed doublets. For *quarks* we have

$$Q_{iL} = \begin{pmatrix} u'_i \\ d'_i \end{pmatrix}_L : (3,2,1,1/3) \qquad Q_{iR} = \begin{pmatrix} u'_i \\ d'_i \end{pmatrix}_R : (3,1,2,1/3),$$

and for *leptons*

$$L_{iL} = \begin{pmatrix} \nu'_i \\ \ell'_i \end{pmatrix}_L : (1,2,1,-1) \qquad L_{iR} = \begin{pmatrix} \nu'_i \\ \ell'_i \end{pmatrix}_R : (1,1,2,-1). \tag{4.1}$$

The first three integers in the parentheses are dimensions of $SU(3)_C, SU(2)_L$ and $SU(2)_R$ representations respectively, while the fourth number characterizes the $B-L$ quantum number. The primes are used to remind that these are not mass eigenstates but gauge eigenstates.

We will now briefly discuss the scalar sector and spontaneous symmetry breaking in LRSM. After that we will explore the gauge sector and the fermion sector of this model.

4.1 Spontaneous Symmetry Breaking Pattern

The full LR symmetric gauge group is

$$SU(3)_C \otimes SU(2)_L \otimes SU(2)_R \otimes U(1)_{B-L}. \tag{4.2}$$

Symmetry breaking occurs in two steps which can be schematically illustrated in the following manner:

$$\begin{array}{c} SU(2)_L \otimes \underbrace{SU(2)_R \otimes U(1)_{B-L}} \\ \Big\downarrow \langle\Delta_R\rangle \text{ or } \langle H_R\rangle \\ \underbrace{SU(2)_L \otimes U(1)_Y} \\ \Big\downarrow \langle\Phi\rangle \text{ and } \langle\Delta_L\rangle \text{ or } \langle H_L\rangle \\ U(1)_{EM}. \end{array} \tag{4.3}$$

The $SU(2)_R \otimes U(1)_{B-L}$ is broken to $U(1)_Y$ at a scale higher than the EW symmetry breaking one. Thus the hypercharge generator is a linear combination of $SU(2)_R$ and $U(1)_{B-L}$ generators. In this model, the hypercharge Y can be reconstructed from the $SU(2)_R$ and $U(1)_{B-L}$ quantum numbers as

$$Y = T_{3R} + \frac{B-L}{2}, \tag{4.4}$$

T_{3R} being the third component of the $SU(2)_R$ isospin. This explains the electric charges of particles, which is given by

$$Q_{EM} = T_{3L} + Y. \tag{4.5}$$

Note that the electromagnetic charge consists of physical quantum numbers like baryon number and lepton number along with eigenvalues of the generators of $SU(2)_{L/R}$ gauge groups.

The LR symmetric gauge group $SU(2)_L \otimes SU(2)_R \otimes U(1)_{B-L}$ is broken down to SM gauge group $SU(2)_L \otimes U(1)_Y$ when the neutral component of an $SU(2)_R$ doublet scalar H_R or $SU(2)_R$ triplet scalar Δ_R acquires a vacuum expectation value. This leads to two variants of Minimal Left-Right Symmetric Models (MLRSMs):

- Scalar sector consists of a bi-doublet (Φ), one left-handed triplet (Δ_L), and one right-handed triplet (Δ_R) [12–15].
- Scalar sector consists of a bi-doublet (Φ), one left-handed doublet (H_L), and one right-handed doublet (H_R) [53–55].

4.1.1 LR Model with Triplet Scalars (LRT)

In this case triplet scalars are present in the theory. The explicit structures of the scalars can be presented in the form

$$\Phi = \begin{pmatrix} \phi_1^0 & \phi_1^+ \\ \\ \phi_2^- & \phi_2^0 \end{pmatrix} \quad , \quad \Delta_{L,R} = \begin{pmatrix} \delta_{L,R}^+/\sqrt{2} & \delta_{L,R}^{++} \\ \\ \delta_{L,R}^0 & -\delta_{L,R}^+/\sqrt{2} \end{pmatrix}.$$

These fields transform under the $SU(2)_L \otimes SU(2)_R \otimes U(1)_{B-L}$ gauge group in the following manner:

$$\Phi \equiv (2,2,0), \qquad \Delta_R \equiv (1,3,2), \qquad \Delta_L \equiv (3,1,2). \tag{4.6}$$

Once neutral components of these scalars acquire vacuum expectation values, they can be written in the form,

$$\langle\Phi\rangle = \begin{pmatrix} v_1 & 0 \\ 0 & v_2 e^{i\theta} \end{pmatrix}, \qquad \langle\Delta_L\rangle = \begin{pmatrix} 0 & 0 \\ v_L & 0 \end{pmatrix}, \qquad \langle\Delta_R\rangle = \begin{pmatrix} 0 & 0 \\ v_R & 0 \end{pmatrix}. \tag{4.7}$$

For simplicity we will choose $v_2 = 0$ without loss of generality hereafter. With these structures of the vacuum expectation values, symmetry breaking occurs in two stages.

The most general form of LRT scalar potential is discussed extensively in [56–58] and for our analysis we use the form given in [58], which reads as,

$$\begin{aligned}
V_{LRT}(\Phi,&\Delta_L,\Delta_R) = \\
&-\mu_1^2\Big\{\mathrm{Tr}\big[\Phi^\dagger\Phi\big]\Big\} - \mu_2^2\Big\{\mathrm{Tr}\big[\tilde{\Phi}\Phi^\dagger\big] + \mathrm{Tr}\big[\tilde{\Phi}^\dagger\Phi\big]\Big\} - \mu_3^2\Big\{\mathrm{Tr}\big[\Delta_L^\dagger\Delta_L\big] + \mathrm{Tr}\big[\Delta_R^\dagger\Delta_R\big]\Big\} \\
&+\lambda_1\Big\{\Big(\mathrm{Tr}\big[\Phi^\dagger\Phi\big]\Big)^2\Big\} + \lambda_2\Big\{\Big(\mathrm{Tr}\big[\tilde{\Phi}\Phi^\dagger\big]\Big)^2 + \Big(\mathrm{Tr}\big[\tilde{\Phi}^\dagger\Phi\big]\Big)^2\Big\} + \lambda_3\Big\{\mathrm{Tr}\big[\tilde{\Phi}\Phi^\dagger\big]\mathrm{Tr}\big[\tilde{\Phi}^\dagger\Phi\big]\Big\} \\
&+\lambda_4\Big\{\mathrm{Tr}\big[\Phi^\dagger\Phi\big]\Big(\mathrm{Tr}\big[\tilde{\Phi}\Phi^\dagger\big] + \mathrm{Tr}\big[\tilde{\Phi}^\dagger\Phi\big]\Big)\Big\} + \lambda_5\Big\{\Big(\mathrm{Tr}\big[\Delta_L\Delta_L^\dagger\big]\Big)^2 + \Big(\Delta_R\Delta_R^\dagger\Big)^2\Big\} \\
&+\lambda_6\Big\{\mathrm{Tr}\big[\Delta_L\Delta_L\big]\ \mathrm{Tr}\big[\Delta_L^\dagger\Delta_L^\dagger\big] + \mathrm{Tr}\big[\Delta_R\Delta_R\big]\ \mathrm{Tr}\big[\Delta_R^\dagger\Delta_R^\dagger\big]\Big\} + \lambda_7\Big\{\mathrm{Tr}\big[\Delta_L\Delta_L^\dagger\big]\ \mathrm{Tr}\big[\Delta_R\Delta_R^\dagger\big]\Big\} \\
&+\lambda_8[\Delta_L\Delta_L^\dagger]\Big\{\mathrm{Tr}\big[\Delta_L\Delta_L^\dagger\big]\ \mathrm{Tr}\big[\Delta_R\Delta_R^\dagger\big]\Big\} + \lambda_9\Big\{\mathrm{Tr}\big[\Phi^\dagger\Phi\big]\Big(\mathrm{Tr}\big[\Delta_L\Delta_L^\dagger\big] + \mathrm{Tr}\big[\Delta_R\Delta_R^\dagger\big]\Big)\Big\} \\
&+(\lambda_{10} + i\,\lambda_{11})\Big\{\mathrm{Tr}\big[\Phi\tilde{\Phi}^\dagger\big]\mathrm{Tr}\big[\Delta_R\Delta_R^\dagger\big] + \mathrm{Tr}\big[\Phi^\dagger\tilde{\Phi}\big]\mathrm{Tr}\big[\Delta_L\Delta_L^\dagger\big]\Big\} \\
&+(\lambda_{10} - i\,\lambda_{11})\Big\{\mathrm{Tr}\big[\Phi^\dagger\tilde{\Phi}\big]\mathrm{Tr}\big[\Delta_R\Delta_R^\dagger\big] + \mathrm{Tr}\big[\tilde{\Phi}^\dagger\Phi\big]\mathrm{Tr}\big[\Delta_L\Delta_L^\dagger\big]\Big\} \\
&+\lambda_{12}\Big\{\mathrm{Tr}\big[\Phi\Phi^\dagger\Delta_L\Delta_L^\dagger\big] + \mathrm{Tr}\big[\Phi^\dagger\Phi\Delta_R\Delta_R^\dagger\big]\Big\} + \lambda_{13}\Big\{\mathrm{Tr}\big[\Phi\Delta_R\Phi^\dagger\Delta_L^\dagger\big] + \mathrm{Tr}\big[\Phi^\dagger\Delta_L\Phi\Delta_R^\dagger\big]\Big\} \\
&+\lambda_{14}\Big\{\mathrm{Tr}\big[\tilde{\Phi}\Delta_R\Phi^\dagger\Delta_L^\dagger\big] + \mathrm{Tr}\big[\tilde{\Phi}^\dagger\Delta_L\Phi\Delta_R^\dagger\big]\Big\} + \lambda_{15}\Big\{\mathrm{Tr}\big[\Phi\Delta_R\tilde{\Phi}^\dagger\Delta_L^\dagger\big] + \mathrm{Tr}\big[\Phi^\dagger\Delta_L\tilde{\Phi}\Delta_R^\dagger\big]\Big\},
\end{aligned} \tag{4.8}$$

where all the coupling constants are real.

The symmetry group $SU(2)_L \otimes SU(2)_R \otimes U(1)_{B-L}$ breaks down to $SU(2)_L \otimes U(1)_Y$ by v_R at high scale. Subsequently, the vacuum expectation value v_1 of the bi-doublet breaks $SU(2)_L \otimes U(1)_Y$ to $U(1)_{EM}$. So the total number of Goldstone bosons are six. Now the Higgs sector has twenty degrees of freedom (eight real field for the bi-doublet and six each for the triplet fields). Hence, the remaining fourteen fields will be physical scalars and they are

1. Two doubly charged scalars $(H_1^{\pm\pm}, H_2^{\pm\pm})$,
2. Two singly charged scalars $(H_1^{\pm}, H_2^{\pm})$,
3. Four neutral CP-even scalars $(H_0^0,\ H_1^0,\ H_2^0,\ H_3^0\ )$,
4. Two neutral CP-odd pseudo scalars $(A_0^0,\ A_1^0\ )$.

We have already mentioned that the scale v_R is much higher than that of the electro-weak breaking *vev* v_1. The scalar masses can be expressed in leading order* [59, 60]

$$\begin{aligned} M^2_{H_0^0} &\simeq 2\,\lambda_1\,v_1^2, \\ M^2_{H_1^0} &\simeq \frac{1}{2}\lambda_{12}\,v_R^2, \\ M^2_{H_2^0} \simeq M^2_{A_1^0} \simeq M^2_{H_2^\pm} &\simeq 2\,\lambda_5\,v_R^2, \\ M^2_{H_3^0} \simeq M^2_{A_2^0} \simeq M^2_{H_1^\pm} \simeq M^2_{H_1^{\pm\pm}} &\simeq \frac{1}{2}(\lambda_7 - 2\lambda_5)\,v_R^2, \\ M^2_{H_2^{\pm\pm}} &\simeq 2\,\lambda_6\,v_R^2. \end{aligned} \tag{4.9}$$

$M_{H_0^0}$ is the Standard Model Higgs boson and will be denoted by M_h from here onwards. It is important to note that the remaining quartic couplings only contribute to the scalar masses as sub-leading terms and proportional to the v_1^2 at the EWSB scale. Hence, $\lambda_2, \lambda_3, \lambda_4, \lambda_8, \lambda_9, \lambda_{10}, \lambda_{11}$ induce only the relative mass splittings among these heavy scalars which are almost phenomenologically inaccessible at present experiments.

*These leading order terms match exactly with the masses of the heavy scalars at scale v_R, i.e., before electro-weak symmetry breaking (EWSB). After the EWSB, some correction terms are generated which are proportional to v_1^2. But as $v_R \gg v_1$, the splitting among the masses of these heavy scalars are negligible compared to their relative masses. It is important to note that this '$\simeq$' will be replaced by '$=$' in Eq. 4.9 when these masses are given at v_R scale.

4.1.2 LR Model with Doublet Scalars (LRD)

In this case the scalar sector consists of a bi-doublet (Φ), one left-handed doublet (H_L), and one right-handed doublet (H_R). The $SU(2)_L \otimes SU(2)_R \otimes U(1)_{B-L}$ quantum numbers of these fields can be written as

$$\Phi \equiv (2,2,0), \qquad H_L \equiv (2,1,1), \qquad \text{and,} \quad H_R \equiv (1,2,1), \tag{4.10}$$

and the structure of $H_{L/R}$ can be written as

$$H_{L/R} = \begin{pmatrix} h^0_{L/R} \\ \\ h^+_{L/R} \end{pmatrix}. \tag{4.11}$$

The neutral components of Φ and $H_{L/R}$ acquire the vacuum expectation values:

$$\langle\Phi\rangle = \begin{pmatrix} v_1 & 0 \\ 0 & v_2 e^{i\theta} \end{pmatrix}, \qquad \langle H_L\rangle = \begin{pmatrix} 0 \\ v_L \end{pmatrix}, \qquad \langle H_R\rangle = \begin{pmatrix} 0 \\ v_R \end{pmatrix}. \tag{4.12}$$

As before, we put $v_2 = 0$. The scalar sector consists of sixteen real scalar fields out of which six are Goldstone bosons. Finally we have four CP-even scalars, two CP-odd scalars and two charged scalars. Among the CP-even scalars one is the Standard Model Higgs boson with mass M_h and the other three are taken as degenerate heavy scalars having mass M_H. The parameters in the Higgs potential can be recast in terms of the masses of the neutral and charged scalars. Details about the scalar sector have been discussed in [61].

The scalar potential for the LR model with doublet scalars can be written as

$$\begin{aligned} V_{LRD}(\Phi, H_L, H_R) \;=\;& 4\lambda_1\Big(\mathrm{Tr}[\Phi^\dagger\Phi]\Big)^2 + 4\lambda_2\Big(\mathrm{Tr}[\Phi^\dagger\tilde{\Phi}] + \mathrm{Tr}[\Phi\tilde{\Phi}^\dagger]\Big)^2 + \\ & 4\lambda_3\Big(\mathrm{Tr}[\Phi^\dagger\tilde{\Phi}] - \mathrm{Tr}[\Phi\tilde{\Phi}^\dagger]\Big)^2 \\ & + \frac{\kappa_1}{2}\Big(H_L^\dagger H_L + H_R^\dagger H_R\Big)^2 + \frac{\kappa_2}{2}\Big(H_L^\dagger H_L - H_R^\dagger H_R\Big)^2 \\ & + \beta_1\Big(\mathrm{Tr}[\Phi^\dagger\tilde{\Phi}] + \mathrm{Tr}[\Phi\tilde{\Phi}^\dagger]\Big)\Big(H_L^\dagger H_L + H_R^\dagger H_R\Big) \\ & + f_1\Big(H_L^\dagger(\tilde{\Phi}\tilde{\Phi}^\dagger - \Phi\Phi^\dagger)H_L - H_R^\dagger(\Phi^\dagger\Phi - \tilde{\Phi}^\dagger\tilde{\Phi})H_R\Big). \end{aligned}$$

In the limit $v_R \gg v_1$ and assuming that all the heavy scalars are degenerate, we have

$$f_1 = (M_H/v_R)^2 = \kappa_1 = -\kappa_2, \tag{4.13}$$

whereas, minimization of the potential requires:

$$\frac{v_1^2}{v_R^2} = \frac{f_1 - 2\beta_1}{4\lambda_1}.$$

4.2 Gauge Sector

4.2.1 LR Model with Triplet Scalars

The kinetic energy term of the scalar part of LRSM with triplet scalars can be written as

$$\mathcal{L}_{kin} = \mathrm{Tr}\Big[(D_\mu\Phi)^\dagger(D^\mu\Phi)\Big] + \mathrm{Tr}\Big[(D_\mu\Delta_L)^\dagger(D^\mu\Delta_L)\Big] + \mathrm{Tr}\Big[(D_\mu\Delta_R)^\dagger(D^\mu\Delta_R)\Big], \tag{4.14}$$

where

$$\begin{aligned} D_\mu\Phi &= \Big(\partial_\mu + ig_{2L}T^aW^a_{L\mu} + ig_{2R}T^aW^a_{R\mu}\Big)\Phi, \\ D_\mu\Delta_{(L/R)} &= \partial_\mu\Delta_{(L/R)} - ig_{(2L/2R)}\Big[T^aW^a_{(L/R)\mu}, \Delta_{(L/R)}\Big] - ig_{B-L}\mathbb{I}\,B_\mu\Delta_{(L/R)}. \end{aligned} \tag{4.15}$$

After spontaneous symmetry breaking the charged W boson mass terms can be written,

$$\mathcal{L}_{charged} = \begin{pmatrix} W_L^{+\mu} & W_R^{+\mu} \end{pmatrix} (\mathcal{M}^\pm)^2 \begin{pmatrix} W^-_{L\mu} \\ W^-_{R\mu} \end{pmatrix} + h.c \tag{4.16}$$

where $\mathcal{M}^\pm$ is the charged gauge boson mass matrix

$$(\mathcal{M}^\pm)^2 = \frac{1}{4}g^2 \begin{pmatrix} v_1^2 & 0 \\ 0 & v_1^2 + 2v_R^2 \end{pmatrix} \qquad \text{(here } g_{2L} = g_{2R} \equiv g\text{)}. \tag{4.17}$$

Note that since we have taken $v_2 = 0$ there is no mixing between left and right charged W bosons and $W_{L\mu}$ is the SM charged gauge boson.

The neutral part of the Lagrangian is

$$\mathcal{L}_{neutral} = \begin{pmatrix} W_L^{3\mu} & W_R^{3\mu} & B^\mu \end{pmatrix} \frac{1}{2}(\mathcal{M}^0)^2 \begin{pmatrix} W_{L\mu}^3 \\ W_{R\mu}^3 \\ B_\mu \end{pmatrix}, \tag{4.18}$$

with

$$\frac{1}{2}(\mathcal{M}^0)^2 = \begin{pmatrix} g^2 v_1^2 & -g^2 v_1^2 & 0 \\ -g^2 v_1^2 & g^2(v_1^2 + 4v_R^2) & -4g g_{\text{B-L}} v_R^2 \\ 0 & -4g g_{\text{B-L}} v_R^2 & 4g_{\text{B-L}}^2 v_R^2 \end{pmatrix}. \tag{4.19}$$

Diagonalization of this mass matrix yields two massive neutral gauge bosons, Z_1^μ and Z_2^μ, and one neutral boson A^μ. The lighter vector boson Z_1 is identified as the SM Z boson.

4.2.2 LR Model with Doublet Scalars

The gauge sector for the LR model with doublet scalar is very similar to that of the LR model with triplet scalars. The kinetic term of scalar part can be written as

$$\mathcal{L}_{kin} = \text{Tr}\Big[(D_\mu \Phi)^\dagger (D^\mu \Phi)\Big] + (D_\mu H_L)^\dagger (D^\mu H_L) + (D_\mu H_R)^\dagger (D^\mu H_R), \tag{4.20}$$

where

$$D_\mu \Phi = \Big(\partial_\mu + i g_{2L} T^a W_{L\mu}^a + i g_{2R} T^a W_{R\mu}^a\Big)\Phi \tag{4.21}$$

$$D_\mu H_{(L/R)} = \partial_\mu H_{(L/R)} - i g_{(2L/2R)}\Big[T^a W_{(L/R)\mu}^a, H_{(L/R)}\Big] - i g_{B-L} \mathbb{I}\, B_\mu H_{(L/R)} \tag{4.22}$$

After symmetry breaking the mass eigenvalues appear to be the same as in the LR model with triplet scalars and we do not write them explicitly here.

4.3 Yukawa sector

Unlike the gauge sector, the Yukawa sector of LRSM depends on the structure of the scalar sector. Here we will discuss the Yukawa sector separately for LRSM with triplet scalars and with doublet scalars.

4.3.1 LRSM with triplet scalars

Under the gauge group $SU(2)_L \otimes SU(2)_R$ quarks and leptons are doublets, as written in Eq. 4.1. The most general lepton Yukawa Lagrangian can be written as

$$-\mathcal{L}_Y = \Big[\overline{L_L}\Big((y^l)\Phi + (\tilde{y}^l)\tilde{\Phi}\Big)L_R + h.c\Big] + \overline{L_R^c}\Sigma_L(y^h)\,L_L + \overline{L_L^c}\Sigma_R(y^h)\,L_R, \quad (4.23)$$

here $\tilde{\Phi} = i\sigma_2\Phi^*$ and $\Sigma_{L/R} = i\sigma_2\Delta_{L/R}$. The triplet scalars $\Delta_{L/R}$ are defined in 4.1.1. The matrices y^l, $\tilde{y}^l$ and y^h are the Yukawa coupling matrices.

The neutral fermion masses are generated once the Φ and Δ_L acquire *vev*. The neutral fermion mass matrix is given by

$$M_\nu = \begin{pmatrix} m_\nu^{II} & m_D \\ m_D^T & m_R \end{pmatrix}, \quad m_D = \frac{1}{\sqrt{2}}y^l v_1, \;\; m_R = \sqrt{2}y^h v_R, \;\; m_\nu^{II} = \sqrt{2}y^h v_L. \quad (4.24)$$

Thus the light neutrino mass matrix

$$m_{\nu_l} = m_\nu^{II} - m_D^T m_R^{-1} m_D, \quad (4.25)$$

is generated through type-I and type-II seesaw mechanisms. The first term comes from type-II seesaw and hence the superscript II. The second term originates via type-I seesaw.

After Higgs bi-doublet and triplet scalars get *vev*, the neutrino part of the above Lagrangian can be rewritten as

$$-\mathcal{L}_\nu = \frac{1}{2}\Big(\overline{n_L^c}M_\nu n_R + \overline{n_R^c}M_\nu^* n_L\Big), \quad (4.26)$$

with mass matrix M_ν where,

$$n_R = \begin{pmatrix} \nu_R^c \\ \nu_R \end{pmatrix}, \quad n_L = \begin{pmatrix} \nu_L \\ \nu_l^c \end{pmatrix}, \quad n_{L/R}^c = C\bar{\nu}_{L/R}^T. \quad (4.27)$$

In the left-right symmetric model with triplet scalars neutrino masses are generated through type-I and type-II seesaw mechanisms. As the *vev* of the left-handed triplet scalar is constrained from ρ parameter, it cannot be larger than $\mathcal{O}$(few GeV). Thus it is indeed possible to generate light neutrino masses $\sim$eV with $v_L \sim$eV, while the neutrino Yukawa coupling can be $\mathcal{O}(1)$. The heavy neutrino mass m_R is also generated through the Yukawa terms. It can be noted that with $m_R \sim \mathcal{O}(\text{TeV})$, m_D needs to be very small to generate light neutrino masses $\sim \mathcal{O}(\text{eV})$. But y^h can be as large as $\mathcal{O}(1)$ when v_R is around the TeV scale. Thus, a successful light neutrino mass generation cannot constrain y^h. But y^h affects the vacuum stability of the scalar potential in this model as the heavy neutrino is also coupled to the SM like Higgs and thus gets constrained. We will discuss later how these parameters are constrained from vacuum stability, triviality and perturbativity of the couplings.

4.3.2 LRSM with doublet scalars

In Left-Right symmetric model with doublet Higgs, the leptonic part of the Yukawa interaction can be written as

$$-\mathcal{L}_l = \bar{l}_L \Big(y_1 \Phi + y_2 \tilde{\Phi} \Big) l_R + h.c. \tag{4.28}$$

where $SU(2)_L \otimes SU(2)_R$ quantum numbers of l_L and l_R are (2,1) and (1,2) respectively. So from this Lagrangian the neutrino mass (Dirac type) can be written as

$$m_D = y_1 v_1 + y_2 (v_2 e^{i\theta})^*. \tag{4.29}$$

Unlike the case of triplet scalars it is not possible here to write a Majorana mass term for right handed neutrinos. But we can write dimension-5 terms which can give rise to Majorana mass terms

$$\mathcal{L}_{D-5} = \frac{\eta_L}{M_L} l_L l_L H_L H_L + \frac{\eta_R}{M_R} l_R l_R H_R H_R \tag{4.30}$$

where M_L and M_R are some very high scales.

With the assumption that $\langle H_L \rangle = 0$ we have effectively

$$m_R \simeq \frac{\eta_R v_R^2}{M_R}.$$

With this effective operator Majorana mass term, the neutrino mass matrix becomes

$$M_\nu = \begin{pmatrix} 0 & m_D \\ m_D^T & m_R \end{pmatrix}. \tag{4.31}$$

After diagonalization, the light neutrino mass matrix can be written as

$$m_{\nu_l} = -m_D^T\, m_R^{-1}\, m_D \tag{4.32}$$

which is the double see-saw formula.

In the left-right symmetric model with two doublet scalars instead of two triplets, neutrino masses cannot be generated through type-II seesaw mechanism. Type-I seesaw is the natural choice in this case. But the right-handed neutrino masses are generated through an effective operator that does not include any Yukawa couplings. Thus with TeV scale right-handed neutrinos light neutrino masses arise if and only if the Dirac-type neutrino Yukawa coupling is very small. Then vacuum stability is automatically satisfied. Thus, only the quartic couplings get constrained through vacuum stability, triviality and perturbativity of the couplings. Within this framework it is indeed possible to generate light neutrino masses of the correct order without lowering the Yukawa coupling as the light neutrino masses are independent of v_R but suppressed by some heavy scale. In that case the vacuum stability constraints cannot be avoided and play the most crucial role in constraining the Yukawa couplings and other parameters.

4.4 Vacuum Stability in LRSM

In this section we will discuss how vacuum stability can constrain parameters in the LR symmetric model. We have already discussed the tools we need to adjudge vacuum stability, viz. positivity of quadratic form and copositivity in Chapter2.

Here we will use those methods to calculate the stability criteria. Imposing the condition that the vacuum should be stable all the way till the Planck scale, the parameter space of the model will be constrained.

We consider the LR model with doublet scalar first because of its simplicity.

4.4.1 LR Model with Doublet Scalars

The scalar sector of this model is discussed in detail in 4.1.2. In appendix B we have calculated the conditions for copositivity, or in other words, conditions for vacuum stability of the Left-Right symmetric model with doublet scalars. Here we have first expanded the full scalar potential in terms of the component fields†. We then construct quadratic forms considering 2-, 3-, and 4-fields directions. As there are maximum four component fields $(\phi_1^0, \phi_1^+, h_R^0, h_R^+)$, in our analysis all the possible quadratic forms have been considered.

One can easily follow the copositivity conditions derived from the given quadratic form of the potential written in a symmetric matrix. These conditions directly follow from our previous discussion on general matrix. At this point, we would like to note and discuss some interesting situations which arise during these calculations. Notice that while constructing the matrix form in some of the cases, we have to introduce one or more extra unphysical parameters to accommodate the most general multi-field terms of the potentials. For instance, if we consider the quadratic form like Eq. B.10 we have to construct a matrix that contains such new parameters‡ in the form of C and K. That bears interesting consequences of generating nontrivial conditions for different regions of these parameters. How-

†We have considered only those scalar multiplets whose components acquire non-zero vacuum expectation values. Our assumption simplifies the analysis but does not spoil the spirit of our formalism. The most general structure surely envelopes all field directions but that might weaken the clarity of this formalism.

‡These situations arise when some of the fields appear in linear form in the scalar quartic terms. They also create another problem due to the linearity in one of the fields. All the basis elements are not guaranteed now to belong in $\Re_n^+$, which can be taken care of by introducing suitable phases in the respective couplings. Now, in general, stability of the scalar potential can be ensured by demanding copositivity of the matrix form of the potential. However, one may not get a simpler set of conditions to ensure stability of the scale potential as we have obtained in our model. This is the generic problem while dealing with multi-component scalar field models, for example see ref. [62] where the author had discussed the most general Two Higgs Doublet Model(2HDM). An alternative approach for this 2HDM can be found in Ref. [63, 64].

ever, one needs to note that C and K are not the physical parameters as they do not exist at the Lagrangian level. Thus, we expect final conditions on stability of the potentials to be independent of these parameters. To discuss further, we rewrite the 4-field direction conditions as computed in B.10:

$$\lambda_1 \geq 0 \quad \& \quad C(f_1 + 2\beta_1) \geq 0 \quad \& \quad K(f_1 + 2\beta_1) \geq 0$$
$$\& \quad C\,K \left(\frac{f_1 + 2\beta_1}{2}\right)^2 - f_1^2 \geq 0.$$

These conditions can be examined along with additional conditions we already derived from 2- and 3-field directions. These existing conditions being independent of these unphysical parameters, put constraint over them. So, using such conditions: $\lambda_1 \geq 0$ and $\beta_1 \geq |f_1|/2$, one readily notes that both C and K have to be non-negative. Hence, following this argument, the last condition can be rewritten as $(2\beta_1 + f_1) \geq 2|f_1|/(CK)$. Our intention is to find the largest parameter space which is compatible with the vacuum stability. In other words, one can simply evade these superficial parameters involving C and K by fixing their values leading to the largest allowed parameter space. Following this principle, the product CK which can have any non-negative value is favored when it approaches infinity. Thus the largest parameter space is allowed when the constraint is given as $(2\beta_1 + f_1) \geq 0$. Thus the final vacuum stability conditions read $\lambda_1 \geq 0$ and $\beta_1 \geq |f_1|/2$.

We have also noted the required RGEs for our analysis in appendix A.4 [65]. In Fig. 4.1 we constrain the universal quartic coupling λ_u ($\equiv \lambda_2$, -λ_3) for LR model with doublet scalars in low v_R region for different values of heavy scalar mass M_H. Similar to the previous case, the yellow shaded region in the plot is disallowed by low energy data ($M_{W_R} > 3.5$ TeV) and the green shaded region is excluded by direct search at LHC ($M_{W_R} > 2.5$ TeV).

As we can see in Fig. 4.1, for any particular heavy scalar mass (M_H), universal quartic coupling λ_u is disallowed above the corresponding line. For example, as seen from the plot, the maximum allowed value of the universal quartic coupling is 0.033, if one considers LR breaking scale at 10 TeV and heavy scalar mass of

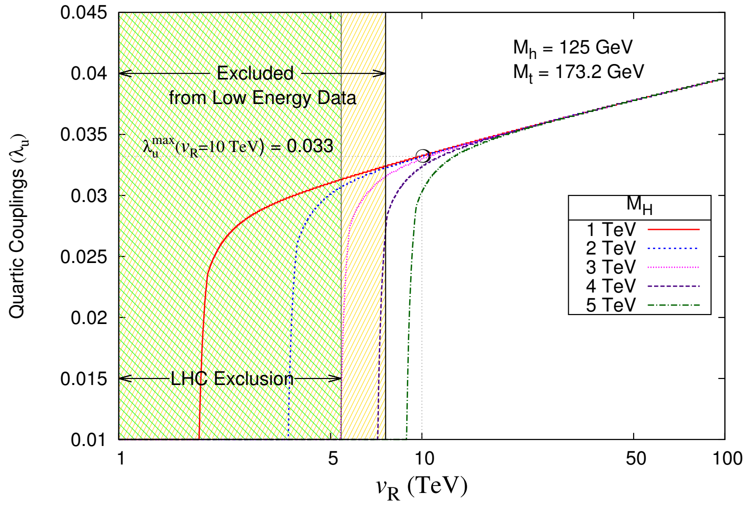

Figure 4.1: Constraints on the universal quartic coupling λ_u ($\equiv \lambda_2$, -λ_3) for LR model with doublet scalars in low v_R region for different values of heavy scalar mass M_H. Yellow shaded region is disallowed by low energy data ($M_{W_R} > 3.5$ TeV) and green shaded region is excluded by direct search at LHC ($M_{W_R} > 2.5$ TeV).

1 TeV. As before, the allowed maximum quartic coupling is lowered for heavier scalar.

In Fig. 4.2 we check the compatibility for stable vacuum in $v_R - M_H$ plane for LR model with doublet scalars. Each color represents a particular set of light Higgs mass (M_h) and top mass (M_t) in respective plot. In Fig. 4.2(a) Higgs mass is fixed at 125 GeV and top quark mass is varying from 170 GeV to 175 GeV where as, in Fig. 4.2(b) top quark mass is fixed at 173.2 GeV and Higgs mass is varying from 122 GeV to 127 GeV. Upper-left region (shaded with light blue) above the line $M_H = v_R$ is disallowed since quartic couplings are non-perturbative at the low scale itself in this domain. The blank (white) strip is also ruled out as the value of the couplings in this region is such that they become non-perturbative before reaching the Planck scale. Lower-right region (shaded with light pink) quartic coupling related with heavy Higgs mass becomes extremely small ($\leq \mathcal{O}(10^{-7})$). We choose universal quartic coupling $\lambda_1 = -\lambda_2 = \lambda_u$ fixed at 0.04. Here, the choice of λ_u allows only $v_R \geq 100$ TeV. Inset to both figures show the higher v_R scale where color patches terminate, representing the very scale where in fact Standard Model breaks down for a particular Higgs mass or top quark mass at one loop.

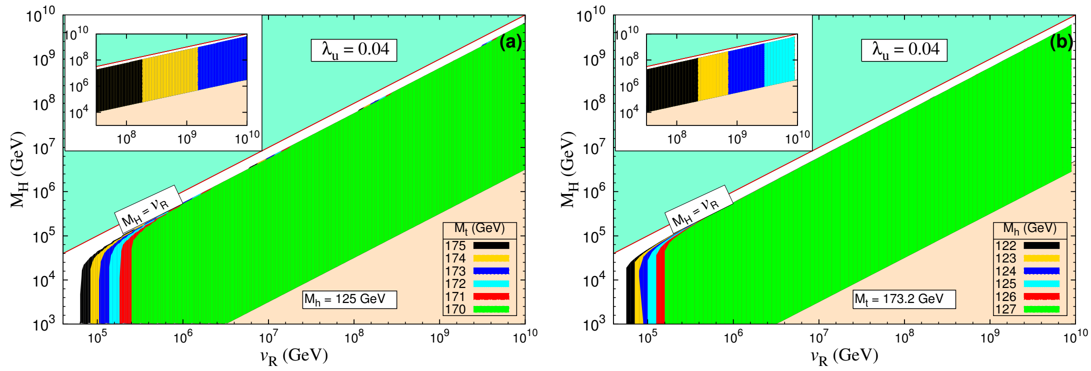

Figure 4.2: Compatibility for stable vacuum in v_R and M_H plane in LR model with doublet scalars. Each color represents a particular set of light Higgs mass (M_h) and top mass (M_t) in respective plot. In figure (a) Higgs mass is fixed at 125 GeV and top quark mass is varying, where as, in figure (b) top quark mass is fixed at 173.2 GeV and Higgs mass is varying. Upper-left region (shaded with light blue) above the line $M_H = v_R$ is disallowed since quartic couplings are non-perturbative at the low scale itself in this domain. Lower-right region (shaded with light pink) quartic coupling related with heavy Higgs mass becomes extremely small ($\leq \mathcal{O}(10^{-7})$). We choose universal quartic coupling λ_u fixed at 0.04. Inset to both figures shows the higher v_R scale where color patches terminate, representing the very scale where in fact Standard Model vacuum becomes unstable for a particular Higgs mass or top quark mass at one loop.

4.4.2 LR Model with Triplet Scalars

This model contains triplets scalar along with the Higgs bi-doublet and the scalar structure is discussed in 4.1.1. For this model, while computing the COP conditions we have also encountered the similar situations as in section 4.4.1 and have dealt them with the same spirit. We consider one such example where a single symmetric matrix coming from two different directions ${}^{3F}V_6$ and ${}^{3F}V_7$. Corresponding quadratic forms are followed in Eqs. B.26 or B.27. Similar to our discussion in section 4.4.1, we encounter one such unphysical parameter C. Here we have also illustrated the removal of superficial parameters from the final vacuum stability conditions. Theoretically, as it is stated earlier, in the λ_i parameter space one needs to vary the parameter C for all possible ranges (which is $[-\infty, \infty]$) together with conditions depicted in Eq. B.28 as well as in Eqs. B.29, B.30, B.32 (which are once again listed as follows) and take union of all such allowed regions to achieve the full parameter space. We have categorized the C dependency as follows:

(a) $C \geq 0$ such that $(1-C) \geq 0$, i.e., $C \in [0,1]$:

$$\lambda_5 + 2\,\lambda_6 \geq 0, \tag{4.33}$$

(b) $C \geq 0$ such that $(1-C) \leq 0$, i.e., $C \in (1,\infty]$:

$$\lambda_5 + 2\,\lambda_6 \geq 0 \qquad \& \qquad \lambda_5^2 - (1-C)^2(\lambda_5 + 2\,\lambda_6)^2 \geq 0, \tag{4.34}$$

(c) $C < 0$ such that $(1-C) \geq 0$, i.e., $C \in [-\infty,0)$:

$$\lambda_5 + 2\,\lambda_6 \leq 0 \qquad \& \qquad \lambda_5^2 - (1-C)^2(\lambda_5 + 2\,\lambda_6)^2 \geq 0. \tag{4.35}$$

However, this procedure is highly impractical to implement in real calculations. But, as we have discussed in the previous section, it is possible to remove the presence of C from the final copositive conditions through the careful inspection of all the copositivity criteria. By combining last two cases (b and c) we can write $\lambda_5 \geq |(1-C)(\lambda_5 + 2\lambda_6)|$, with $C \in [-\infty,\infty]$ excluding the range $[0,1]$. It is obvious that the other derived condition $\lambda_5 \geq 0$ is more relaxed for the given range of C. Thus $\lambda_5 \geq 0$ allows larger parameter space than the condition $\lambda_5 \geq |(1-C)(\lambda_5 + 2\lambda_6)|$. Now the case (a) possess the criteria $\lambda_5 + 2\lambda_6 \geq 0$ that leads to the less parameter space than the already derived condition $\lambda_5 + \lambda_6 \geq 0$ for $\lambda_6 < 0$. For $\lambda_6 \geq 0$ both conditions are automatically satisfied as $\lambda_5 \geq 0$.

This can also be demonstrated pictorially in the following manner. Assuming that we are interested in the region of $|\lambda_i| \leq 1$ from perturbativity, we would like to find out particular values of C which actually maximize the allowed regions for a given condition. Thereafter we simply rewrite those conditions at that point and demand that to be the final conditions. In our present example, conditions given in Eqs. 4.34 and 4.35 depend on the parameter C. However, as demonstrated in Fig. 4.3 they maximize the allowed parameters at $C = 1$ and $C = 0$, respectively. Moreover, union of these sets of nontrivial conditions for different ranges of C is equivalent to a simple condition given by $(\lambda_5 + \lambda_6) \geq 0$ which is independent of C. Interestingly, this is not a new condition and already is explored in several

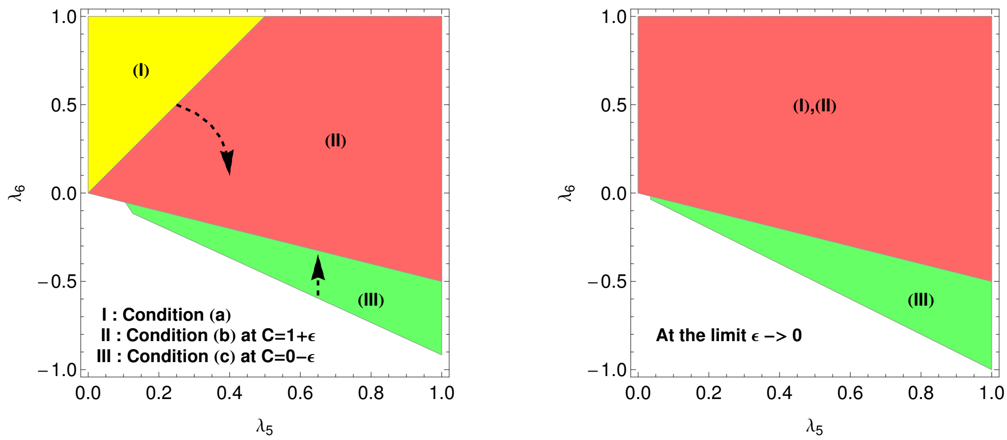

Figure 4.3: Maximizing allowed parameter space the in $\lambda_5 - \lambda_6$ plane corresponds to suitable parameter C in the case of ${}^{3F}V_6$ and ${}^{3F}V_7$. The figure in the left panel is for small value of ϵ $(= 0.2)$ chosen to parametrize C. Black arrows represent the movements of boundary lines for increased values of ϵ satisfying the conditions. In the right panel we demonstrate that at the limit ϵ goes to zero, maximum allowed space is achieved. Clearly these sets of conditions at the C values which maximize the allowed parameters are equivalent to a simple condition given by $(\lambda_5 + \lambda_6) \geq 0$ which is independent of C.

2-field copositivity conditions like ${}^{2F}V_8$ and ${}^{2F}V_{10}$. Final copositivity conditions in this case can be written as B.33. Including all copositive conditions we get a final set of conditions as

$$\lambda_1 \geq 0 \quad \& \quad \lambda_5 \geq 0 \quad \& \quad \lambda_5 + \lambda_6 \geq 0 \quad \& \quad 16\, \lambda_1 \lambda_5 - \lambda_{12}^2 \geq 0.$$

The renormalization group evolutions that we have considered in our analysis are depicted in appendix A.3 [66]. In Fig. 4.4 we show the constraints on universal quartic coupling λ_u $(\equiv \lambda_2,\ \lambda_3,\ \lambda_4,\ \lambda_8,\ \lambda_9,\ \lambda_{10},\ \lambda_{11})$ for LR model with triplet scalars in low v_R region. Yellow shaded region is disallowed from low energy data $(M_{W_R} > 3.5$ TeV$)$ [67–70] and green shaded region is excluded from direct search at LHC $(M_{W_R} > 2.5$ TeV$)$ [71–74]. One can easily translate these bounds to the LR symmetry breaking scale v_R using the relation:

$$M^2_{W_R^\pm} = \frac{1}{4} g_2^2 \left(v_1^2 + v_R^2\right). \tag{4.36}$$

In our analysis we also set Majorana Yukawa, y^h at 0.25. We note that, for any particular heavy scalar mass (M_H), universal quartic coupling λ_u is disallowed above the corresponding line shown in the figure. For example, as seen from the

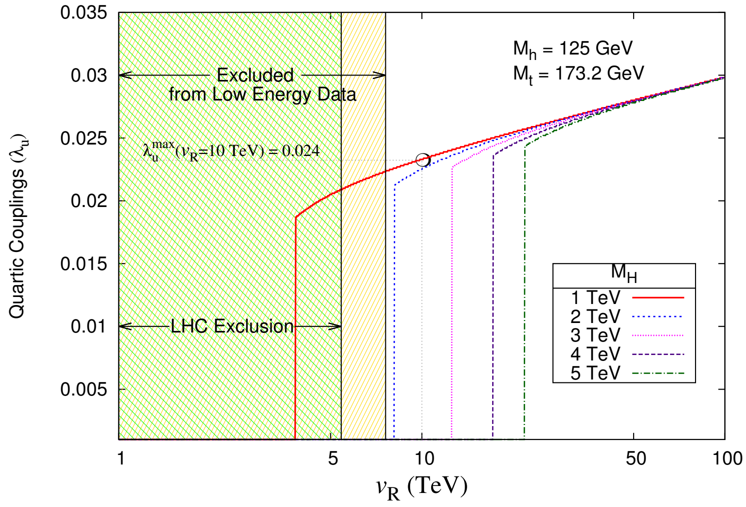

Figure 4.4: Constraints on universal quartic coupling λ_u ($\equiv \lambda_2$, λ_3, λ_4, λ_8, λ_9, λ_{10}, λ_{11}) for LR model with triplet scalars in low v_R region. Yellow Shaded region is disallowed from low energy data ($M_{W_R} > 3.5$ TeV) and green shaded region is excluded from direct search at LHC ($M_{W_R} > 2.5$ TeV).

plot, maximum allowed value of the universal quartic coupling is 0.024 if one considers LR breaking scale at 10 TeV and heavy scalar mass at 1 TeV. Allowed maximum quartic coupling is lowered for heavier scalar which can be understood from vacuum stability and perturbativity.

In Fig. 4.5 we depict the vacuum stability allowed parameter space in LR model with triplet scalar in Left-Right symmetric breaking scale v_R and heavy scalar M_H plane. Each color represents a particular set of light Higgs mass (M_h) and top mass (M_t) in respective plot. In Fig. 4.5(a) Higgs mass is fixed at 125 GeV and top quark mass is varying from 170 GeV to 175 GeV where as, in Fig. 4.5(b) top quark mass is fixed at 173.2 GeV and Higgs mass is varying from 122 GeV to 127 GeV. Upper-left region (shaded with light blue) above the line $M_H = v_R$ is disallowed since quartic couplings are non-perturbative in this domain. The blank (white) strip is also ruled out as the value of the couplings in this region is such that they become non-perturbative before reaching the Planck scale. Lower-right region (shaded with light pink) quartic coupling related with heavy Higgs mass becomes extremely small ($\leq \mathcal{O}(10^{-7})$). We choose universal quartic coupling λ_2, λ_3, λ_4, λ_8, λ_9, λ_{10}, $\lambda_{11} = \lambda_u$ fixed at 0.03. This choice of λ_u allows only $v_R \geq 100$ TeV which can be inferred from Fig. 4.4. Inset to both figures show the higher

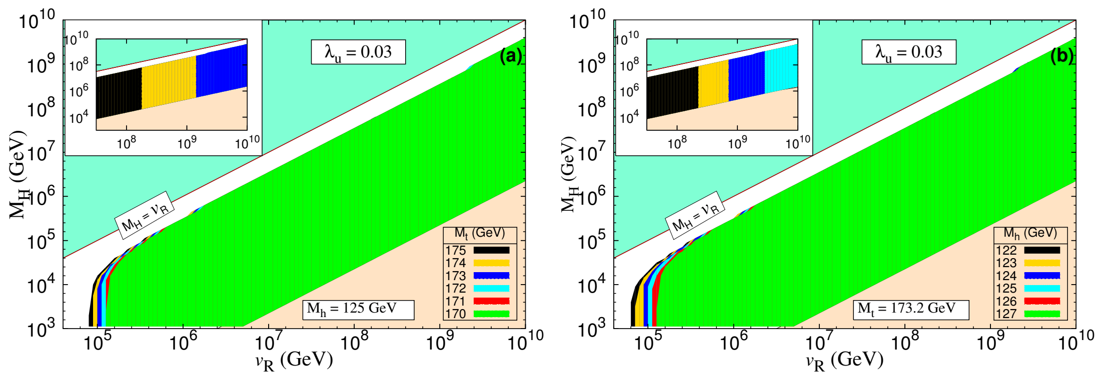

Figure 4.5: Compatibility of stable vacuum in v_R and M_H plane in LR model with triplet scalar. Each color represents a particular set of light Higgs mass (M_h) and top mass (M_t) in respective plot. In figure (a) Higgs mass is fixed at 125 GeV for different top quark mass whereas in figure (b) top quark mass is fixed at 173.2 GeV and Higgs mass is varying. Upper-left region (shaded with light blue) above the line $M_H = v_R$ is disallowed since quartic couplings are non-perturbative in this domain. Lower-right region (shaded with light pink) quartic coupling related with heavy scalar mass becomes extremely small ($\leq \mathcal{O}(10^{-7})$). We choose universal quartic coupling λ_u fixed at 0.03. Inset to both figures show the higher v_R scale where the Standard Model vacuum becomes unstable.

v_R scale where color patches terminate, representing the very scale where in fact Standard Model breaks down for a particular Higgs mass or top quark mass at one loop.

We have computed the vacuum stability conditions using copositivity and to construct the symmetric matrices we have to chose a particular basis. Recently we have found that it is indeed possible to choose a different basis where the stability conditions can be relaxed. We are working to find the stability conditions via copositivity in a basis independent way which can provide the necessary and sufficient conditions.

4.5 Unitarity constraints in LRSM with Triplet Scalars

To illustrate the effect of unitarity, we consider the quartic couplings $\lambda_2, \lambda_3, \lambda_4, \lambda_8$, λ_9, λ_{10} ($=\lambda_u$) to be universal as they only contribute in mass splittings between the heavy scalar states. Since these couplings are not accessible at the collider, they can only be constrained by using vacuum stability, perturbativity and unitarity. While the effect of vacuum stability and perturbativity was extensively discussed

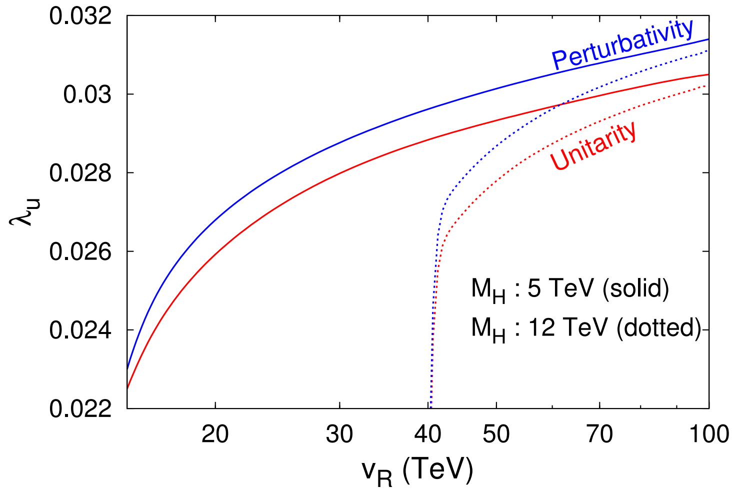

Figure 4.6: Constraints on the universal quartic coupling λ_u for LR model coming from unitarity (red) and perturbativity (blue) bounds for multi-TeV region of Left-Right symmetry breaking scale v_R. Also, v_R scale is heavy enough ($>$ 10 TeV) to satisfy the constraints. Stringent bounds are coming from unitarity. Two different sets of heavy scalar states (M_H), viz., 5 TeV and 12 TeV are considered for demonstration.

in the previous section, here we would like to analyze the bound from unitarity of the S-matrix and demonstrate combined results together. In the appendix C we included all the explicit calculations done using MATHEMATICA to compute unitarity constraints for LR model with triplet scalars. The MATHEMATICA notebook files can be obtained from the URL: http://www.prl.res.in/~konar/data.html or from the source file in arXiv [75].

Using the RGE equations [65], we extract maximum allowed values for quartic couplings keeping all heavy scalar masses degenerate satisfying constraints coming from unitarity, vacuum stability and perturbativity. We have adopted v_R to be heavy enough ($>$ 10 TeV) for our analysis so that the bounds on W_R are easily satisfied.

Figure 4.6 demonstrates both the constraints coming from unitarity (red-dotted curves), as well as perturbativity (blue-solid curves) on the universal quartic coupling λ_u for Left-Right symmetric model. Multi-TeV region of Left-Right symmetry breaking scale v_R is considered. Also, two different sets of heavy scalar states (M_H), assuming heavy scalar states are nearly degenerate, are considered for presentation. Clearly, for a particular value of Left-Right symmetry breaking scale (v_R) unitarity bounds put severe constraints on quartic couplings compared to that of coming from perturbativity bounds. We have implemented the perturbativity bound as $|\lambda_i| < 4\pi,\ \forall\, i \in [0, 15]$.

4.5.1 Constraints on Physical Scalar Masses

So far in this section we have demonstrated the usefulness of unitarity to constrain the quartic coupling in the Left-Right symmetric model. Now, we turn to look for some more phenomenologically useful aspects, in an era, when the LHC is expected to explore new physics at multi-TeV scale. Here we use vacuum stability along with unitarity and perturbativity to constrain the physical scalar mass states. Vacuum stability criteria for this model are calculated using copositivity of symmetric matrices in [17] and combined conditions read as:

$$\lambda_1 \geq 0 \quad \wedge \quad \lambda_5 \geq 0 \quad \wedge \quad \lambda_5 + \lambda_6 \geq 0 \quad \wedge \quad 16\, \lambda_1\, \lambda_5 - \lambda_{12}^2 \geq 0. \tag{4.37}$$

To explore the allowed mass range of physical scalars, at LR symmetry breaking scale (*i.e.*, v_R scale) we randomly vary the quartic couplings§ $\lambda_5, \lambda_6, \lambda_7$ and λ_{12} in their allowed range¶ $[0, 4\pi]$ and estimate the corresponding mass scales. These quartic couplings run according to their respective RGEs [65] and we ensure that the quartic couplings obey all the conditions coming from vacuum stability, unitarity, as well as perturbativity at each scale below M_{Pl}. The input quartic couplings which obey these conditions, till M_{Pl}, are interpreted as the accepted mass scale of physical scalars using Eq. 4.9.

In Fig. 4.7 we demonstrate the allowed mass range for four sets of heavy scalar states listed in Eq. 4.9 (except first one, which is actually input parameter mass) after imposing all constraints as described above. Below we present the detailed discussion about each of these sets of heavy scalars. This is demonstrated for two different LR symmetry breaking scale viz. 30 TeV and 100 TeV and corresponding mass ranges are also tabulated in Table 4.1. We also display, in

§The parameter $(\lambda_7 - 2\lambda_5)$ sets mass scale for some scalars and instead of λ_7 we randomly vary the difference $(\lambda_7 - 2\lambda_5)$ in the range $[0, 4\pi]$ to ensure that no unphysical mass scale appears in the model.

¶In general quartic coupling can take any value from $[-4\pi, 4\pi]$ but here these couplings cannot be negative as it will lead to tachyonic states.

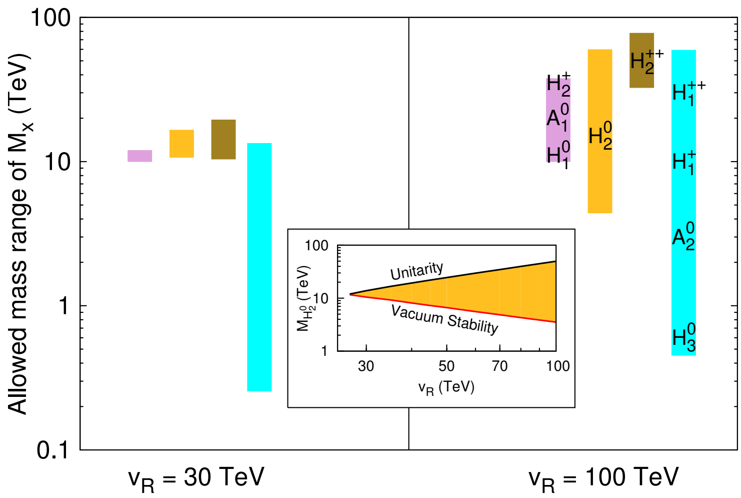

Figure 4.7: Allowed mass range for four sets of heavy scalar states (M_X) after imposing all constraints coming from vacuum stability, unitarity, as well as perturbativity at each scale all the way up to the Planck scale (M_{Pl}). Two different sets of Left-Right symmetry breaking scale v_R are considered, which are 30 TeV and 100 TeV. The bound $M_{H_1^0} > 10$ TeV has also been taken into account. Here λ_u is set to the value 0.01 which is much below the unitarity bound and this is evident from the Fig. 4.6. Inset shows how one set of heavy scalar mass (e.g., $M_{H_2^0}$) is constrained from vacuum stability (red) and unitarity (black) bounds over a continuous range of v_R.

the inset of Fig. 4.7, how one set of heavy scalar mass (e.g., $M_{H_2^0}$) is constrained from vacuum stability (red) and unitarity (black) over a continuous range of v_R.

From these considerations one can make following observations about the allowed mass range:

- To suppress the FCNC effects the fields H_1^0 and A_1^0 should be heavy $\simeq 10$ TeV [76–78]. We use this information to limit the corresponding quartic coupling λ_{12} from below at v_R scale, and, on the other hand perturbativity restricts the coupling from above. This can be seen in the purple bar (left most region) where allowed mass range for $M_{H_1^0}, M_{A_1^0}$ and $M_{H_2^\pm}$ is very narrow for small v_R value. Large v_R relaxes the perturbativity bound and larger region is allowed. This also sets a minimum allowed value of LR breaking scale v_R coming from vacuum stability and perturbativity, which can also be marked from the inset plot. However, this would make sense only if FCNC bound is robust. Non-minimal LR model can avoid FCNC bound and few TeV scale H_1^0 is allowed [79].

- Allowed range of $M_{H_2^0}(= 2\,\lambda_5\, v_R^2)$ is depicted in orange/yellow band. To explain its behavior we add an inset in the Fig. 4.7 where a continuous variation of $M_{H_2^0}$ with v_R is shown. Since λ_5 and λ_{12} are coupled through vacuum stability condition (cf. Eq. 4.37) the minimum allowed value of λ_5 is fixed at v_R scale which sets the scale of $M_{H_2^0}$. For fixed $M_{H_1^0}$ (10 TeV), higher value of v_R supports lower λ_{12} which eventually decreases minimum allowed value for λ_5. Maximum allowed value of λ_5 is restricted from unitarity. As evident from the figure, $M_{H_2^0}$ can be light enough *i.e.,* $\mathcal{O}$ (TeV) for higher values of v_R.

- Mass of $M_{H_2^{\pm\pm}}$ is defined by the quartic coupling λ_6. With low initial value, this coupling decreases with energy and eventually becomes negative, leading to tachyonic states. To get rid of tachyonic states the boundary value for λ_6 at v_R scale should be high enough and this leads to relatively higher mass states for $M_{H_2^{\pm\pm}}$ as shown in olive band.

- The parameter $(\lambda_7 - 2\lambda_5)$ governs mass scale for[‖] $M_{H_3^0}$, $M_{A_2^0}$, $M_{H_1^\pm}$, and $M_{H_1^{\pm\pm}}$ and it can become very small as it is not constrained from below via vacuum stability. But the mass scale will shift as there are secondary contributions coming from universal quartic couplings and EW breaking *vev* v_1. The cyan bar represents the allowed range for these scalars. In principle contribution to these scalars coming from LR breaking *vev* can be zero and in that case the secondary contribution of $\mathcal{O}(100)$ GeV will set the mass scale. The minimum values shown in Fig. 4.7 are nothing but numerical artifact where the coupling is already very small ($\sim 10^{-5}$).

4.6 Conclusion

Being a very simple gauge group extension of the SM and giving a rich dividend in BSM phenomena, Left-Right symmetric models are phenomenologically interesting in their own right. The scalar sector of this model is quite rich due to the fact that an enlarged scalar sector is required to get a mechanism for breaking

[‖]Note that LEP II data yields a lower bound on the mass of H_3^0, which is about 55 GeV [80].

v_R (TeV)	$M_{H_1^0}, M_{A_1^0}, M_{H_2^\pm}$ (TeV)	$M_{H_2^0}$ (TeV)	$M_{H_2^{\pm\pm}}$ (TeV)	$M_{H_3^0}, M_{A_2^0}, M_{H_1^\pm}, M_{H_1^{\pm\pm}}$ (TeV)
30	$10-12$	$10.5-16.5$	$10.5-20$	$\mathcal{O}(0.1)-13.5$
100	$10-37.5$	$4.4-60$	$33-78$	$\mathcal{O}(0.1)-59$

Table 4.1: Allowed mass range in TeV for two different v_R scale. These are approximated values as there will be secondary contributions which will shift masses upward by $\mathcal{O}(100)$ GeV which is insignificant except for the lower limit of the last column.

the Left-Right symmetric group to the SM gauge group. In the present work we analyzed the scalar sector of the Left-Right symmetric model in the light of various theoretical and experimental constraints.

We have computed the criteria for the potential to be bounded from below, i.e., the conditions for vacuum stability. We also perform the renormalization group evolutions of the parameters (couplings) of these models at the one loop level with proper matching conditions. We have shown how the phenomenologically inaccessible couplings can be constrained for different choices of scales of new physics. They in turn also affect the RGEs of the other couplings. We have noted that the new physics effects must be switched on before the SM vacuum faces the instability. This helps the vacuum stability of the full scalar potential and achieve a consistent spontaneous symmetry breaking. We have analyzed these aspects varying Higgs and top quark mass over their allowed ranges.

Also, we constrain the masses of the other physical scalars by using the unitarity constraints. We obtain these constraints by evaluating the zeroth order partial wave amplitude of various $2 \to 2$ scatterings. We find that for any Left-Right symmetry breaking scale, unitarity bounds put severe constraints on quartic couplings compared to that of coming from perturbativity. We also demonstrated that some of the physical scalars can have the mass in the TeV range which can have interesting LHC prospects. It is to be noted that the masses of these scalars are dependent on the Left-Right symmetry breaking scale v_R, and consequently, obtained bounds are highly sensitive to this v_R.

Chapter 5

TeV Scale Seesaw Model

Convincing indications of BSM physics have emerged from the phenomenon of neutrino oscillation observed in terrestrial experiments. These results have conclusively established that neutrinos have non-zero masses and flavor mixing. Oscillation data together with the cosmological bound on the sum of neutrino masses ($\Sigma m_i < 0.23$ eV including the PLANCK data [81]) indicate that neutrino masses are much smaller than those of other fermions in the SM. Such small masses can be generated naturally by the seesaw mechanism. The origin of seesaw is the dimension 5 effective operator $\frac{c_5}{M} LLHH$, where $L(H)$ is the SM lepton(Higgs) doublet, c_5 is a dimensionless coupling and M is the mass scale at which the effective operator is being generated [82]. The smallness of neutrino masses in these models is related to the scale of lepton number violation which is required to be very high $\sim \mathcal{O}(10^{15}$ GeV) to generate neutrino masses in the right ballpark. The most economical in terms of particle content is the type-I seesaw in which heavy singlet right-handed neutrinos are added to the SM Lagrangian [83–87]. However, the natural seesaw scale is far beyond the reach of the LHC. To have signatures of seesaw models at the LHC, the heavy neutrino (N) mass needs to be $\sim \mathcal{O}$ (TeV).

Seesaw models which lead to light neutrino masses are studied in the context of (meta)stability of the electroweak vacuum [88–97], lepton flavor violating (LFV) decay [98–100], and new physics signatures of such models at present colliders [101–122]. Seesaw models which consist of extra heavy fields added to the

SM can predict a hierarchical light neutrino mass spectrum as well as a degenerate light neutrino mass spectrum [83–87, 123]. With recent results from Planck data [47], a degenerate mass spectrum becomes severely restricted, although a quasi-degenerate (QD) mass spectrum [83–87, 123] is not fully ruled out. It is worthwhile to study QD models in the light of new constraints coming from vacuum (meta)stability and lepton flavor violation (LFV) and also to investigate the possibility of observing signatures of these models at the upcoming 14 TeV LHC.

5.1 The model

We extend the Standard Model (SM) particle spectrum by adding three heavy right handed neutrinos having masses at the TeV scale. The additional part of the Lagrangian is given by

$$\mathcal{L}_{ext} = -\,\tilde{\Phi}^{\dagger}\overline{N}_R Y_\nu l_L - \frac{1}{2}\overline{N}_R\, M\, N_R^c + \text{h.c.}\,, \tag{5.1}$$

where l_L is the left handed lepton doublet, Φ is the SM Higgs doublet and $\tilde{\Phi}$ is given by $\tilde{\Phi} = i\sigma^2\Phi^*$. The right handed singlet heavy neutrino field is denoted by N_R and $(Y_\nu)_{ji}$ are the elements of the Dirac Yukawa coupling matrix of dimension (3×3) in the present model with the first(second) index assigned to heavy(light) neutrinos. After spontaneous symmetry breaking the Higgs field acquires a vacuum expectation value v. Consequently the light neutrino mass matrix is given by,

$$m_\nu = m_D^T\, M^{-1} m_D, \tag{5.2}$$

where the Dirac mass term is given by $m_D = Y_\nu v/\sqrt{2}$. Using the parameterization *à la* Casas and Ibarra [124], the texture of the Yukawa coupling matrix Y_ν can be expressed as*

$$Y_\nu = \frac{\sqrt{2}}{v}\sqrt{M^d}\, R\sqrt{m_\nu^d}\, U^\dagger_{\texttt{PMNS}}, \tag{5.3}$$

*For the two heavy neutrino case, the parameterization has been studied by Ibarra et.al. [125].

where M^d and m_ν^d are the heavy and light neutrino mass matrices respectively in their diagonal basis[†]. $U_{\texttt{PMNS}}$ is the light neutrino mixing matrix, given by

$$U_{\texttt{PMNS}} = \begin{pmatrix} c_{12}\,c_{13} & s_{12}\,c_{13} & s_{13}\,e^{-i\delta} \\ -\,c_{23}\,s_{12} - s_{23}\,s_{13}\,c_{12}\,e^{i\delta} & c_{23}\,c_{12} - s_{23}\,s_{13}\,s_{12}\,e^{i\delta} & s_{23}\,c_{13} \\ s_{23}\,s_{12} - \,c_{23}\,s_{13}\,c_{12}\,e^{i\delta} & -\,s_{23}\,c_{12} - c_{23}\,s_{13}\,s_{12}\,e^{i\delta} & c_{23}\,c_{13} \end{pmatrix} P\,, \quad (5.4)$$

with $c_{mn} = \cos\theta_{mn}$, $s_{mn} = \sin\theta_{mn}$ and δ the CP-violating Dirac phase. The matrix P is the Majorana phase matrix, expressed as $P = \mathrm{diag}(e^{-i\alpha_1/2}, e^{-i\alpha_2/2}, 1)$. For this parameterization of Y_ν, it is evident that the measurable parameters from the low energy neutrino experiments enters through m_ν^d and $U_{\texttt{PMNS}}$, whereas all unknown parameters are originate from M^d as well as from complex the orthogonal matrix R. For simplicity M^d has been approximated with a single parameter of heavy neutrino mass (i.e. all the heavy neutrinos are degenerate). Elements of the matrix R are completely arbitrary and can be very large which eventually elevate the Yukawa couplings (cf. Eq. 5.3) to $\mathcal{O}(1)$. On the other hand, owing to the relation $RR^T = I$, these arbitrary elements do not effect the determination of m_ν in Eq. 5.2. In other words, the matrix R acts like a fine tuning parameter which helps to generate sufficiently large Yukawa couplings along with TeV scale M_R.

Orthogonality ensures that the matrix R can be written as,

$$R = O\,e^{iA}, \quad (5.5)$$

where O and A are real orthogonal[‡] and real antisymmetric matrices respectively. For nearly degenerate light neutrinos one can absorb O in $U_{\texttt{PMNS}}$ [126]. The general form of the antisymmetric matrix A can be expressed in terms of three unknown

[†]In the present work we have taken M to be diagonal which implies M and M^d are equivalent.
[‡]Satisfying $det[O] = det[R]$.

parameters

$$A = \begin{pmatrix} 0 & a & b \\ -a & 0 & c \\ -b & -c & 0 \end{pmatrix}, \tag{5.6}$$

with $a, b, c \in \Re$. Expanding and rewriting in terms of a new parameter $\omega = \sqrt{a^2 + b^2 + c^2}$ one would obtain

$$e^{iA} = \mathbb{1} - \frac{\cosh\omega - 1}{\omega^2} A^2 + i\,\frac{\sinh\omega}{\omega} A\,. \tag{5.7}$$

In order to reduce the number of free parameters in our analysis, we choose $a = b = c = \omega/\sqrt{3}$. Now, we are left with a single unknown parameter ω (together with single unknown heavy neutrino mass scale M_R as diagonal entries of matrix M^d) that will be constrained by imposing the bound of metastability of the electroweak vacuum and non-observation of LFV decay processes. These constraints would in turn be reflected in terms of the norm for Yukawa coupling matrix which is extremely crucial the production of the heavy neutrinos and essentially determine the discovery potential at the collider. Since Y_ν is a complex square matrix of dimension three, magnitude of which can be best represented in terms of the norm of Y_ν,

$$\begin{aligned} \mathrm{Tr}[Y_\nu^\dagger Y_\nu] &= \frac{2\,M_R}{v^2}\,\mathrm{Tr}\left[\sqrt{m_\nu^d}\,R^\dagger R\,\sqrt{m_\nu^d}\right], \\ &= \frac{2\,M_R}{v^2}\,m_0\,(1 + 2\cosh(\,2\,\omega))\,. \end{aligned} \tag{5.8}$$

One can arrive at this much compact expression[§] in terms of the parameter ω, as shown in the last equation, assuming an exact degenerate common light neutrino mass scale m_0. For demonstration, contours of constant values of $(\mathrm{Tr}[Y_\nu^\dagger Y_\nu])^{1/2}$ is shown in Fig. 5.1 with these parameters. For our analysis, the common mass scale for light neutrinos is chosen to be $m_0 \simeq 0.07$ eV, whereas heavy neutrino mass

[§]Note that, choice of equal a, b, c parameters does not affect this expression. However, unequal parameters would significantly complicate the LFV calculation in Eq. 5.21. Also note that if one of the parameters (a, b or c) is zero, then also it is possible to satisfy LFV bound, but it is not the case when two parameters are zero.

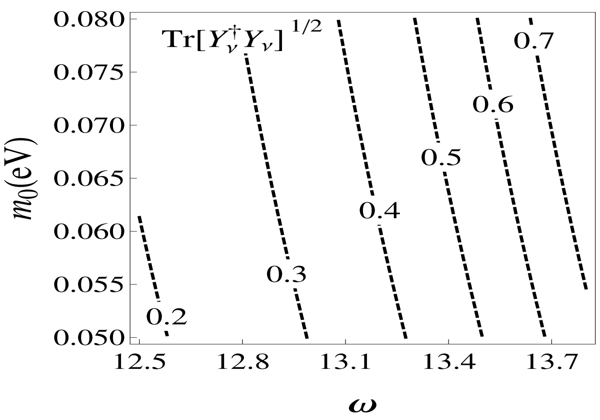

Figure 5.1: Parametric plot of $(\mathrm{Tr}[Y_\nu^\dagger Y_\nu])^{1/2}$ with ω and the common light neutrino mass scale m_0. The heavy neutrino mass is fixed at 100 GeV. The numbers in the plot indicate the corresponding values for the different set of parameters ω and m_0.

is fixed at 100 GeV. We note that the present allowed light neutrino mass can maximally access the quasi-degenerate range, and hence the hierarchical neutrino mass is no more can be neglected completely. One can parameterize this effect so that the observed neutrino mass hierarchy can be correctly accommodated within this framework of quasi-degenerate neutrinos. We classify them as 'normal' and 'inverted' hierarchy of masses over the common mass scale for light neutrinos. As evident from the figure, for a fixed value of m_0, different values of $(\mathrm{Tr}[Y_\nu^\dagger Y_\nu])^{1/2}$ can be obtained by varying ω accordingly [127]. To present one example, for this particular choice of degenerate light (heavy) neutrino mass of 0.07 eV (100 GeV), the norm $(\mathrm{Tr}[Y_\nu^\dagger Y_\nu])^{1/2} \simeq 0.5$ can be considered for choice of the parameter ¶ $\omega = 13.4$.

5.2 Metastability bound

The SM potential at tree level is given by

$$\mathcal{V}(\phi) = \lambda \left(\phi^\dagger \phi\right)^2 - m^2 \, \phi^\dagger \phi \; . \tag{5.9}$$

¶Note that, for this value of ω, elements of the matrix e^{iA} of Eq. 5.5 are of $\mathcal{O}(10^6)$ which enhances the Yukawa coupling matrix as in Eq. 5.3.

The physical Higgs mass, in the above convention, is defined as $m_h^2 = 2\lambda\, v^2$. The Renormalization Group equation for λ can be expressed up to i^{th} loop as

$$\frac{d\lambda}{d\ln\mu} = \sum_i \frac{\beta_\lambda^{(i)}}{(16\pi^2)^i}\,, \tag{5.10}$$

where μ is the renormalization scale. The β-function at one loop is given by,

$$\beta_\lambda^{(1)} = 24\,\lambda^2 - \left(\frac{9}{5}\,g_1^2 + 9\,g_2^2\right)\lambda + \frac{27}{200}\,g_1^4 + \frac{9}{20}\,g_1^2\,g_2^2 + \frac{9}{8}\,g_2^2 + 4T\lambda - 2Y\ , \tag{5.11}$$

where,

$$\begin{aligned} T &= \mathrm{Tr}\left[3\,{Y_u}^\dagger Y_u + 3\,{Y_d}^\dagger Y_d + {Y_l}^\dagger Y_l + Y_\nu^\dagger Y_\nu\right]\ , && (5.12)\\ Y &= \mathrm{Tr}\left[3(Y_u^\dagger Y_u)^2 + 3(Y_d^\dagger Y_d)^2 + ({Y_l}^\dagger Y_l)^2 + (Y_\nu^\dagger Y_\nu)^2\right] && (5.13)\end{aligned}$$

and g_i's are the gauge coupling constants. GUT modification for the $U(1)$ gauge coupling has been taken into account. Y_u, Y_d and Y_l denote the Yukawa coupling matrices for the up type quark, down type quark and charged lepton respectively. Expectedly, the dominant contribution comes from the top Yukawa (up type quark) running and the one-loop β function is governed by the following equation:

$$\beta_{Y_u}^{(1)} = Y_u\left[\frac{3}{2}{Y_u}^\dagger Y_u + \frac{3}{2}{Y_d}^\dagger Y_d + T - \left(\frac{17}{20}g_1^2 + \frac{9}{4}g_2^2 + 8g_3^2\right)\right]. \tag{5.14}$$

Three-loop RGE for the Higgs self coupling (λ), the top Yukawa coupling and the gauge couplings has been used in the numerical analysis [128–135]. Matching corrections for the top Yukawa coupling has been taken up to three-loop QCD [136], one-loop electroweak [137,138] and $\mathcal{O}(\alpha\alpha_s)$ [139,140] while for the Higgs self coupling, they have been taken up to two loop [141, 142]. The Higgs self coupling also receives an additional contribution from the higher order corrections of the effective potential. The loop corrected[‖] effective self coupling denoted by $\tilde{\lambda}$, is

[‖]We incorporated two loop correction due to the SM and one loop correction due to neutrino Yukawa couplings.

given by [93, 143, 144],

$$\begin{aligned}
\tilde{\lambda} \;=\; & \lambda - \frac{1}{32\,\pi^2}\Bigg[\frac{3}{8}\left(g_1^2+g_2^2\right)^2\left(\frac{1}{3}-\ln\frac{(g_1^2+g_2^2)}{4}\right)+6\,y_t^4\left(\ln\frac{y_t^2}{2}-1\right) \\
& +\frac{3}{4}\,g_2^4\left(\frac{1}{3}-\ln\frac{g_2^2}{4}\right)+\,([Y_\nu^\dagger Y_\nu]_{ii})^2\left(\ln\frac{[Y_\nu^\dagger Y_\nu]_{ii}}{2}-1\right) \\
& +([Y_\nu\,Y_\nu^\dagger]_{jj})^2\left(\ln\frac{[Y_\nu\,Y_\nu^\dagger]_{jj}}{2}-1\right)\Bigg]+\frac{Y_t^4}{(16\pi^2)^2}\times\Bigg[g_3^2\Bigg\{24\left(\ln\frac{Y_t^2}{2}\right)^2 \\
& -64\ln\frac{Y_t^2}{2}+72\Bigg\}-\frac{3}{2}\,Y_t^2\left\{3\left(\ln\frac{Y_t^2}{2}\right)^2-16\ln\frac{Y_t^2}{2}+23+\frac{\pi^2}{3}\right\}\Bigg],
\end{aligned} \tag{5.15}$$

where $i\,,j$ denote the generation index of light and heavy neutrinos respectively. The absolute stability of the electroweak vacuum implies $\tilde{\lambda} \geq 0$ up to Planck scale. However, as shown in [141], the absolute stability is highly restrictive. In this light we shall consider metastability i.e., transition time from a metastable vacuum towards instability should be greater than the age of the universe. In other words the transition probability through quantum tunneling should be less than unity.

The tunneling probability within the semi-classical approximation is given by (at zero temperature) [145–148],

$$p = \max_{\mu<\Lambda} V_U\,\mu^4\,\exp\left(-\frac{8\pi^2}{3|\lambda(\mu)|}\right), \tag{5.16}$$

where Λ is the cutoff scale and V_U is volume of the past light-cone, taken as τ^4. Here τ is the age of the universe taken from Planck data as $\tau = 4.35\times10^{17}$ sec. For the vacuum to be metastable, one should have $p<1$ which can be recast in terms of a lower bound on λ given by

$$|\lambda| < \lambda_{\rm meta}^{\rm max} = \frac{8\pi^2}{3}\frac{1}{4\ln(\tau\mu)}. \tag{5.17}$$

The above equation can be utilized to put an upper bound on $\mathrm{Tr}[Y_\nu^\dagger Y_\nu]$ from the running of λ as a function of the heavy neutrino mass M_R. This has been displayed in Fig. 5.3 by horizontal slanting lines corresponding to different choices of the top mass and strong coupling. Now, the region below this line is consistent with the metastability bound.

5.3 Lepton Flavor Violation bound

Lepton flavor violating decay processes get significant contribution from the heavy neutrino due to its relatively low mass scale compared to the canonical seesaw mechanism. The experimental upper limit on $\mu \to e\,\gamma$ processes can be translated to an upper bound on $\mathrm{Tr}[Y_\nu^\dagger Y_\nu]$ as a function of M_R. The branching ratio for $\mu \to e\gamma$ [149] is given by

$$\mathrm{Br}\,(\mu \to e\gamma) = \frac{3\,\alpha}{8\,\pi}\left|\sum_j V_{ej} V_{j\mu}^\dagger f(x_j)\right|^2 , \tag{5.18}$$

where the dependence on the heavy neutrino mass is expressed in terms of the dimensionless parameter $x_j = (M_{R_j}^2/m_W^2)$ by a slowly varying function,

$$f(x) = \frac{x\,(1 - 6\,x + 3\,x^2 + 2\,x^3 - 6\,x^2 \ln x)}{2\,(1-x)^4} \,. \tag{5.19}$$

In present case, right handed neutrinos are degenerate, *i.e.*, $M_{R_j} = M_R$. The light-heavy mixing matrix V is obtained through the diagonalization of the full neutral lepton mass matrix and is given by [152],

$$V = m_D^\dagger \left(M^{-1}\right)^* U_R \,, \tag{5.20}$$

where U_R is a unitary matrix** that diagonalizes M. Using Eq. 5.3 and 5.20 with Eq. 5.18 one gets,

$$\mathrm{Br}\,(\mu \to e\gamma) = \frac{3\,\alpha}{8\,\pi\,M_R^2}\left[f\left(\frac{M_R^2}{m_W^2}\right)\right]^2 \left|U_{\mathtt{PMNS}}\sqrt{m_\nu^d}\,R^\dagger R\,\sqrt{m_\nu^d}\,U_{\mathtt{PMNS}}^\dagger\right|^2 \tag{5.21}$$

and $\mathrm{Tr}[Y_\nu^\dagger Y_\nu]$ is given by Eq. 5.8. From Eq. 5.21, 5.8 and 5.8 one can see that the angular and phase dependence of the branching ratio comes from the $U_{\mathtt{PMNS}}$,

**U_R is the identity matrix in the present scenario as M is diagonal.

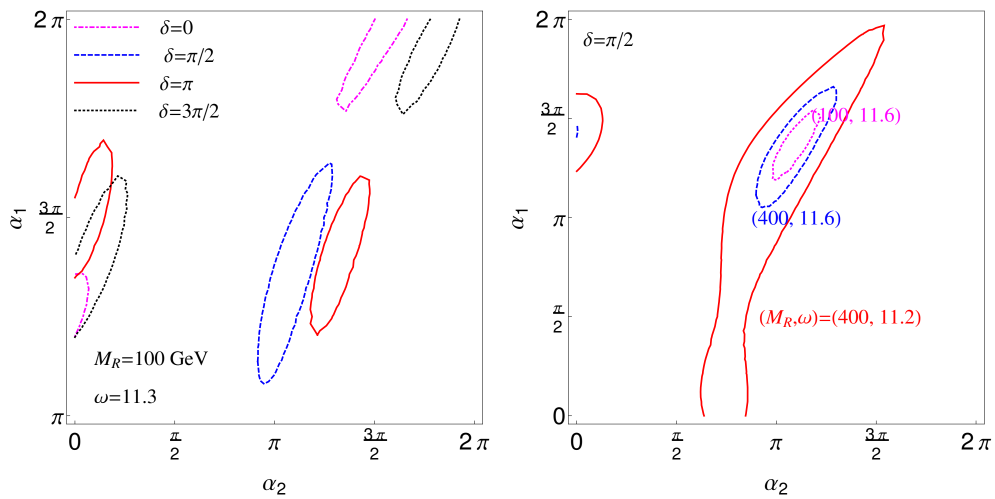

Figure 5.2: (Left panel) Contours of allowed lepton flavor violating regions with Br $(\mu \to e\gamma) = 5.7 \times 10^{-13}$ in the parameter plane of Majorana phases α_1 and α_2 with different values of Dirac CP phase δ. Taking all the neutrino oscillation parameters and mass differences at the global best-fit values, the area within each contours are consistent with the experimental LFV upper bound from the decay rate of $\mu \to e\,\gamma$. The Right panel demonstrates the variation of these LFV equality contours for different choices of the heavy neutrino mass M_R and parameter ω considering one example ($\delta = \pi/2$) contour from the left panel. As expected, on decreasing M_R or increasing ω the area under the contour shrinks, retaining a smaller window for choices of these unknown parameters.

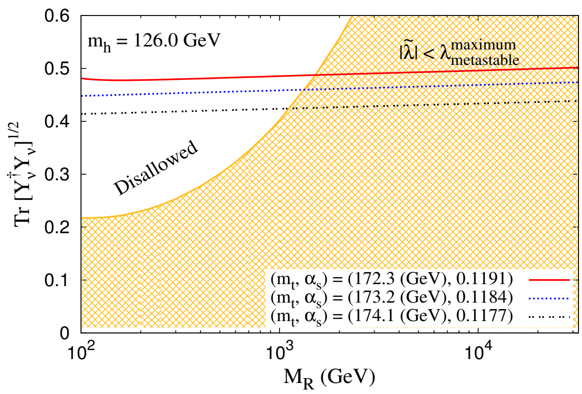

Figure 5.3: Allowed region of the Yukawa norm $\mathrm{Tr}[Y_\nu^\dagger Y_\nu]$ as a function of the heavy neutrino mass M_R by imposing combined constraints coming from metastability of the electroweak vacuum as well as lepton flavor violating decay $(\mu \to e\,\gamma)$. The SM Higgs mass is fixed at $m_h = 126$ GeV. The horizontal slanting lines represent the upper bound on $\mathrm{Tr}[Y_\nu^\dagger Y_\nu]$ consistent with the metastability bound, as in Eq. 5.17. The three lines are due to three different sets of values for the top mass and the strong coupling [150, 151]. The shaded area below the curved line is allowed from the lepton flavor violating constraint as given in Eq. 5.22. The yellow line corresponds to $\omega = 11.9$ and gives us the best choice for study within the bound of LFV. Hence, the region marked "Disallowed" is ruled out from LFV for such choice of ω.

whereas the magnitude of the branching ratio is encoded in $\sqrt{m_\nu^d}\, R^\dagger R\, \sqrt{m_\nu^d}$ whose modulus is proportional to $\mathrm{Tr}[Y_\nu^\dagger Y_\nu]$. The analytical expression of $\mathrm{Br}(\mu \to e\gamma)$ is somewhat lengthy and hence omitted here. Subjected to the present experimental upper bound on the $\mu \to e\,\gamma$ process [153]

$$\mathrm{Br}\,(\mu \to e\gamma) \leq 5.7 \times 10^{-13}, \tag{5.22}$$

one would obtain, numerically, an upper bound on $\mathrm{Tr}[Y_\nu^\dagger Y_\nu]$ by inverting Eq. 5.21.

In a numerical calculation with a very high degree of precision, it is observed that the $3\,\sigma$ uncertainty of the oscillation parameters together with all the phases varied in the full range [154] would not bound $\mathrm{Tr}[Y_\nu^\dagger Y_\nu]$. Hence an effective bound on $\mathrm{Tr}[Y_\nu^\dagger Y_\nu]$ is coming only from vacuum metastability. To probe this a little further, in Fig. 5.2 (left panel) we demonstrate the contours of allowed lepton flavor violating regions in the parameter plane of Majorana phases α_1 and α_2 with different values of Dirac CP phase[††] δ. Taking all neutrino oscillation parameters and mass differences at the global best-fit values the area within each contours are consistent with the experimental LFV upper bound from the decay rate of $\mu \to e\,\gamma$. Although not conspicuous from the analytic form of the multi-parameter expression from Eq. 5.21, one can estimate that a suitable and precise choice of δ and α parameters within such contours can indeed evade the bound. In the right panel of Fig. 5.2 we demonstrate the variation of these LFV equality contours for different choices of the heavy neutrino mass M_R and the parameter ω considering once such example ($\delta = \pi/2$) contour from the left panel. As expected, decreasing M_R or increasing ω would make the contour narrower retaining a smaller window of choices for these unknown parameters.

From our discussion above, it is clear that one can choose a parameter for any phenomenological analysis bounded by metastability. However, we took an approach to consider a conservative estimate for $\mathrm{Tr}[Y_\nu^\dagger Y_\nu]$ satisfying both LFV and vacuum metastability bounds. To begin with, we choose a particular set of oscillation parameters such as the global best-fit values of oscillation parameters. Now, if one examines the particular choices of these unknown phases which would be just enough to satisfy the equality of Eq. 5.22, they are essentially all the points

[††] In the 3σ range of oscillation parameters, the Dirac CP phase δ is allowed in its full range (0-2π). Also the Majorana phases $\alpha_{1,2}$ are not constrained by oscillation experiments, hence are varied in full range (0-2π). These three phases are considered here as unknown parameters.

residing over the contours shown in Fig. 5.2. All the points inside the contours will give BR($\mu \to e\gamma$) $< 5.7 \times 10^{-13}$. Since all the contours are drawn with a fixed ω value, the norm Tr[$Y_\nu^\dagger Y_\nu$] will be the same for all the contours shown in Fig. 5.2(left panel).

The dependence of the norm Tr[$Y_\nu^\dagger Y_\nu$] as a function of the heavy neutrino mass is depicted in Fig. 5.3. The upper bound on the norm is depicted by the golden solid line for $\omega = 11.9$. This gives us the best choice to study within the bound of LFV for this particular value of ω. The yellow shaded area below the curve is allowed[‡‡] from the lepton flavor violating constraint as used in Eq. 5.22. Hence, the region marked "Disallowed" is strictly ruled out from LFV for such choice of ω.

5.4 Neutrino Less Double Beta Decay

In this section we briefly discuss the contribution of this particular model towards neutrino less double beta decay ($0\nu\beta\beta$). The general expression of half-life for $0\nu\beta\beta$ in the context of Type-I seesaw is given by [155, 156]

$$T_{\frac{1}{2}}^{-1} = G\,\frac{|\mathcal{M}_\nu|^2}{m_e^2}\left|\sum_i \left(U_{\texttt{PMNS}}\right)_{e\,i}^2\,\left(m_\nu^d\right)_i + \sum_j \langle p^2\rangle \frac{V_{e\,j}^2}{M_{R_j}}\right|^2 , \tag{5.23}$$

where $G = 7.93 \times 10^{-15}$ yr^{-1}, $\mathcal{M}_\nu$ is the nuclear matrix element due to light neutrino exchange and m_e being the electron mass. $\langle p^2\rangle$ in the second term, which is due to the contributions from heavy singlet neutrinos, is given by [157]

$$\langle p^2\rangle = -\,m_e\,m_p \frac{\mathcal{M}_N}{\mathcal{M}_\nu}\,, \tag{5.24}$$

which is taken to be $\langle p^2\rangle = -\,(182\text{ MeV})^2$ [155]. Here m_p is the proton mass and $\mathcal{M}_N$ is the nuclear matrix element due to heavy neutrino exchange.

The first and the second term in Eq. 5.23 represent contributions from light and heavy neutrinos respectively and thus summed over corresponding number of light(heavy) neutrinos. Accordingly with the help of Eq. 5.3 and 5.20, the second

[‡‡]This is over the choice of decreasing values of ω parameters.

term can be expressed as,

$$\frac{\langle p^2 \rangle}{M_R^2} \left(U_{\texttt{PMNS}} \sqrt{m_\nu^d}\, R^\dagger R^* \sqrt{m_\nu^d}\, U_{\texttt{PMNS}}^T \right)_{e\,e} = \frac{\langle p^2 \rangle}{M_R^2} \left(U_{\texttt{PMNS}} \right)_{e\,i}^2 \left(m_\nu^d \right)_i \,. \tag{5.25}$$

Consequently Eq. 5.23 becomes

$$T_{\frac{1}{2}}^{-1} = G \, \frac{|\mathcal{M}_\nu|^2}{m_e^2} \left(1 + \frac{\langle p^2 \rangle}{M_R^2} \right)^2 \left| \left(U_{\texttt{PMNS}} \right)_{e\,i}^2 \left(m_\nu^d \right)_i \right|^2 \,. \tag{5.26}$$

One can notice that the contribution on $0\nu\beta\beta$ from heavy neutrinos is extremely tiny, *e.g.* only 0.001% of the light neutrino contribution can come towards the half-life of $0\nu\beta\beta$ even for a heavy neutrino mass of 100 GeV. This contribution is even suppressed as the mass increased. Although light neutrino contribution to the neutrino less double beta decay can be sizable and can possibly be explored in the future experiments [158], the heavy neutrino contribution in this scenario can be neglected. This outcome is not surprising if one follows from Eq. 5.25. The large values in the matrix R, which is essential to obtain large Dirac Yukawa, gets canceled. Finally we get very small value of $(VV^T)_{\ell\ell}$ for same sign di-lepton (SSDL) production. In the same ground collider production of SSDL is suppressed and hence not considered although the heavy neutrino is of Majorana type. Interestingly, this is a general consequence of Casas-Ibarra parameterization when the heavy neutrinos are degenerate. At the same time large Yukawa makes the opposite sign di-lepton (OSDL) cross section (which is proportional to $(VV^\dagger)_{\ell\ell}$) sizable. Large SM background in this channel compelled us to consider for tri-lepton signal at the LHC. In the next section, we would explore the production of these heavy neutrinos at the collider and discuss the discovery potential for 14 TeV large hadron Collider.

5.5 Collider Phenomenology

Heavy neutrinos can be produced dominantly by s-channel W-boson exchange at the hadron collider. We also explore the corresponding vector boson fusion (VBF) production associated with two forward jets. At the leading order, parton

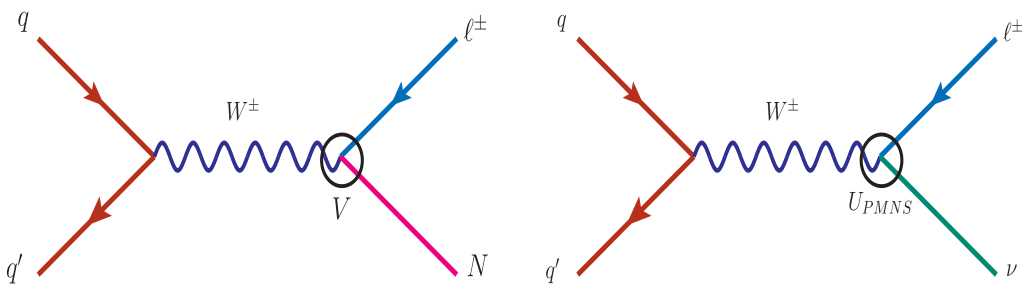

Figure 5.4: (Left panel)Production of heavy neutrino via the $s-$ channel W boson production mode. The corresponding $W-\ell-N$ vertex is the heavy-light mixing matrix, V as defined in Eq. 5.20. (Right panel) The corresponding Standard Model production channel $W \to \ell\nu$, where the $W-\ell-\nu$ vertex is the U_{PMNS} matrix element.

level processes producing heavy neutrinos (N) in the mass basis are as follows:

$$\begin{aligned} q\bar{q}' &\longrightarrow W^{\pm *} \longrightarrow l^{\pm}\, N \quad \text{(s-channel)}, \\ qq' &\longrightarrow l^{\pm}\, N\, q\, q'' \quad \text{(VBF)}\ , \end{aligned} \tag{5.27}$$

where q represents a suitable parton and the associated leptons are $l \equiv (e,\, \mu,\, \tau)$. In Fig. 5.4 (left panel) we have shown the s-channel production model of the heavy neutrino associated with a charged lepton. The heavy-light mixing matrix V is responsible for this channel as shown in the figure. The matrix V is defined as $V = m_D^{\dagger}\,(M^{-1})^*\,U_R$ where $m_D = Y_{\nu}\dfrac{v}{\sqrt{2}}$. As we have shown in Fig. 5.1 the value of the Dirac Yukawa coupling (Y_{ν}) can be large and it is possible to probe heavy neutrinos at the LHC. For comparison we have also shown the corresponding Standard Model production channel. For the SM the $W-\ell-\nu$ vertex is proportional to the PMNS matrix as defined in Eq. 5.4.

In Fig. 5.5 (left panel) the total cross section for these processes is shown as a function of the heavy neutrino mass after applying the pre-selection cuts i.e., $p_{T_l} > 20$ GeV and $|\eta_l| < 2.5$. The solid (dashed) line shows the leading order production cross section through the s-channel (VBF) process. From the figure it is evident that the VBF cross section is insufficient for discovery at the LHC, and we shall not discuss this production mechanism afterwards and concentrate only on s-channel process for phenomenological analysis.

For our simulation we consider the maximum allowed value coming from $\mathrm{Tr}[Y_{\nu}^{\dagger}Y_{\nu}]$ satisfying combined LFV and metastability bounds as depicted in Fig. 5.3,

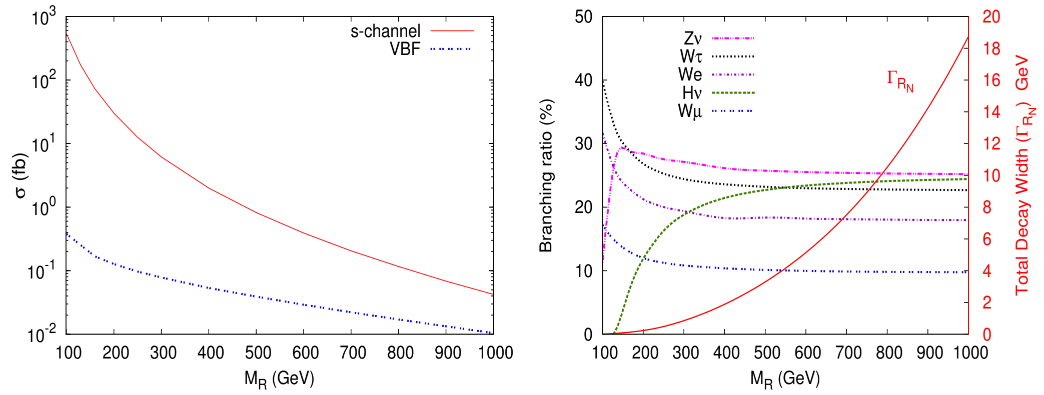

Figure 5.5: (Left panel) Total cross section is plotted for leading order s-channel heavy neutrino production (solid line) associated with charged lepton at the 14 TeV LHC. Basic pre-selection cuts $p_{T\ell} \geq 20$ GeV and $|\eta_\ell| \leq 2.5$ are applied and choice of parameters are compatible with the neutrino oscillation data constrained with vacuum metastability and LFV. The dotted line shows the corresponding VBF production cross section, where basic VBF cuts were used in addition to the pre-selection cuts. (Right panel) Demonstration of the decay branching ratios of the heavy neutrino in different channels as a function of mass. Total decay width is also shown with red-solid line.

together with the neutrino oscillation data within their uncertainties. One can notice that the higher values of Yukawa coupling are permitted from these constraints once we move towards higher masses of heavy neutrinos. We have used `MadGraph5` [160] to simulate the production and decay of heavy neutrinos. Parton distribution functions `CTEQ6L1` [161] have been used and the factorization scale is set at the heavy neutrino mass.

A heavy neutrino can decay into weak gauge bosons $(W^\pm, Z)$ or the Higgs boson (H) in association with leptons because of mixing between light and heavy neutrinos:

$$N \longrightarrow W^\pm l^\mp / Z\nu_l / H\nu_l. \tag{5.28}$$

Branching ratios of N in these channels are shown in Fig. 5.5 (right panel) with varying heavy neutrino mass M_R. In this plot the red-solid line shows the total decay width (Γ_N) of the heavy neutrino. The figure manifests that the $W\tau$ channel is the dominant decay mode for the low mass region and saturates at $\sim 22\%$ for $M_R \gtrsim 400$ GeV. Both $H\nu$ and $Z\nu$ channels saturate at $\sim 25\%$ in the high mass region leaving approximately 18%(10%) for the $We(W\mu)$ channel.

To analyze signals for heavy neutrino, we have implemented this model in

Selection Criteria	
Lepton identification criteria	$\|\eta_\ell\| < 2.5$ and $p_{T\ell} > 20$ GeV
Detector efficiency for leptons	Electron efficiency (for e^- & e^+): 0.7 (70%) Muon efficiency (for μ^- & μ^+): 0.9 (90%)
Smearing	Gaussian smearing of electron energy and muon p_T
Jet reconstruction	`PYCELL` cone algorithm in `PYTHIA`
Lepton-jet separation	$\Delta R_{lj} \geq 0.4$ (for all jets)
Lepton-lepton separation	$\Delta R_{ll} \geq 0.2$
Lepton-photon separation	$\Delta R_{l\gamma} \geq 0.2$ for all $p_{T_\gamma} > 10$ GeV
Hadronic activity (To consider leptons with very less hadronic activity around them.)	Hadronic activity for each lepton: $\frac{\sum p_{T_{hadron}}}{p_{T_l}} \leq 0.2$ ($\equiv$ radius of the cone around the lepton)
Final p_T cuts for leptons	$p_{T_{l_1}} > 30$ GeV, $p_{T_{l_2}} > 30$ GeV and $p_{T_{l_3}} > 20$ GeV
Missing p_T cut	$\not{p}_T > 30$ GeV
Z-veto[a]	$\|m_{\ell_1\ell_2} - M_Z\| \geq 6\Gamma_Z$
VBF Cuts	
Central jet veto	On any additional jet with $p_{T3} > 20$ GeV, and $\|\eta_0\| < 2$ events are discarded. Pseudorapidity difference between the average of the two forward jets and the third jet: $\eta_0 = \eta_3 - (\eta_1 + \eta_2)/2$.
Pseudorapidity [159] of charged leptons	$\eta_{j,min} < \eta_\ell < \eta_{j,max}$
Cut applied to jets	$p_{T\,j_1,j_2} > 20$ GeV $M_{j_1j_2} > 600$ GeV $\eta_{j_1} \cdot \eta_{j_2} < 0$ and $\|\eta_{j_1} - \eta_{j_2}\| > 4$

Table 5.1: Selection criteria used in simulation.

[a]Z-veto: Invariant mass for the same flavored and opposite sign lepton pair, $m_{\ell_1\ell_2}$, must be sufficiently away from Z pole.

`FeynRules` [162] to generate the Feynman rules compatible with `MadGraph`. Parton level cross sections were generated using `MadGraph5` and for showering and hadronization of the lhe [163] event file, `PYTHIA6` [164] has been used.

To enhance the signal over background, selection criteria tabulated in Table. 5.1 have been implemented. In the top portion of this table, all selection parameters and efficiencies are listed. Cuts entitled "VBF cuts" are applied only for the VBF part of the analysis. For detail see references [118, 122].

Signal Estimation

Following from our earlier discussion on heavy neutrino production and decay, we are looking for tri-lepton production at the LHC,

$$pp \to \ell^\pm N \to \ell^\pm(W^\pm\ell^\mp/Z\nu) \to e^\pm e^\pm e^\mp/e^\pm\mu^\pm e^\mp/e^\pm\mu^\pm\mu^\mp/\mu^\pm\mu^\pm\mu^\mp + \not{E}_T.$$

Total signal cross section (fb)	Flavor allocated cross section (fb)			
	eee	$ee\mu$	$e\mu\mu$	$\mu\mu\mu$
2.732	0.318	1.144	1.030	0.2

Table 5.2: Final tri-lepton with $\not{E}_T$ signal cross section in fb produced through s-channel heavy neutrino for the benchmark mass $M_R = 100$ GeV at the 14 TeV LHC. All event selection cuts were applied (Table 5.1) except the VBF cuts as described in the text. We have also classified total tri-lepton signals into four different flavor combination of leptons and presented expected cross section in each category.

Cross section of final tri-lepton signal through s-channel heavy neutrino production at 14 TeV LHC for a benchmark point of $M_R = 100$ GeV is listed in Table 5.2. Here we have incorporated all event selection criteria except the VBF cuts. Total contribution from all the light leptons (e, μ) as well as the differential contributions from the four flavor combinations are also presented.

Background Analysis

All the Standard Model channels which can mimic this tri-lepton signal with missing E_T are considered for the estimation of the SM background. For such simulation, events are generated using `ALPGEN` [165] at the parton level and then passed on `PYTHIA` for hadronization and showering. We have used the same selection criteria as tabulated in Table 5.1. The inclusive cross section for the $\ell^\pm\ell^\pm\ell^\mp\nu_\ell$ final state from the SM is 32.722 fb. Details of contributions from individual channels towards the SM background can be found in [118, 122, 166].

Discovery potential at the LHC

With our understanding of the signal strength for producing tri-leptons from heavy neutrino and possible sources of leading background, it is convenient to present our result in terms of significance which we express as $S/\sqrt{S+B}$, where $S\,(B) = \mathcal{L}\,\sigma_{S\,(B)}$. $\mathcal{L}$ is the integrated luminosity of available data from the experiment and $\sigma_{S(B)}$ is the final cross section of the signal (background) after all event selection cuts and with model parameters satisfying metastability and LFV bounds. Fig. 5.6 depicts 3σ(magenta) and 5σ(blue) constant significance contours

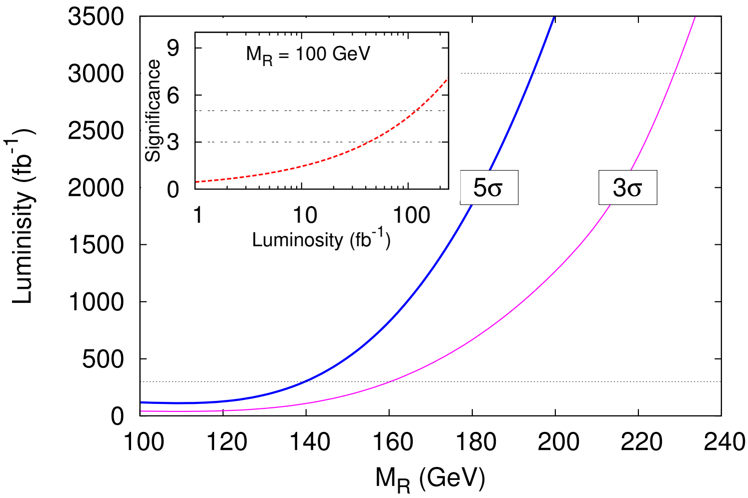

Figure 5.6: Contours of constant 3σ and 5σ significance at the 14 TeV LHC in terms of heavy neutrino mass M_R and integrated luminosity. With 300fb^{-1} data tri-lepton signal can probe upto M_R = 160(140) GeV with $3\sigma(5\sigma)$ significance, whereas with 3000fb^{-1} luminosity LHC can reach up to 230(190) GeV. Inset shows variation of significance for the s-channel tri-lepton production signal and backgrounds with heavy neutrino mass $M_R = 100$ GeV.

at the 14 TeV LHC in terms of heavy neutrino mass and integrated luminosity. Horizontal black-dotted lines represent integrated luminosities of 300 fb^{-1} and 3000 fb^{-1}. This model can be probed through tri-lepton signals at the 14 TeV LHC upto M_R = 160(140) GeV with $3\sigma(5\sigma)$ significance with integrated luminosity of $300 fb^{-1}$. Whereas with higher luminosity of 3000fb^{-1} it can be probed upto $\sim 230(190)$ GeV. Inset of the figure demonstrates the expected significance of the s-channel tri-lepton production from heavy neutrino with mass $M_R = 100$ GeV as a function of integrated luminosity. We note that $3\,\sigma(5\,\sigma)$ significance can be achieved with integrated luminosity $\sim 43(120)$fb^{-1}.

5.6 Conclusion

In this chapter we have considered a TeV scale seesaw model that leads to quasi degenerate light neutrino mass spectrum. The model is fully reconstructible from oscillation parameters apart from an unknown factor parameterized by a constant ω for a particular light and heavy neutrino mass scale, m_ν^d and M_R respectively. We have demonstrated that the norm of Yukawa, Tr$[Y_\nu^\dagger Y_\nu]$, can have arbitrary magnitude with different choices of ω and the common light neutrino mass scale

m_0. Consequently, we have obtained bounds on $\mathrm{Tr}[Y_\nu^\dagger Y_\nu]$ from both the consideration of the metastability of the electroweak vacuum as well as lepton flavor violation. Mass scale of QD light neutrinos is set at $m_0 = 0.07$ eV. Extremely fine-tuned choices of unknown phases evade bounds on $\mathrm{Tr}[Y_\nu^\dagger Y_\nu]$ from LFV. However, bulk region of parameters allows us a stronger LFV bound than that of metastability in the low M_R regions. Beyond that mass range, LFV bound becomes weaker than the metastability bound. The later remains slowly varying with M_R. However, contribution of the heavy neutrino towards neutrinoless double beta decay is insignificant in this model compared to the light neutrino contribution.

The constrained model parameters were then used to study the production and decay modes of the heavy neutrino at the LHC. Due to suppressed same sign di-lepton signal in this model, we have studied tri-lepton associated with missing E_T signal coming from the s-channel production of the heavy neutrino with realistic selection criteria as well as detailed simulation. However, a similar signal along with two forward tagged jets, coming through the production of heavy neutrino perceived in vector boson fusion comes with much smaller cross section at the present scenario. With a benchmark point of heavy neutrino mass $M_R = 100$ GeV, we have presented the discovery potential of heavy neutrino, fitted to the model, with $3\,\sigma\,(5\,\sigma)$ significance for integrated luminosity $\sim 42(120)$ fb^{-1} at the 14 TeV LHC. Moreover, this model can be probed (at $3\,\sigma$) for heavy neutrino mass upto 160(230) GeV for low(high) luminosity options.

Chapter 6

Summary and Outlook

Quest for the SM Higgs boson finally comes to an end after the observation of the Higgs boson at the LHC by CMS and ATLAS collaborations. The discovery completes the SM and obtained data do not show any major deviation from the SM expectations as yet. This leads us to a precision era, and, precise measurements of the Higgs boson couplings are very crucial. The measured mass of the Higgs boson is

$$m_H = 125.09 \pm 0.21 \ \ (\text{stat}) \ \pm 0.11 \ \ (\text{syst}) \quad \text{GeV}. \tag{6.1}$$

It has been noted that the SM vacuum is not stable up to the Planck scale for most values in the allowed range for the top-quark mass, the Higgs mass and the strong coupling α_s. This indicates the existence of new physics which can take care of the stability issue. Also there are several other experimental evidences for BSM scenarios, neutrino oscillation being one of them. Neutrino oscillation indicates that neutrino have a tiny mass and there must be some mechanism to generate it. The most popular mechanism of neutrino mass generation is the 'seesaw' mechanism.

In the run-I, the LHC has delivered the long sought Higgs boson and is now running with a higher energy of 13 TeV to find signatures of BSM. Since BSM scenarios often contain extended scalar sectors, it is worthwhile to study and constrain the parameter space of the scalar sector of these models. This helps to search for these models at colliders like LHC. Any good theory should follow some properties like unitarity, perturbativity and also vacuum stability which is used to constrain new physics models.

One of the minimal extensions of the SM is the gauged $U(1)_{B-L}$ model, where an extra $U(1)$ gauge group is appended to the SM gauge group. Three RH neutrinos naturally arise for the sake of anomaly cancellation which also help to generate light neutrino masses via the seesaw mechanism. Apart from the heavy neutrinos there exist a neutral gauge boson Z' and a heavy Higgs boson along with the SM particles. The model can have interesting phenomenology at the LHC owing to signatures for Z' or RH neutrinos. Also this model can accommodate a dark matter(DM) candidate provided the DM is stable due to an additional $\mathbb{Z}_2$ symmetry. We have studied vacuum stability and perturbativity and constrained different parameters of the model. In another study we have explored the possibility that the $B-L$ gauge symmetry can be broken at a very high energy scale, say $\sim 10^{16}$ GeV. In this case the tree level threshold correction can be crucial to stabilize the EW vacuum. This model with high-scale $B-L$ breaking can explain inflationary dynamics where the heavy Higgs boson is the inflaton.

We have also studied the Left-Right symmetric model. Being a very simple gauge group extension of the SM and giving a rich dividend in BSM phenomena, Left-Right symmetric models are phenomenologically interesting in their own right. The scalar sector of this model is quite rich due to the fact that an enlarged scalar sector is required for breaking the Left-Right symmetric group to the SM gauge group. We analyzed the scalar sector of the Left-Right symmetric standard model with triplet scalars in the light of various theoretical and experimental constraints. The scalar sector comprising of one bi-doublet, one left handed and one right handed triplet ultimately gives rise to fourteen physical scalars. The lightest among them is expected to be the recently discovered Higgs boson with mass around 125 GeV. We constrain the masses of the other physical scalars by using unitarity constraints. We obtain these constraints by evaluating the various zeroth order partial wave amplitude for $2 \to 2$ scattering. We find that for any Left-Right symmetry breaking scale, unitarity bounds put severe constraints on quartic couplings compared to those coming from perturbativity. We also demonstrated that some of the physical scalars can have the masses in the TeV range and can have interesting LHC prospects. It is to be noted that the masses of these scalars are dependent on the Left-Right symmetry breaking scale v_R and consequently the obtained bounds are highly sensitive to this v_R.

Both the models discussed above are gauge extension of the SM, whereas it is also possible to extend only the particle content of the SM to explain neutrino mass generation keeping the gauge group same as that of the SM. We have considered this kind of model where the new particles are of TeV mass scale. The model is fully reconstructible from oscillation parameters apart from an unknown factor parameterized by a constant ω for specific light and heavy neutrino mass scales, m_ν^d and M_R respectively. We have demonstrated that the norm of the Yukawa matrix, $\mathrm{Tr}[Y_\nu^\dagger Y_\nu]$ can be chosen of arbitrary magnitude with different choices of ω and the common light neutrino mass scale m_0. Consequently we have obtained bounds on $\mathrm{Tr}[Y_\nu^\dagger Y_\nu]$ both from the consideration of the metastability of the electroweak vacuum as well as lepton flavor violation. The mass scale of quasi-degenerate light neutrinos is set at $m_0 = 0.07$ eV. Extremely fine-tuned choices of unknown phases evade the bound on $\mathrm{Tr}[Y_\nu^\dagger Y_\nu]$ from LFV. However bulk of the region of parameters allows us a stronger LFV bound than that of the metastability in the low M_R regions. Beyond that mass range, the LFV bound becomes weaker than the metastability bound. The latter remains slowly varying with M_R. However, the contribution of the heavy neutrino towards the neutrinoless double beta decay is insignificant in this model compared to the light neutrino contribution.

The constrained model parameters were then used to study the production and decay modes of the heavy neutrino at the LHC. Due to the suppressed signature of the same sign di-lepton signal in this model, we have studied tri-lepton associated with missing E_T signal coming from the s-channel production of the heavy neutrino with realistic selection criteria as well as detailed simulation. However, a similar signal along with two forward tagged jets, coming through the production of heavy neutrino through vector boson fusion comes with a much smaller cross section in the present scenario. With a benchmark point of heavy neutrino mass $M_R = 100$ GeV, we have presented the discovery potential for the heavy neutrino, fitted to the model, with $3\,\sigma\,(5\,\sigma)$ significance for integrated luminosity $\sim 42(120)$ fb^{-1} at the 14 TeV LHC. Moreover, this model can be probed for heavy neutrino mass upto 160(230) GeV for low(high) luminosity options.

To summarize, we have studied scale dependent properties like vacuum stability, unitarity and perturbativity for different BSM scenarios. All the scenarios under consideration can explain generation of tiny neutrino masses. In our study we have shown how the scale dependent properties can restrict the parameters of BSM scenarios. We have also shown that for LRSM with triplet scalars the quartic couplings which are inaccessible to colliders like LHC can be constrained solely from perturbativity or unitarity. Mostly the scalar sector of the models is constrained, but in the case of TeV scale seesaw model the Dirac Yukawa couplings are restricted.

Appendix A

Renormalization Group Evolution Equations

A.1 Standard Model RGEs

For Standard Model we have used renormalization group evolution equations from [19] with matching conditions for top Yukawa and Higgs quartic coupling at their pole masses.

A.2 $U(1)_{B-L}$ Model

Gauge RG Equations

Renormalization group equations for $SU(3)_C$ and $SU(2)_L$ gauge couplings g_3 and g_2:

$$\begin{aligned}
16\pi^2 \frac{d}{dt} g_3 &= g_3^3 \Big[-1 + \frac{4}{3} n_g \Big] = \frac{g_3^3}{16\pi^2} \Big[-7 \Big] \\
16\pi^2 \frac{d}{dt} g_2 &= g_2^3 \Big[-\frac{22}{3} + \frac{4}{3} n_g + \frac{1}{6} \Big] = \frac{g_2^3}{16\pi^2} \Big[-\frac{19}{6} \Big]
\end{aligned}$$

where n_g is number of generations.

Renormalization group equations for Abelian gauge couplings $g_1,\ g_{B-L}$ and $\widetilde{g}$:

$$
\begin{aligned}
16\pi^2 \frac{d}{dt} g_1 &= \left[\frac{41}{6}\ g_1^3\right] \\
16\pi^2 \frac{d}{dt} g_{B-L} &= \left[12\ g_{B-L}^3 + \frac{32}{3} g_{B-L}\widetilde{g} + \frac{41}{6} g_{B-L}\widetilde{g}^2\right] \\
16\pi^2 \frac{d}{dt}\widetilde{g} &= \left[\frac{41}{6}\ \widetilde{g}(\widetilde{g}^2 + 2g_1^2) + \frac{32}{3}\ g_{B-L}(\widetilde{g}^2 + g_1^2) + 12\ g_{B-L}^2\widetilde{g}\right]
\end{aligned}
$$

Fermion RG Equations

RG evolution equation for top quark Yukawa coupling Y_t:

$$
16\pi^2 \frac{d}{dt} Y_t = Y_t \left[\frac{9}{2} Y_t^2 - 8g_3^2 - \frac{9}{4} g_2^2 - \frac{17}{12} g_1^2 - \frac{17}{12}\widetilde{g}^2 - \frac{2}{3} g_{B-L}^2 - \frac{5}{3}\widetilde{g} g_{B-L}\right]
$$

In case of RH neutrinos RGEs we are considering degenerate RH neutrino Yukawa coupling and we are in a basis where these couplings are diagonal, then we have :

$$
16\pi^2 \frac{d}{dt} y_i^h = y_i^h \left[4(y_i^h)^2 + 2\ \mathrm{Tr}\big[(y^h)^2\big] - 6g_{B-L}^2\right]
$$

Scalar RG Equations

RGEs for the scalar couplings $\lambda_1,\ \lambda_2$ and λ_3 are :

$$
\begin{aligned}
16\pi^2 \frac{d}{dt}\lambda_1 &= \Big[24\lambda_1^2 + \lambda_3^2 - 6Y_t^4 + \frac{9}{8} g_2^4 + \frac{3}{8} g_1^4 + \frac{3}{4} g_2^2 g_1^2 + \frac{3}{4} g_2^2\widetilde{g}^2 + \frac{3}{4} g_1^2\widetilde{g}^2 \\
&\quad + \frac{3}{8}\widetilde{g}^4 + 12\lambda_1 Y_t^2 - 9\lambda_1 g_2^2 - 3\lambda_1 g_1^2 - 3\lambda_1\widetilde{g}^2\Big] \\
8\pi^2 \frac{d}{dt}\lambda_2 &= \left[10\lambda_2^2 + \lambda_3^2 - \frac{1}{2}\mathrm{Tr}\big[(y^h)^4\big] + 48 g_{B-L}^4 + 4\lambda_2 \mathrm{Tr}\big[(y^h)^2\big] - 24\lambda_2 g_{B-L}^2\right] \\
8\pi^2 \frac{d}{dt}\lambda_3 &= \lambda_3\left[6\lambda_1 + 4\lambda_2 + 2\lambda_3 + 3Y_t^2 - \frac{3}{4}(3g_2^2 - g_1^2 - \widetilde{g}^2) + 2\ \mathrm{Tr}\big[(y^h)^2\big] - 12 g_{B-L}^2\right] \\
&\quad + 6\widetilde{g}^2 g_{B-L}^2
\end{aligned}
$$

A.3 LR Model with Triplet Scalars

Gauge RG Equations

$$\begin{aligned}
16\pi^2 \frac{d}{dt} g_3 &= g_3^3 \Big(-7 \Big) \\
16\pi^2 \frac{d}{dt} g_2 &= g_2^3 \Big(-\frac{15}{6} \Big) \\
16\pi^2 \frac{d}{dt} g_{B-L} &= g_{B-L}^3 \Big(\frac{28}{9} \Big)
\end{aligned}$$

Note that in our case $g_{2L} = g_{2R} = g_2$.

Fermion RG Equations

$$\begin{aligned}
16\pi^2 \frac{d}{dt} Y_t &= \Big[8Y_t^3 - Y_t \big(\frac{2}{3} g_1^2 - \frac{9}{2} g_2^2 - 8 g_3^2 \big) \Big] \\
16\pi^2 \frac{d}{dt} Y_i^M &= \Big[2Y_i^M \Big(-\frac{3}{4} g_1^2 - \frac{9}{4} g_2^2 \Big) + 2Y_i^M \mathrm{Tr}\big[(Y^M)^2 \big] + 6(Y_i^M)^3 \Big]
\end{aligned}$$

Scalar RG Equations

To write down scalar RG equations, We classified 15 scalar couplings into three categories depending on how they coupled with scalar fields.

- **Coefficients with Φ^4**

$$\begin{aligned}
16\pi^2 \frac{d}{dt} \lambda_1 &= 32\lambda_1^2 + \frac{5}{3}\lambda_{12}^2 + \frac{1}{2}\lambda_{13}^2 + 2\lambda_{14}^2 + 64\lambda_2^2 + 16\lambda_1\lambda_3 + 16\lambda_3^2 \\
&\quad + 48\lambda_4^2 + 6\lambda_{12}\lambda_9 + 6\lambda_9^2 + 12\lambda_1 Y_t^2 - 6Y_t^4 - 18\lambda_1 g_2^2 + 3g_2^4 \\
16\pi^2 \frac{d}{dt} \lambda_2 &= 6(\lambda_{10}^2 - \lambda 11^2) + \frac{3}{2}\lambda_{14}\lambda_{15} + 24\lambda_1\lambda_2 + 48\lambda_2\lambda_3 \\
&\quad +12\lambda_4^2 + 12\lambda_2 Y_t^2 - 18\lambda_2 g_2^2 \\
16\pi^2 \frac{d}{dt} \lambda_3 &= 12(\lambda_{10}^2 + \lambda_{11}^2) - (\lambda_{12}^2 - \lambda_{13}^2) - \frac{1}{2}(\lambda_{14}^2 + \lambda_{15}^2) + 128\lambda_2^2 \\
&\quad +24\lambda_1\lambda_3 + 16\lambda_3^2 + 24\lambda_4^2 + 12\lambda_3 Y_t^2 + 3Y_t^4 - 18\lambda_3 g_2^2 + \frac{3}{2} g_2^2 \\
16\pi^2 \frac{d}{dt} \lambda_4 &= 48\lambda_4(\lambda_1 + 2\lambda_2 + \lambda_3) + 6\lambda_{10}(2\lambda_9 + \lambda_{12}) \\
&\quad + \frac{3}{2}\lambda_{13}(\lambda_{14} + \lambda_{15}) + 12\lambda_4 Y_t^2 - 18\lambda_4 g_2^2
\end{aligned}$$

- **Coefficients with Δ^4**

$$
\begin{aligned}
16\pi^2\frac{d}{dt}\lambda_5 &= 28\lambda_5^2+16\lambda_6(\lambda_5+\lambda_6)+16(\lambda_{10}^2+\lambda_{11}^2)+2\lambda_{12}^2+3\lambda_7^2\\
&\quad +4\lambda_9(\lambda_9+\lambda_{12})+2\lambda_5Y_t^2-16Y_t^4-12\lambda_5g_{_{B-L}}^2\\
&\quad +6g_{_{B-L}}^4+12g_{_{B-L}}^2g_2^2-24\lambda_5g_2^2+9g_2^4\\
16\pi^2\frac{d}{dt}\lambda_6 &= 12\lambda_6(\lambda_6+2\lambda_5-g_{_{B-L}}^2-2g_2^2)+12\lambda_8^2\\
&\quad -\lambda_{12}^2+8Y_t^4+8\lambda_6Y_t^2-12g_{_{B-L}}^2g_2^2+3g_2^4\\
16\pi^2\frac{d}{dt}\lambda_7 &= 4\lambda_7^2+16\lambda_7(2\lambda_5+\lambda_6)+32(\lambda_{10}^2-\lambda_{11}^2)+2(\lambda_{12}^2+\lambda_{13}^2)\\
&\quad +4(\lambda_{14}^2+\lambda_{15}^2)+32\lambda_8^2+8\lambda_{12}\lambda_9+\lambda_9^2\\
&\quad +8\lambda_7Y_t^2-12\lambda_7(g_{_{B-L}}^2+g_2^2)+12g_{_{B-L}}^4\\
16\pi^2\frac{d}{dt}\lambda_8 &= \lambda_{13}^2+4\lambda_{14}\lambda_{15}+8\lambda_8(\lambda_5+5\lambda_6+\lambda_7+Y_t^2)-12\lambda_8(2g_{_{B-L}}^2+g_2^2)
\end{aligned}
$$

- **Coefficients with $\Phi^2\Delta^2$**

$$
\begin{aligned}
16\pi^2\frac{d}{dt}\lambda_9 &= \lambda_9\Big(20\lambda_1+8\lambda_3+16\lambda_5+8\lambda_6+6\lambda_7+4\lambda_9+6Y_t^2+4\mathrm{Tr}\big[(Y^M)^2\big]\\
&\quad -6g_{_{B-L}}^2-21g_2^2\Big)+6g_2^4+16(\lambda_{10}^2+\lambda_{11}^2)+\lambda_{12}(8\lambda_1+\lambda_{12})+3\lambda_{13}^2\\
&\quad +12\lambda_{14}^2+8\lambda_{12}\lambda_3+48\lambda_{10}\lambda_4+\lambda_{12}(6\lambda_5+8\lambda_6+3\lambda_7)\\
16\pi^2\frac{d}{dt}\lambda_{10} &= \lambda_{10}\Big(4\lambda_1+4\lambda_{12}+48\lambda_2+16\lambda_3+16\lambda_4+16\lambda_5+8\lambda_6+6\lambda_7+8\lambda_9\\
&\quad +6Y_t^2+4\mathrm{Tr}\big[(Y^M)^2\big]-6g_{_{B-L}}^2-21g_2^2\Big)-3\lambda_{13}(\lambda_{14}+\lambda_{15})+12\lambda_4\lambda_9\\
16\pi^2\frac{d}{dt}\lambda_{11} &= \lambda_{11}\Big(4\lambda_1+4\lambda_{12}-48\lambda_2+16\lambda_3+16\lambda_5+8\lambda_6-6\lambda_7\\
&\quad +8\lambda_9+6Y_t^2+4\mathrm{Tr}\big[(Y^M)^2\big]-6g_{_{B-L}}^2-21g_2^2\Big)\\
16\pi^2\frac{d}{dt}\lambda_{12} &= \lambda_{12}\Big(4\lambda_1+4\lambda_{12}-8\lambda_3+4\lambda_5-8\lambda_6+8\lambda_9+6Y_t^2\\
&\quad 4\mathrm{Tr}\big[(Y^M)^2\big]-6g_{_{B-L}}^2-21g_2^2\Big)-12(\lambda_{14}^2-\lambda_{15}^2)\\
16\pi^2\frac{d}{dt}\lambda_{13} &= \lambda_{13}\Big(4\lambda_1+4\lambda_{12}+8\lambda_3+2\lambda_7+8\lambda_8+8\lambda_9+3Y_t^2+\mathrm{Tr}\big[(Y^M)^2\big]\\
&\quad -6g_{_{B-L}}^2-21g_2^2\Big)+\big(8\lambda_4+16\lambda_{10}\big)\big(\lambda_{14}+\lambda_{15}\big)
\end{aligned}
$$

$$\begin{aligned}
16\pi^2\frac{d}{dt}\lambda_{14} &= \lambda_{14}\Big(4\lambda_1-4\lambda_{12}+2\lambda_7+8\lambda_9+6Y_t^2+4\mathrm{Tr}\big[(Y^M)^2\big]-6g^2_{_{B-L}}-21g_2^2\Big)\\
&\quad +4\lambda_{13}(\lambda_4+2\lambda_{10})+8\lambda_{15}(2\lambda_2+\lambda_8)\\
16\pi^2\frac{d}{dt}\lambda_{15} &= \lambda_{15}\Big(4\lambda_1+12\lambda_{12}+2\lambda_7+8\lambda_9+6Y_t^2+4\mathrm{Tr}\big[(Y^M)^2\big]-6g^2_{_{B-L}}-21g_2^2\Big)\\
&\quad +4\lambda_{13}(\lambda_4+4\lambda_{10})+8\lambda_{14}(2\lambda_2+\lambda_8)
\end{aligned}$$

A.4 LR Model with Doublet Scalars

Gauge RG Equations

$$\begin{aligned}
16\pi^2\frac{d}{dt}g_3 &= g_3^3\Big(-7\Big)\\
16\pi^2\frac{d}{dt}g_2 &= g_2^3\Big(-\frac{17}{6}\Big)\\
16\pi^2\frac{d}{dt}g_{_{B-L}} &= g_{B-L}^3\big(3\big)
\end{aligned}$$

Note that in our case $g_{_{2L}}=g_{_{2R}}=g_{_2}$.

Fermion RG Equations

$$64\pi^2\frac{d}{dt}Y_t=\Big(-\frac{2}{9}g^2_{_{B-L}}-9g_2^2-32g_3^2\Big)Y_t+7Y_t^3$$

Scalar RG Equations

- **Coefficients with Φ^4**

$$\begin{aligned}
128\pi^2\frac{d}{dt}\lambda_1 &= \lambda_1\Big(-72g_2^2+256\big(\lambda_1+\lambda_2-\lambda_3\big)+24Y_t^2\Big)\\
&+\ 1024(\lambda_1^2+\lambda_2^2)+32\beta_1^2+8f_1^2+9g_2^4-12Y-Y_t^4\\
512\pi^2\frac{d}{dt}\lambda_2 &= \lambda_2\Big(-288g_2^2+768\lambda_1+3072\lambda_2+1024\lambda_3+96Y_t^2\Big)\\
&\quad -8f_1^2+3g_2^4-3Y_t^4\\
256\pi^2\frac{d}{dt}\lambda_3 &= \lambda_3\Big(-144g_2^2-384\lambda_1-512\lambda_2-1536\lambda_3+48Y_t^2\Big)\\
&\quad +4f_1^2-3g_2^4-3Y_t^4
\end{aligned}$$

- **Coefficients with** $H_{L/R}^4$

$$
\begin{aligned}
512\pi^2 \frac{d}{dt}\kappa_1 &= \kappa_1\big(-96 g_{_{B-L}}^2 - 144 g_2^2 + 576\kappa_1 + 384\kappa_2 \big) \\
&+ 192\kappa_2^2 + 256\beta_1^2 + 128 f_1^2 + 24 g_{B-l}^4 + 12 g_{_{B-L}}^2 g_2^2 + 9 g_2^4 \\
512\pi^2 \frac{d}{dt}\kappa_2 &= \kappa_2\big(-96 g_{_{B-L}}^2 - 144 g_2^2 + 512\kappa_1 + 384\kappa_2 \big) + 128 f_1^2 \\
& \quad +12 g_{_{B-L}}^2 g_2^2 + 9 g_2^4
\end{aligned}
$$

- **Coefficeients with** $\Phi^2 H_{L/R}^2$

$$
\begin{aligned}
256\pi^2 \frac{d}{dt}\beta_1 &= -4\beta_1 \Big[-8\beta_1 + 6 g_{_{B-L}}^2 + 27 g_2^2 - 2\big(20\kappa_1 + 4\kappa_2 + 40\lambda_1 \\
& \quad +32\lambda_2 - 32\lambda_3 + 3 Y_t^2 \big) \Big] + 24 f_1^2 + 9 g_2^4 \\
256\pi^2 \frac{d}{dt} f_1 &= f_1 \Big(16\beta_1 - 6 g_{_{B-L}}^2 - 27 g_2^2 + 8(\kappa_1 + \kappa_2) + 16(\lambda_1 - 4\lambda_2) \\
& \quad +64\lambda_3 + 6 Y_t^2 \Big)
\end{aligned}
$$

Appendix B

Conditions of COP for LR Model

B.1 LR Model With Doublet Scalars

B.1.1 2-Field Directions and Stability Conditions

(I)

$$^{2F}V_1(\phi_1^0\,,\,\phi_1^+) = \lambda_1\,\left(\phi_1^{0^2} + \phi_1^{+^2}\right)^2. \tag{B.1}$$

Here we would like to note that all the field directions are evaluated in terms of the modulus of each field, i.e., $\phi_1^0 \equiv |\phi_1^0|$, and we have used the same notation through out the thesis.

In matrix form it can be represented in basis $(\phi_1^{0^2}, \phi_1^{+^2})$:

$$\begin{pmatrix} \lambda_1 & \lambda_1 \\ & \lambda_1 \end{pmatrix}.$$

Copositivity condition:

$$\lambda_1 \geq 0.$$

(II)

$$^{2F}V_2(\phi_1^+\,,\,h_R^+) = \lambda_1\,\phi_1^{+^4} + \frac{2\beta_1 + f_1}{2} h_R^{+^2} \phi_1^{+^2}. \tag{B.2}$$

$$^{2F}V_3(\phi_1^0\,,\,h_R^0) = \lambda_1\,\phi_1^{0\,4} + \frac{2\beta_1 + f_1}{2} h_R^{0\,2} \phi_1^{0\,2}. \tag{B.3}$$

In matrix form each of them can be represented in basis ($\phi_1^{+\,2} \Leftrightarrow \phi_1^{0\,2}, h_R^{+\,2} \Leftrightarrow h_R^{0\,2}$):

$$\begin{pmatrix} \lambda_1 & \frac{2\beta_1+f_1}{4} \\ & 0 \end{pmatrix}.$$

Here two different quadratic forms are represented by the same matrix in different basis and the *sign* '$\Leftrightarrow$' implies the mutual exchange of fields leading one quadratic form to other one. For example, if we replace $\phi_1^{+\,2}$ and $h_R^{+\,2}$ in $^{2F}V_2(\phi_1^+\,,\,h_R^+)$ by $\phi_1^{0\,2}$ and $h_R^{0\,2}$ simultaneously then we achieve $^{2F}V_3(\phi_1^0\,,\,h_R^0)$. We have used the same notation through out the text.

Copositivity condition:

$$\lambda_1 \geq 0, \qquad 2\beta_1 + f_1 \geq 0.$$

(III)

$$^{2F}V_4(\phi_1^0\,,\,h_R^+) = \lambda_1\,\phi_1^{0\,4} + \frac{2\beta_1 - f_1}{2} h_R^{+\,2} \phi_1^{0\,2}. \tag{B.4}$$

$$^{2F}V_5(\phi_1^+\,,\,h_R^0) = \lambda_1\,\phi_1^{+\,4} + \frac{2\beta_1 - f_1}{2} h_R^{0\,2} \phi_1^{+\,2}. \tag{B.5}$$

In matrix form both of them can be represented in basis ($\phi_1^{0\,2} \Leftrightarrow \phi_1^{+\,2}, h_R^{+\,2} \Leftrightarrow h_R^{0\,2}$):

$$\begin{pmatrix} \lambda_1 & \frac{2\beta_1-f_1}{4} \\ & 0 \end{pmatrix}.$$

Copositivity condition:

$$\lambda_1 \geq 0, \qquad 2\beta_1 - f_1 \geq 0.$$

B.1.2 3-Field Directions and Stability Conditions

(I)

$$
\begin{aligned}
{}^{3F}V_1(\phi_1^0\,,\,\phi_1^+\,,\,h_R^0) &= h_R^{0\,2}\left(\beta_1(\phi_1^{0 2}+\phi_1^{+ 2})+\frac{1}{2}f_1(\phi_1^{0 2}-\phi_1^{+ 2})\right)\\
&+ \lambda_1\left(\phi_1^{0 2}+\phi_1^{+ 2}\right)^2 .
\end{aligned} \tag{B.6}
$$

$$
\begin{aligned}
{}^{3F}V_2(\phi_1^0\,,\,\phi_1^+\,,\,h_R^+) &= h_R^{+ 2}\left(\beta_1(\phi_1^{0 2}+\phi_1^{+ 2})+\frac{1}{2}f_1(\phi_1^{+ 2}-\phi_1^{0 2})\right)\\
&+ \lambda_1\left(\phi_1^{0 2}+\phi_1^{+ 2}\right)^2 .
\end{aligned} \tag{B.7}
$$

In matrix form each can be represented in basis $(\phi_1^{0 2}, \phi_1^{+ 2}, h_R^{0\,2} \Leftrightarrow h_R^{+ 2})$:

$$
\begin{pmatrix}
\lambda_1 & \lambda_1 & \frac{2\beta_1-f_1}{4}\\
 & \lambda_1 & \frac{2\beta_1+f_1}{4}\\
 & & 0
\end{pmatrix}.
$$

<u>Copositivity conditions</u>:

$$
\lambda_1 \geq 0, \qquad 2\beta_1 - f_1 \geq 0, \qquad 2\beta_1 + f_1 \geq 0.
$$

(II)

$$
{}^{3F}V_3(\phi_1^0\,,\,h_R^0\,,\,h_R^+) = \frac{1}{2}\phi_1^{0 2}\left(f_1\left(h_R^{0\,2}-h_R^{+ 2}\right)+2\beta_1\left(h_R^{0\,2}+h_R^{+ 2}\right)+2\lambda_1\phi_1^{0 2}\right). \tag{B.8}
$$

$$
{}^{3F}V_4(\phi_1^+\,,\,h_R^0\,,\,h_R^+) = \frac{1}{2}\phi_1^{+ 2}\left(f_1\left(h_R^{+ 2}-h_R^{0\,2}\right)+2\beta_1\left(h_R^{0\,2}+h_R^{+ 2}\right)+2\lambda_1\phi_1^{+ 2}\right). \tag{B.9}
$$

In matrix form both can be represented in basis $(\phi_1^{0 2} \Leftrightarrow \phi_1^{+ 2}, h_R^{0\,2}, h_R^{+ 2})$:

$$\begin{pmatrix} \lambda_1 & \frac{2\beta_1+f_1}{4} & \frac{2\beta_1-f_1}{4} \\ & 0 & 0 \\ & & 0 \end{pmatrix}.$$

Copositivity condition:

$$\lambda_1 \geq 0, \qquad 2\beta_1 - f_1 \geq 0, \qquad 2\beta_1 + f_1 \geq 0.$$

B.1.3 4-Field Directions and Stability Conditions

(I)

$$\begin{aligned} {}^{4F}V_1(\phi_1^0, \phi_1^+, h_R^0, h_R^+) \;=\; & \frac{1}{2}\Bigg(f_1 \left(h_R^+(\phi_1^0 - \phi_1^+) + h_R^0(\phi_1^0 + \phi_1^+) \right) \\ & \left(h_R^0(\phi_1^0 - \phi_1^+) - h_R^+(\phi_1^0 + \phi_1^+) \right) + 2({\phi_1^0}^2 + {\phi_1^+}^2) \\ & \left(({h_R^0}^2 + {h_R^+}^2)\beta_1 + \lambda_1({\phi_1^0}^2 + {\phi_1^+}^2) \right) \Bigg). \end{aligned} \tag{B.10}$$

In matrix form it can be represented in basis $({\phi_1^0}^2, {\phi_1^+}^2, {h_R^0}^2, {h_R^+}^2, \phi_1^0\phi_1^+, h_R^0 h_R^+)$:

$$\begin{pmatrix} \lambda_1 & \lambda_1 & \frac{(1-C)}{2}\frac{f_1+2\beta_1}{2} & \frac{(1-K)}{2}\frac{2\beta_1-f_1}{2} & 0 & 0 \\ & \lambda_1 & \frac{2\beta_1-f_1}{4} & \frac{f_1+2\beta_1}{4} & 0 & 0 \\ & & 0 & 0 & 0 & 0 \\ & & & 0 & 0 & 0 \\ & & & & C\frac{f_1+2\beta_1}{2} & -f_1 \\ & & & & & K\frac{f_1+2\beta_1}{2} \end{pmatrix}.$$

Copositivity conditions :

$$\lambda_1 \geq 0, \qquad C(2\beta_1 + f_1) \geq 0, \qquad K(2\beta_1 + f_1) \geq 0,$$

$$C\ K\left(\frac{2\beta_1 + f_1}{2}\right)^2 - f_1^2 \geq 0.$$

In this case we do not have any other four field directions. Thus we can find the conditions which ensure that the potential is bounded from below by combining all COP criteria. From 2- and 3-fields directions we find the following conditions: $\lambda_1 \geq 0, \beta_1 \geq |f_1|/2$. We can eliminate both the unphysical parameters C and K from the COP emerged from 4-field direction by demanding the maximisation of the parameter space. Detailed discussion is in section 4.4.1 which leads to a condition we already have from 2- and 3-field directions.

B.2 LR Model With Triplet Scalars

B.2.1 2-Field Directions and Stability Conditions

(I)

$$^{2F}V_1(\phi_1^0\,,\,\phi_1^+) = \lambda_1\big(\phi_1^{0^2} + \phi_1^{+^2}\big)^2. \tag{B.11}$$

This can be represented as a symmetric matrix (Λ) of order two in basis $(\phi_1^{0^2}, \phi_1^{+^2})$:

$$\begin{pmatrix} \lambda_1 & \lambda_1 \\ & \lambda_1 \end{pmatrix}.$$

<u>Copositivity condition:</u>

$$\lambda_1 \geq 0.$$

(II)

$$^{2F}V_2(\phi_1^0\,,\,\delta^0) = \lambda_5\,\delta^{0^4} + \lambda_1\,\phi_1^{0^4}. \tag{B.12}$$

$$^{2F}V_3(\phi_1^+\,,\,\delta^{++}) = \lambda_5\,\delta^{++^4} + \lambda_1\,\phi_1^{+^4}. \tag{B.13}$$

In matrix form both of them can be represented in basis $(\phi_1^{0^2} \Leftrightarrow \phi_1^{+^2}, \delta^{0^2} \Leftrightarrow \delta^{++^2})$:

$$\begin{pmatrix} \lambda_1 & 0 \\ & \lambda_5 \end{pmatrix}.$$

Copositivity conditions:

$$\lambda_1 \geq 0, \qquad \lambda_5 \geq 0.$$

(III)

$${}^{2F}V_4(\phi_1^0\,,\,\delta^+) = (\lambda_5+\lambda_6)\delta^{+^4} + \lambda_1\,\phi_1^{0^4} + \frac{1}{2}(\lambda_{12}+2\lambda_9)\,\delta^{+^2}\phi_1^{0^2}. \tag{B.14}$$

$${}^{2F}V_5(\phi_1^+\,,\,\delta^+) = (\lambda_5+\lambda_6)\,\delta^{+^4} + \lambda_1\,\phi_1^{+^4} + \frac{1}{2}(\lambda_{12}+2\lambda_9)\,\delta^{+^2}\phi_1^{+^2}. \tag{B.15}$$

In matrix form both can be represented in basis ($\phi_1^{0^2} \Leftrightarrow \phi_1^{+^2}, \delta^{+^2}$):

$$\begin{pmatrix} \lambda_1 & \frac{1}{4}(\lambda_{12}+2\,\lambda_9) \\ & \lambda_5+\lambda_6 \end{pmatrix}.$$

Copositivity condition:

$$\lambda_1 \geq 0, \qquad \lambda_5+\lambda_6 \geq 0.$$

(IV)

$${}^{2F}V_6(\phi_1^0\,,\,\delta^{++}) = \lambda_5\,\delta^{++^4} + \lambda_1\,\phi_1^{0^4} + \lambda_{12}\,\delta^{++^2}\phi_1^{0^2}. \tag{B.16}$$

$${}^{2F}V_7(\phi_1^+\,,\,\delta^0) = \lambda_5\,\delta^{0^4} + \lambda_1\,\phi_1^{+^4} + \lambda_{12}\,\delta^{0^2}\phi_1^{+^2}. \tag{B.17}$$

In matrix form each of them can be represented in basis ($\phi_1^{0^2} \Leftrightarrow \phi_1^{+^2}, \delta^{++^2} \Leftrightarrow \delta^{0^2}$):

$$\begin{pmatrix} \lambda_1 & \frac{\lambda_{12}}{2} \\ & \lambda_5 \end{pmatrix}.$$

Copositivity conditions:

$$\lambda_1 \geq 0, \qquad \lambda_5 \geq 0.$$

(V)

$$^{2F}V_8(\delta^0\,,\,\delta^+) = \lambda_5\big(\delta^{0^2} + \delta^{+^2}\big)^2 + \lambda_6\;\delta^{+^4}. \tag{B.18}$$

$$^{2F}V_9(\delta^+\,,\,\delta^{++}) = \lambda_5\big(\delta^{+^2} + \delta^{++^2}\big)^2 + \lambda_6\;\delta^{+^4}. \tag{B.19}$$

In matrix form both can be represented in basis $(\delta^{+^2}, \delta^{0^2} \Leftrightarrow \delta^{++^2})$:

$$\begin{pmatrix} \lambda_5 & \lambda_5 \\ & \lambda_5 + \lambda_6 \end{pmatrix}.$$

Copositivity condition:

$$\lambda_5 \geq 0, \qquad \lambda_5 + \lambda_6 \geq 0.$$

(VI)

$$^{2F}V_{10}(\delta^0\,,\,\delta^{++}) = \lambda_5\big(\delta^{0^2} + \delta^{++^2}\big)^2 + 4\lambda_6\;\delta^{+^2}\delta^{0^2}. \tag{B.20}$$

In matrix form it can be represented in basis $(\delta^{0^2}, \delta^{++^2})$:

$$\begin{pmatrix} \lambda_5 & \lambda_5 + 2\lambda_6 \\ & \lambda_5 \end{pmatrix}.$$

Copositivity conditions:

$$\lambda_5 \geq 0, \qquad \lambda_5 + \lambda_6 \geq 0.$$

B.2.2 3-Field Directions and Stability Conditions

(I)

$$ {}^{3F}V_1(\phi_1^0\,,\,\phi_1^+\,,\,\delta^0) = \lambda_1\,\left({\phi_1^0}^2 + {\phi_1^+}^2\right)^2 + \lambda_5\,{\delta^0}^2 + \lambda_{12}\,{\delta^0}^2{\phi_1^0}^2. \tag{B.21} $$

$$ {}^{3F}V_2(\phi_1^0\,,\,\phi_1^+\,,\,\delta^{++}) = \lambda_1\,\left({\phi_1^0}^2 + {\phi_1^+}^2\right)^2 + \lambda_5\,{\delta^{++}}^4 + \lambda_{12}\,{\phi_1^0}^2{\delta^{++}}^2. \tag{B.22} $$

In matrix form both of them can be represented in basis $({\phi_1^0}^2, {\phi_1^+}^2, {\delta^0}^2 \Leftrightarrow {\delta^{++}}^2)$:

$$ \begin{pmatrix} \lambda_1 & \lambda_1 & \frac{\lambda_{12}}{2} \\ & \lambda_1 & 0 \\ & & \lambda_5 \end{pmatrix}. $$

<u>Copositivity conditions</u>:

$$ \lambda_1 \geq 0, \qquad \lambda_5 \geq 0. $$

(II)

$$ {}^{3F}V_3(\phi_1^0\,,\,\phi_1^+\,,\,\delta^+) = \lambda_1\,\left({\phi_1^0}^2 + {\phi_1^+}^2\right)^2 + (\lambda_5+\lambda_6){\delta^+}^4 + \frac{1}{2}(\lambda_{12}+2\lambda_9)\,\left({\phi_1^0}^2+{\phi_1^+}^2\right){\delta^+}^2. \tag{B.23} $$

In matrix form it can be represented in basis $({\phi_1^0}^2, {\phi_1^+}^2, {\delta^+}^2)$:

$$ \begin{pmatrix} \lambda_1 & \lambda_1 & \frac{1}{4}(\lambda_{12}+2\,\lambda_9) \\ & \lambda_1 & \frac{1}{4}(\lambda_{12}+2\,\lambda_9) \\ & & \lambda_5+\lambda_6 \end{pmatrix}. $$

<u>Copositivity condition</u>:

$$ \lambda_1 \geq 0, \qquad \lambda_5+\lambda_6 \geq 0. $$

(III)

$$^{3F}V_4(\phi_1^0\,,\,\delta^0\,,\,\delta^+) = \lambda_1\;\phi_1^{04} + \lambda_5\;\left(\delta^{02}+\delta^{+2}\right)^2 + \lambda_6\delta^{+4} + \frac{1}{2}(\lambda_{12}+2\lambda_9)\;\phi_1^{02}\delta^{+2}. \tag{B.24}$$

$$^{3F}V_5(\phi_1^+\,,\,\delta^{++}\,,\,\delta^+) = \lambda_1\;\phi_1^{+4} + \lambda_5\;\left(\delta^{+2}+\delta^{++2}\right)^2 + \lambda_6\delta^{+4} + \frac{1}{2}(\lambda_{12}+2\lambda_9)\;\phi_1^{+2}\delta^{+2}. \tag{B.25}$$

In matrix form both can be represented in basis ($\phi_1^{02} \Leftrightarrow \phi_1^{+2}, \delta^{02} \Leftrightarrow \delta^{++2}, \delta^{+2}$):

$$\begin{pmatrix} \lambda_1 & 0 & \frac{1}{4}(\lambda_{12}+2\,\lambda_9) \\ & \lambda_5 & \lambda_5 \\ & & \lambda_5+\lambda_6 \end{pmatrix}.$$

<u>Copositivity condition:</u>

$$\lambda_1 \geq 0, \qquad \lambda_5 \geq 0, \qquad \lambda_5+\lambda_6 \geq 0.$$

(IV)

$$\begin{aligned} ^{3F}V_6(\phi_1^0\,,\,\delta^0\,,\,\delta^{++}) &= \lambda_5\;\left(\delta^{02}+\delta^{++2}\right)^2 + \lambda_1\;\phi_1^{04} + 4\lambda_6\;{\delta_0}^2\delta^{++2} \\ &\quad +\lambda_{12}\;\delta^{++2}\;\phi_1^{02} + 2\,\lambda_9\,\delta^0\,\delta^{++}\;\phi_1^{02}. \end{aligned} \tag{B.26}$$

$$\begin{aligned} ^{3F}V_7(\phi_1^+\,,\,\delta^0\,,\,\delta^{++}) &= \lambda_5\;\left(\delta^{02}+\delta^{++2}\right)^2 + \lambda_1\;\phi_1^{+4} + 4\lambda_6\;{\delta_0}^2\delta^{++2} \\ &\quad +\lambda_{12}\;\delta^{02}\;\phi_1^{+2} + 2\,\lambda_9\,\delta^0\,\delta^{++}\;\phi_1^{+2}. \end{aligned} \tag{B.27}$$

In matrix form both of them can be represented in basis ($\phi_1^{0\,2} \Leftrightarrow \phi_1^{+\,2}, \delta^{0\,2}, \delta^{++\,2}$):

$$
\begin{pmatrix}
\lambda_1 & 0 & \frac{\lambda_{12}}{2} & \lambda_9 \\
 & \lambda_5 & (1-C)(\lambda_5 + 2\,\lambda_6) & 0 \\
 & & \lambda_5 & 0 \\
 & & & 2C(\lambda_5 + 2\lambda_6)
\end{pmatrix}.
$$

Copositivity conditions:

$$\lambda_1 \geq 0, \qquad \lambda_5 \geq 0, \qquad C(\lambda_5 + 2\,\lambda_6) \geq 0. \tag{B.28}$$

Here we encounter three possibilities in respect to the last condition for three ranges of the unphysical parameter C:

(a) $C \geq 0$ such that $(1 - C) \geq 0$, i.e., $C \in [0, 1]$:

$$\lambda_5 + 2\,\lambda_6 \geq 0. \tag{B.29}$$

(b) $C \geq 0$ such that $(1 - C) < 0$, i.e., $C \in (1, \infty]$:

$$\lambda_5 + 2\,\lambda_6 \geq 0 \qquad \& \qquad \lambda_5^2 - (1-C)^2(\lambda_5 + 2\,\lambda_6)^2 \geq 0. \tag{B.30}$$

(c) $C < 0$ such that $(1 - C) \geq 0$, i.e., $C \in [-\infty, 0)$:

$$\lambda_5 + 2\,\lambda_6 \leq 0 \qquad \& \qquad \lambda_5^2 - (1-C)^2(\lambda_5 + 2\,\lambda_6)^2 \geq 0. \tag{B.31}$$

As C is a free parameter we can rewrite this condition as:

$$\lambda_5 + 2\,\lambda_6 \leq 0 \qquad \& \qquad \lambda_5^2 - C^2(\lambda_5 + 2\,\lambda_6)^2 \geq 0, \tag{B.32}$$

with $C \in (1, \infty]$.

In principle, union of exhaustive scan over all possible C values would provide us total allowed region in the parameter space. That is indeed possible in much simpler way by finding the particular C values which maximise the allowed region. Thus one can eliminate this extra unphysical parameter by writing unified condition which remain allowed. Detailed discussion is in section 4.4.2. Similar method would be implemented in many other cases as follows. Thus the final copositivity conditions in this case can be written as,

$$\lambda_1 \geq 0, \qquad \lambda_5 \geq 0, \qquad (\lambda_5 + \lambda_6) \geq 0. \tag{B.33}$$

(V)

$$\begin{aligned} {}^{3F}V_8(\phi_1^0\,,\,\delta^+\,,\,\delta^{++}) &= \lambda_1\,\phi_1^{0^4} + \lambda_5\left(\delta^{++^2} + \delta^{+^2}\right)^2 + \lambda_6\,\delta^{+^4} \\ &+ \frac{1}{2}\lambda_{12}\,\phi_1^{0^2}(2\delta^{++^2} + \delta^{+^2}) + \lambda_9\,\phi_1^{0^2}\,\delta^{+^2}. \end{aligned} \tag{B.34}$$

$$\begin{aligned} {}^{3F}V_9(\phi_1^+\,,\,\delta^0\,,\,\delta^+) &= \lambda_1\,\phi_1^{+^4} + \lambda_5\left(\delta^{0^2} + \delta^{+^2}\right)^2 + \lambda_6\,\delta^{+^4} \\ &+ \frac{1}{2}\lambda_{12}\,\phi_1^{+^2}(2\delta^{0^2} + \delta^{+^2}) + \lambda_9\,\phi_1^{+^2}\,\delta^{+^2}. \end{aligned} \tag{B.35}$$

In matrix form both can be represented in basis ($\phi_1^{0^2} \Leftrightarrow \phi_1^{+^2}, \delta^{++^2} \Leftrightarrow \delta^{0^2}, \delta^{+^2}$):

$$\begin{pmatrix} \lambda_1 & \frac{1}{4}(\lambda_{12} + 2\,\lambda_9) & \frac{\lambda_{12}}{2} \\ & \lambda_5 + \lambda_6 & \lambda_5 \\ & & \lambda_5 \end{pmatrix}.$$

<u>Copositivity conditions:</u>

$$\lambda_1 \geq 0, \qquad \lambda_5 \geq 0, \qquad \lambda_5 + \lambda_6 \geq 0.$$

(VI)

$$ {}^{3F}V_{10}(\delta^0\,,\,\delta^+\,,\,\delta^{++}) = \lambda_5\,\left(\delta^{0\,2}+\delta^{+\,2}+\delta^{++\,2}\right)^2+\lambda_6\,\left(\delta^{+\,2}+2\delta^0\delta^{++}\right)^2. \quad \text{(B.36)} $$

In matrix form it can be represented in basis $(\delta^{0\,2}, \delta^{+\,2}, \delta^{++\,2})$:

$$ \begin{pmatrix} \lambda_5 & \lambda_5 & (1-C)(\lambda_5+2\,\lambda_6) & 0 \\ & \lambda_5+\lambda_6 & \lambda_5 & 2\lambda_6 \\ & & \lambda_5 & 0 \\ & & & 2C(\lambda_5+2\lambda_6) \end{pmatrix}. $$

<u>Copositivity condition</u>:

$$ \lambda_1 \geq 0, \qquad \lambda_5 \geq 0, \qquad \lambda_5+\lambda_6 \geq 0, \qquad C(\lambda_5+2\,\lambda_6) \geq 0. $$

Possible three cases are:

(a) <u>$C > 0,\ (1-C) \geq 0, \text{i.e.},\ C \in [0:1]$</u>

$$ \lambda_5+2\,\lambda_6 \geq 0 \qquad \& \qquad 2C\,(\lambda_5+\lambda_6)\,(\lambda_5+2\,\lambda_6) - 4\,\lambda_6^2 \geq 0 $$

(b) <u>$C > 0,\ (1-C) \leq 0, \text{i.e.},\ C \in [1:\infty]$</u>

$$ \lambda_5+2\,\lambda_6 \geq 0 \qquad \& \qquad \lambda_5^2-(1-C)^2(\lambda_5+2\,\lambda_6)^2 \geq 0. $$

$$ 2C\,(\lambda_5+\lambda_6)\,(\lambda_5+2\,\lambda_6) - 4\,\lambda_6^2 \geq 0 $$

(c) <u>$C > 0,\ (1-C) \leq 0, \text{i.e.},\ C \in [-\infty:0)$</u>

$$ \lambda_5+2\,\lambda_6 \leq 0 \qquad \& \qquad \lambda_5^2-(1-C)^2(\lambda_5+2\,\lambda_6)^2 \geq 0. $$

$$ 2C\,(\lambda_5+\lambda_6)\,(\lambda_5+2\,\lambda_6) - 4\,\lambda_6^2 \geq 0 $$

We have already discussed the similar situation in detail in the section 4.4.2.

Final conditions in this case can be calculated as:

$$\lambda_1 \geq 0, \qquad \lambda_5 \geq 0, \qquad \lambda_5 + \lambda_6 \geq 0.$$

B.2.3 4-Field Directions and Stability Conditions

(I)

$$\begin{aligned} {}^{4F}V_1(\phi_1^0\,,\,\phi_1^+\,,\,\delta^0\,,\,\delta^+) \quad &= \lambda_5\,\left(\delta^{0^2}+\delta^{+^2}\right)^2 + \lambda_6\,\delta^{+^4} + \lambda_1\,\left(\phi_1^{0^2}+\phi_1^{+^2}\right)^2 \\ &+\frac{1}{2}\lambda_{12}\,\left(2\delta^{0^2}\phi_1^{+^2} + 2\sqrt{2}\phi_1^0\phi_1^+\delta^0\delta^+ + \delta^{+^2}\big(\phi_1^{0^2}+\phi_1^{+^2}\big)\right) \\ &+\lambda_9\,\delta^{+^2}\big(\phi_1^{0^2}+\phi_1^{+^2}\big). \end{aligned} \tag{B.37}$$

In matrix form it can be represented in basis $(\phi_1^{0^2}, \phi_1^{+^2}, \delta^{+^2}, \delta^{++^2}, \phi_1^0\,\phi_1^+, \delta^+\,\delta^{++})$:

$$\begin{pmatrix} \lambda_1 & (1-C)\lambda_1 & \frac{1}{4}(\lambda_{12}+2\,\lambda_9) & \frac{1}{4}(\lambda_{12}+2\,\lambda_9) & 0 & 0 \\ & \lambda_1 & 0 & \frac{\lambda_{12}}{2} & 0 & 0 \\ & & \lambda_5+\lambda_6 & (1-K)\lambda_5 & 0 & 0 \\ & & & \lambda_5 & 0 & 0 \\ & & & & 2\,C\lambda_1 & \frac{\lambda_{12}}{\sqrt{2}} \\ & & & & & 2\,K\lambda_5 \end{pmatrix}.$$

<u>Copositivity condition:</u>

$$\lambda_1 \geq 0, \qquad \lambda_5 \geq 0, \qquad \lambda_5+\lambda_6 \geq 0, \qquad C \geq 0, \qquad K \geq 0.$$

Here the two possibilities are:

(I) <u>$(1-C) \leq 0$, i.e., $C \in (1,\infty]$</u>

$$\lambda_1\,\lambda_1 - (1-C)^2\,\lambda_1^2 \geq 0 \qquad \Rightarrow \qquad C \in [0,2].$$

(II) $\underline{(1-K) \leq 0, \text{i.e., } K \in (1,\infty]}$

$$\lambda_5\left(\lambda_5+\lambda_6\right)-(1-K)^2\,\lambda_5^2 \geq 0.$$

The last condition leads to $\lambda_5+\lambda_6 \geq (1-K)^2\lambda_5$, and this condition is maximally relaxed for $K=1$ as $\lambda_5 \geq 0$. It is also possible to confirm numerically that $K=1$ allows the largest parameter space. So, $K=1$ and $C \in [0,2]$ are the possible choices.

Then final conditions are

$$\lambda_1 \geq 0, \qquad \lambda_5 \geq 0, \qquad \lambda_5+\lambda_6 \geq 0.$$

(II)

$$\begin{aligned}
{}^{4F}V_2(\phi_1^0\,,\,\phi_1^+\,,\,\delta^0\,,\,\delta^{++}) \;=\;& \lambda_5\left({\delta^0}^2+{\delta^{++}}^2\right)^2+4\lambda_6\,{\delta^0}^2{\delta^{++}}^2+\lambda_1\left({\phi_1^0}^2+{\phi_1^+}^2\right)^2 \\
&+\lambda_{12}\left(\left({\delta^{++}}^2{\phi_1^0}^2+{\delta^0}^2{\phi_1^+}^2\right)+\delta^0\,\delta^{++}\left({\phi_1^0}^2+{\phi_1^+}^2\right)\right) \\
&+2\lambda_9\,\delta^0\,\delta^{++}\left({\phi_1^0}^2+{\phi_1^+}^2\right). \qquad \text{(B.38)}
\end{aligned}$$

In matrix form it can be represented in basis $({\phi_1^0}^2, {\phi_1^+}^2, {\delta^0}^2, {\delta^{++}}^2)$:

$$\begin{pmatrix}
\lambda_1 & \lambda_1 & 0 & \frac{\lambda_{12}}{2} & \lambda_9 \\
 & \lambda_1 & \frac{\lambda_{12}}{2} & 0 & \lambda_9 \\
 & & \lambda_5 & (1-C)(\lambda_5+2\,\lambda_6) & 0 \\
 & & & \lambda_5 & 0 \\
 & & & & 2C(\lambda_5+2\,\lambda_6)
\end{pmatrix}.$$

<u>Copositivity conditions</u>:

$$\lambda_1 \geq 0, \qquad \lambda_5 \geq 0, \qquad C(\lambda_5+2\,\lambda_6) \geq 0.$$

The possible three cases are:

(a) $\underline{C > 0,\ (1-C) \geq 0, \text{i.e.},\ C \in [0,1]}$

$$\lambda_5 + 2\,\lambda_6 \geq 0.$$

(b) $\underline{C > 0,\ (1-C) \leq 0, \text{i.e.},\ C \in (1,\infty]}$

$$\lambda_5 + 2\,\lambda_6 \geq 0 \qquad \& \qquad \lambda_5^2 - (1-C)^2(\lambda_5 + 2\,\lambda_6)^2 \geq 0.$$

(c) $\underline{C < 0,\ (1-C) \geq 0, \text{i.e.},\ C \in [-\infty,0)}$

$$\lambda_5 + 2\,\lambda_6 \leq 0 \qquad \& \qquad \lambda_5^2 - (1-C)^2(\lambda_5 + 2\,\lambda_6)^2 \geq 0.$$

We have already discussed the similar situation in detail in the section 4.4.2. Final conditions in this case can be calculated as:

$$\lambda_1 \geq 0, \qquad \lambda_5 \geq 0, \qquad \lambda_5 + \lambda_6 \geq 0$$

(III)

$$\begin{aligned} {}^{4F}V_3(\phi_1^0\,,\,\phi_1^+\,,\,\delta^0\,,\,\delta^+) \;=\; & \lambda_5\left(\delta^{0^2} + \delta^{+^2}\right)^2 + \lambda_6\,\delta^{+^4} + \lambda_1\left(\phi_1^{0^2} + \phi_1^{+^2}\right)^2 \\ & + \frac{1}{2}\lambda_{12}\left(2\delta^{0^2}\phi_1^{+^2} - 2\sqrt{2}\phi_1^0\phi_1^+\delta^0\delta^+ + \delta^{+^2}\big(\phi_1^{0^2} + \phi_1^{+^2}\big)\right) \\ & + \lambda_9\,\delta^{+^2}\big(\phi_1^{0^2} + \phi_1^{+^2}\big). \end{aligned} \tag{B.39}$$

In matrix form it can be represented in basis $(\phi_1^{0^2}, \phi_1^{+^2}, \delta^{+^2}, \delta^{++^2}, \phi_1^0\,\phi_1^+, \delta^+\,\delta^{++})$:

$$\begin{pmatrix} \lambda_1 & (1-C)\lambda_1 & \frac{1}{4}(\lambda_{12}+2\,\lambda_9) & \frac{1}{4}(\lambda_{12}+2\,\lambda_9) & 0 & 0 \\ & \lambda_1 & 0 & \frac{\lambda_{12}}{2} & 0 & 0 \\ & & \lambda_5+\lambda_6 & (1-K)\lambda_5 & 0 & 0 \\ & & & \lambda_5 & 0 & 0 \\ & & & & 2C\lambda_1 & -\frac{\lambda_{12}}{\sqrt{2}} \\ & & & & & 2K\lambda_5 \end{pmatrix}.$$

<u>Copositivity condition:</u>

$$\lambda_1 \geq 0, \qquad \lambda_5 \geq 0, \qquad \lambda_5 + \lambda_6 \geq 0, \qquad C \geq 0, \qquad K \geq 0 \qquad \text{and}$$

$$4C\,K\,\lambda_1\,\lambda_5 - \frac{\lambda_{12}^2}{2} \geq 0.$$

The two possible cases are:

(i) $\underline{(1-C) \leq 0, \text{i.e.}, C \in (1,\infty]}$

$$\lambda_1\,\lambda_1 - (1-C)^2\,\lambda_1^2 \geq 0 \qquad \Rightarrow \qquad 1 - (1-C)^2 \geq 0.$$

(ii) $\underline{(1-K) \leq 0, \text{i.e.}, K \in (1,\infty]}$

$$\lambda_5\,(\lambda_5 + \lambda_6) - (1-K)^2\,\lambda_5^2 \geq 0.$$

In a similar method discussed in detail in the section 4.4.2, we choose $C = 2$ and $K = 1$ for the last copositivity condition in this present case, e.g., $C\,K\,\lambda_1\,\lambda_5 - \frac{\lambda_{12}^2}{8} \geq 0$. This choice of C and K are made, keeping in mind that these unphysical parameters can be set to values which allows the largest parameter space.

Here we can also argue the maximisation of the allowed parameter space, as suggested in section 4.4.2. As $C, K \geq 0$, we can rewrite the condition as $\lambda_1\lambda_5 \geq |\lambda_{12}^2/(8CK)|$. Thus the largest parameter space can be accessed if we use the conditions $\lambda_1\lambda_5 \geq 0$, which would be achieved for either C or $K \to \infty$. But we have restriction on C as $0 \leq C \leq 2$. The other condition leads to $\lambda_5 + \lambda_6 \geq (1-K)^2\lambda_5$, and this condition is maximally relaxed for $K = 1$ as $\lambda_5 \geq 0$. So as the product $\lambda_1\lambda_5$ can be maximally relaxed for allowed maximum values of C, K which are 2 and 1 respectively we find the following constraint on this product as $\lambda_1\lambda_5 \geq \lambda_{12}^2/16$.

We finally arrived at the conditions as,

$$\lambda_1 \geq 0, \qquad \lambda_5 \geq 0, \qquad \lambda_5 + \lambda_6 \geq 0, \qquad 16\,\lambda_1\,\lambda_5 - \lambda_{12}^2 \geq 0.$$

(IV)

$$
\begin{aligned}
{}^{4F}V_4(\phi_1^0\,,\,\delta^0\,,\,\delta^+\,,\,\delta^{++}) \;=\;& \lambda_5\,\left(\delta^{0\,2}+\delta^{+\,2}+\delta^{++\,2}\right)^2+\lambda_6\,\left(\delta^{+\,2}+2\delta^0\delta^{++}\right)^2 \\
&+\lambda_1\,\phi_1^{0\,4}+\frac{1}{2}\lambda_{12}\,\phi_1^{0\,2}(2\delta^{0\,2}+\delta^{+\,2}) \\
&+\lambda_9\phi_1^{0\,2}\left(\delta^{+\,2}+2\,\delta^0\,\delta^{++}\right). \qquad \text{(B.40)}
\end{aligned}
$$

$$
\begin{aligned}
{}^{4F}V_5(\phi_1^+\,,\,\delta^0\,,\,\delta^+\,,\,\delta^{++}) \;=\;& \lambda_5\,\left(\delta^{0\,2}+\delta^{+\,2}+\delta^{++\,2}\right)^2+\lambda_6\,\left(\delta^{+\,2}+2\delta^0\delta^{++}\right)^2 \\
&+\lambda_1\,\phi_1^{+\,4}+\frac{1}{2}\lambda_{12}\,\phi_1^{+\,2}(2\delta^{0\,2}+\delta^{+\,2}) \\
&+\lambda_9\phi_1^{+\,2}\left(\delta^{+\,2}+2\,\delta^0\,\delta^{++}\right). \qquad \text{(B.41)}
\end{aligned}
$$

Both of them can be represented in basis $(\phi_1^{0\,2} \Leftrightarrow \phi_1^{+\,2}, \delta^{0\,2}, \delta^{+\,2}, \delta^{++\,2}, \delta^0\,\delta^{++})$:

$$
\begin{pmatrix}
\lambda_1 & \frac{\lambda_{12}}{2} & \frac{\lambda_{12}}{4} & 0 & \lambda_9 \\
 & \lambda_5 & \lambda_5 & (1-C)(\lambda_5+2\,\lambda_6) & 0 \\
 & & \lambda_5+\lambda_6 & \lambda_5 & 2\,\lambda_6 \\
 & & & \lambda_5 & 0 \\
 & & & & 2C(\lambda_5+2\lambda_6)
\end{pmatrix}.
$$

<u>Copositivity conditions</u>:

$$
\lambda_1 \geq 0, \qquad \lambda_5 \geq 0, \qquad \lambda_5+\lambda_6 \geq 0, \qquad C(\lambda_5+2\,\lambda_6) \geq 0.
$$

The possible three cases are:

(a) <u>$C > 0,\ (1-C) \geq 0, \text{i.e.},\ C \in [0,1]$</u>

$$
\lambda_5+2\,\lambda_6 \geq 0 \qquad \& \qquad 2\,C(\lambda_5+\lambda_6)(\lambda_5+2\,\lambda_6)-4\,\lambda_6^2 \geq 0.
$$

(b) <u>$C > 0,\ (1-C) \leq 0, \text{i.e.},\ C \in (1,\infty]$</u>

$$
\lambda_5+2\,\lambda_6 \geq 0 \qquad \& \qquad \lambda_5^2-(1-C)^2(\lambda_5+2\,\lambda_6)^2 \geq 0.
$$

$$
\& \qquad 2\,C(\lambda_5+\lambda_6)(\lambda_5+2\,\lambda_6)-4\,\lambda_6^2 \geq 0.
$$

(c) $\underline{C < 0,\ (1-C) \geq 0, \text{i.e.},\ C \in [-\infty, 0)}$

$$\lambda_5 + 2\,\lambda_6 \leq 0 \qquad \& \qquad \lambda_5^2 - (1-C)^2(\lambda_5 + 2\,\lambda_6)^2 \geq 0,$$

$$\& \qquad 2\,C(\lambda_5 + \lambda_6)(\lambda_5 + 2\,\lambda_6) - 4\,\lambda_6^2 \geq 0.$$

We have already discussed the similar situation in detail in the section 4.4.2. Final conditions in this case can be calculated as:

$$\lambda_1 \geq 0, \qquad \lambda_5 \geq 0, \qquad \lambda_5 + \lambda_6 \geq 0.$$

Appendix C

Unitarity in LRSM with Triplet Scalars

Here we present two MATHEMATICA files (which can be obtained from the URL: http://www.prl.res.in/~konar/data.html or from the source file in arXiv [75]) where we spell out the details of the calculation of the unitarity constraints. In the file named LRT_Pot.nb we construct the $2 \to 2$ scattering matrices for all the q-charged 2-particle states. One can also obtain the eigenvalues of those matrices by running that code by appropriately uncommenting some commands. We have collected all the independent eigenvalues of all the scattering matrices in the second file called Eigenvalue_collect.nb.

The MATHEMATICA file LRT_Pot.nb

Construction of the 2 → 2 Scattering Matrices:

In the following we describe the scalar potential for the LRSM. Later we construct the scattering matrices q –charged 2-particle states by properly specifying the basis. (Uncomment and run the command “Eigenvalues[X]” to obtain the eigenvalues of the matrix ‘X’.)
We have collected all the eigenvlaues and put it in a different file.

Defining the scalar potential

```
Clear["Global`*"]
```

$$\phi = \begin{pmatrix} \frac{1}{\sqrt{2}}(\phi10r + I\ \phi10i) & \phi1p \\ \phi2m & \frac{1}{\sqrt{2}}(\phi20r + I\ \phi20i) \end{pmatrix};$$

$$\Delta R = \begin{pmatrix} \frac{\delta Rp}{\sqrt{2}} & \delta Rpp \\ \frac{1}{\sqrt{2}}(\delta R0r + I\ \delta R0i) & -\frac{\delta Rp}{\sqrt{2}} \end{pmatrix};\ \Delta L = \begin{pmatrix} \frac{\delta Lp}{\sqrt{2}} & \delta Lpp \\ \frac{1}{\sqrt{2}}(\delta L0r + I\ \delta L0i) & -\frac{\delta Lp}{\sqrt{2}} \end{pmatrix};$$

$$\sigma = \begin{pmatrix} 0 & -I \\ I & 0 \end{pmatrix};\ \phi t = \sigma.\phi.\sigma;$$

```
V4 = λ1 (Tr[ϕ†.ϕ])^2 + λ2 ((Tr[ϕt.ϕ†])^2 + (Tr[ϕt†.ϕ])^2) + λ3 ((Tr[ϕt.ϕ†]) (Tr[ϕt†.ϕ])) +
   λ4 ((Tr[ϕ†.ϕ]) ((Tr[ϕt†.ϕ]) + (Tr[ϕt.ϕ†]))) + λ5 ((Tr[ΔL.ΔL†])^2 + (Tr[ΔR.ΔR†])^2) +
   λ6 ( (Tr[ΔL.ΔL]) (Tr[ΔL†.ΔL†]) + (Tr[ΔR.ΔR]) (Tr[ΔR†.ΔR†])) + λ7 (Tr[ΔL.ΔL†] Tr[ΔR.ΔR†]) +
   λ8 (Tr[ΔL.ΔL] Tr[ΔR†.ΔR†] + Tr[ΔL†.ΔL†] Tr[ΔR.ΔR]) + λ9 Tr[ϕ†.ϕ] (Tr[ΔL†.ΔL†] + Tr[ΔR†.ΔR†]) +
   (λ10 + i λ11) ((Tr[ϕt†.ϕ]) (Tr[ΔR.ΔR†]) + (Tr[ϕ†.ϕt]) (Tr[ΔL.ΔL†])) +
   (λ10 - i λ11) ((Tr[ϕt†.ϕ]) (Tr[ΔL.ΔL†]) + (Tr[ϕt.ϕ†]) (Tr[ΔR.ΔR†])) +
   λ12 (Tr[ϕ†.ϕ.ΔL.ΔL†] + Tr[ϕ†.ϕ.ΔR.ΔR†]);

replace = {Conjugate[ϕ10r] → ϕ10r, Conjugate[ϕ10i] → ϕ10i,
   Conjugate[ϕ20r] → ϕ20r, Conjugate[ϕ20i] → ϕ20i, Conjugate[ϕ1p] → ϕ1m,
   Conjugate[ϕ2m] → ϕ2p, Conjugate[δR0r] → δR0r, Conjugate[δR0i] → δR0i,
   Conjugate[δRp] → δRm, Conjugate[δRpp] → δRmm, Conjugate[δL0r] → δL0r,
   Conjugate[δL0i] → δL0i, Conjugate[δLp] → δLm, Conjugate[δLpp] → δLmm,
   Conjugate[I ϕ10i + ϕ10r] → {- I ϕ10i + ϕ10r}, Conjugate[I ϕ20i + ϕ20r] → {- I ϕ20i + ϕ20r}};

(*Potential in terms of the fields *)
Vtot = Simplify[V4 /. replace];
```

Construction of scattering amplitude matrix

For neutral two-particle states

```
NCColumn = {
   ϕ1p ϕ1m, ϕ1p ϕ2m, ϕ1p δRm , ϕ1p δLm (*4,4*),
   ϕ2p ϕ1m,  ϕ2p ϕ2m, ϕ2p δRm ,  ϕ2p  δLm (*4,8*),
   δRp ϕ1m, δRp ϕ2m, δRp δRm, δRp δLm(*4,12*),
   δLp ϕ1m, δLp ϕ2m, δLp δRm, δLp δLm(*4,16*),
   ϕ10r ϕ10r, ϕ10r ϕ10i , ϕ10r ϕ20r , ϕ10r ϕ20i ,
   ϕ10r  δR0r, ϕ10r  δR0i , ϕ10r  δL0r, ϕ10r  δL0i  (*8,24*),
   ϕ10i ϕ10i, ϕ10i ϕ20r , ϕ10i ϕ20i , ϕ10i δR0r , ϕ10i δR0i , ϕ10i δL0r , ϕ10i  δL0i(*7,31*),
   ϕ20r  ϕ20r, ϕ20r  ϕ20i, ϕ20r  δR0r, ϕ20r δR0i , ϕ20r  δL0r, ϕ20r δL0i  (*6,37*),
   ϕ20i  ϕ20i, ϕ20i δR0r , ϕ20i δR0i , ϕ20i δL0r  , ϕ20i  δL0i(*5,42*),
   δR0r  δR0r, δR0r δR0i , δR0r  δL0r, δR0r δL0i (*4,46*),
   δR0i δR0i , δR0i δL0r  , δR0i  δL0i (*3,49*),
   δL0r  δL0r, δL0r  δL0i (*2,51*),
   δL0i δL0i(*1,52*),
   δRpp δRmm , δRpp δLmm (*2,54*),
   δLpp  δRmm, δLpp δLmm (*2,56*)
  };
NCRow = {
   ϕ1m ϕ1p, ϕ1m ϕ2p, ϕ1m δRp , ϕ1m δLp (*4,4*),
   ϕ2m ϕ1p,  ϕ2m ϕ2p, ϕ2m δRp ,  ϕ2m  δLp (*4,8*),
   δRm ϕ1p, δRm ϕ2p, δRm δRp, δRm δLp(*4,12*),
   δLm ϕ1p, δLm ϕ2p, δLm δRp, δLm δLp(*4,16*),
   ϕ10r ϕ10r, ϕ10r ϕ10i , ϕ10r ϕ20r , ϕ10r ϕ20i ,
   ϕ10r  δR0r, ϕ10r  δR0i , ϕ10r  δL0r, ϕ10r  δL0i  (*8,24*),
   ϕ10i ϕ10i, ϕ10i ϕ20r , ϕ10i ϕ20i , ϕ10i δR0r , ϕ10i δR0i , ϕ10i δL0r , ϕ10i  δL0i(*7,31*),
   ϕ20r  ϕ20r, ϕ20r  ϕ20i, ϕ20r  δR0r, ϕ20r δR0i , ϕ20r  δL0r, ϕ20r δL0i  (*6,37*),
   ϕ20i  ϕ20i, ϕ20i δR0r , ϕ20i δR0i , ϕ20i δL0r  , ϕ20i  δL0i(*5,42*),
   δR0r  δR0r, δR0r δR0i , δR0r  δL0r, δR0r δL0i (*4,46*),
   δR0i δR0i , δR0i δL0r  , δR0i  δL0i (*3,49*),
   δL0r  δL0r, δL0r  δL0i (*2,51*),
   δL0i δL0i(*1,52*),
   δRmm δRpp , δRmm δLpp (*2,54*),
   δLmm  δRpp, δLmm δLpp (*2,56*)
  };
```

The symmetry factor is introduced to avoid double counting:

```
NCfacList[i_, j_] := FactorList[NCColumn[[i]] NCRow[[j]]];
NCSymFac[i_, j_] := (If[Length[NCfacList[i, j]] == 2, Return[Factorial[4]]];
   If[Length[NCfacList[i, j]] == 3, If[(NCfacList[i, j])[[2, 2]] == 2 &&
      (NCfacList[i, j])[[3, 2]] == 2, Return[4], Return[Factorial[3]]]];
   If[Length[NCfacList[i, j]] == 4, Return[2]];
   If[Length[NCfacList[i, j]] == 5, Return[1]]);

NCcoeff[i_, j_] := Coefficient[Vtot, NCColumn[[i]] NCRow[[j]]];
NCMatFunc[i_, j_] := NCSymFac[i, j] NCcoeff[i, j];

For[i = 1; NCklist = {}, i ≤ 56, i++,
 For[j = 1; NCjlist = {}, j ≤ 56, j++, AppendTo[NCjlist, {NCMatFunc[i, j]}]];
 AppendTo[NCklist, Flatten[NCjlist]]]
(*NCklist//MatrixForm*)
(*Eigenvalues[NCklist]*)
```

For singly charged two-particle states

```
CCColumn = {
   ϕ1p ϕ10r , ϕ1p ϕ10i, ϕ1p ϕ20r, ϕ1p ϕ20i , ϕ1p δR0r, ϕ1p δR0i, ϕ1p δL0r, ϕ1p δL0i (*8,8*),
   ϕ2p ϕ10r, ϕ2p ϕ10i, ϕ2p ϕ20r,
   ϕ2p ϕ20i , ϕ2p δR0r , ϕ2p δR0i, ϕ2p δL0r, ϕ2p δL0i (*8,16*),
   δRp ϕ10r , δRp ϕ10i, δRp ϕ20r, δRp ϕ20i, δRp δL0r,
   δRp δL0i , δRp δR0r , δRp δR0i (*8,24*),
   δLp ϕ10r, δLp ϕ10i, δLp ϕ20r , δLp ϕ20i, δLp δR0r , δLp δR0i, δLp δL0r, δLp δL0i (*8,32*),
   ϕ1p δRmm, ϕ1p δLmm (*2,34*),
   ϕ2p δRmm, ϕ2p δLmm (*2,36*),
   δRp δRmm, δRp δLmm (*2,38*),
   δLp δRmm, δLp δLmm (*2,40*)
  };
CCRow = {ϕ1m ϕ10r , ϕ1m ϕ10i, ϕ1m ϕ20r, ϕ1m ϕ20i , ϕ1m δR0r, ϕ1m δR0i, ϕ1m δL0r, ϕ1m δL0i (**),
   ϕ2m ϕ10r, ϕ2m ϕ10i, ϕ2m ϕ20r, ϕ2m ϕ20i , ϕ2m δR0r , ϕ2m δR0i, ϕ2m δL0r, ϕ2m δL0i (**),
   δRm ϕ10r , δRm ϕ10i, δRm ϕ20r, δRm ϕ20i, δRm δL0r, δRm δL0i, δRm δR0r , δRm δR0i (**),
   δLm ϕ10r, δLm ϕ10i, δLm ϕ20r , δLm ϕ20i, δLm δR0r , δLm δR0i , δLm δL0r, δLm δL0i (**),
   ϕ1m δRpp, ϕ1m δLpp (**),
    ϕ2m δRpp, ϕ2m δLpp (**),
   δRm δRpp, δRm δLpp (**),
   δLm δRpp, δLm δLpp (**)
  };
```

Symmetry factor:

```
CCfacList[i_, j_] := FactorList[CCColumn[[i]] CCRow[[j]]];
CCSymFac[i_, j_] := (If[Length[CCfacList[i, j]] == 2, Return[Factorial[4]]];
   If[Length[CCfacList[i, j]] == 3, If[(CCfacList[i, j])[[2, 2]] == 2 &&
      (CCfacList[i, j])[[3, 2]] == 2, Return[4], Return[Factorial[3]]]];
   If[Length[CCfacList[i, j]] == 4, Return[2]];
   If[Length[CCfacList[i, j]] == 5, Return[1]]);

CCcoeff[i_, j_] := Coefficient[Vtot, CCColumn[[i]] CCRow[[j]]];
CCMatFunc[i_, j_] := CCSymFac[i, j] CCcoeff[i, j];

For[i = 1; CCklist = {}, i ≤ 40, i++,
 For[j = 1; CCjlist = {}, j ≤ 40, j++, AppendTo[CCjlist, {CCMatFunc[i, j]}]]
  AppendTo[CCklist, Flatten[CCjlist]]]
(*CCklist//MatrixForm;*)
(*Eigenvalues[CCklist]*)
```

For quartically charged two-particle states

```
QCColumn = { δRpp δRpp, δRpp δLpp , δLpp δLpp };
QCRow = {δRmm δRmm, δRmm δLmm , δLmm δLmm};
```

Symmetry factor:

```
QCfacList[i_, j_] := FactorList[QCColumn[[i]] QCRow[[j]]];
QCSymFac[i_, j_] := (If[Length[QCfacList[i, j]] == 2, Return[Factorial[4]]];
   If[Length[QCfacList[i, j]] == 3, If[(QCfacList[i, j])[[2, 2]] == 2 &&
      (QCfacList[i, j])[[3, 2]] == 2, Return[4], Return[Factorial[3]]]];
   If[Length[QCfacList[i, j]] == 4, Return[2]];
   If[Length[QCfacList[i, j]] == 5, Return[1]]);
QCcoeff[i_, j_] := Coefficient[Vtot, QCColumn[[i]] QCRow[[j]]];
QCMatFunc[i_, j_] := QCSymFac[i, j] QCcoeff[i, j];

For[i = 1; QCklist = {}, i ≤ 3 , i++,
 For[j = 1; QCjlist = {}, j ≤ 3, j++, AppendTo[QCjlist, {QCMatFunc[i, j]}]];
 AppendTo[QCklist, Flatten[QCjlist]]]
(*QCklist//MatrixForm*)
(*Eigenvalues[QCklist]*)
```

For doubly charged two-particle states

```
DCColumn = {
    ϕ1p ϕ1p, ϕ1p ϕ2p, ϕ1p δRp , ϕ1p δLp (*4,4*),
    ϕ2p ϕ2p, ϕ2p δRp , ϕ2p δLp (*3,7*),
    δRp δRp , δRp δLp (*2,9*),
    δLp δLp (*1,10*),
    δRpp ϕ10r, δRpp ϕ10i, δRpp ϕ20r,
    δRpp ϕ20i, δRpp δR0r , δRpp δR0i, δRpp δL0r, δRpp δL0i (*8,18*),
    δLpp ϕ10r, δLpp ϕ10i, δLpp ϕ20r, δLpp ϕ20i, δLpp δR0r ,
    δLpp δR0i, δLpp δL0r, δLpp δL0i (*8,26*)
   };
DCRow = {
    ϕ1m ϕ1m, ϕ1m ϕ2m, ϕ1m δRm , ϕ1m δLm (**),
    ϕ2m ϕ2m, ϕ2m δRm , ϕ2m δLm (**),
    δRm δRm , δRm δLm (**),
    δLm δLm (**),
    δRmm ϕ10r, δRmm ϕ10i, δRmm ϕ20r,
    δRmm ϕ20i, δRmm δR0r , δRmm δR0i, δRmm δL0r, δRmm δL0i (**),
    δLmm ϕ10r, δLmm ϕ10i, δLmm ϕ20r, δLmm ϕ20i, δLmm δR0r , δLmm δR0i, δLmm δL0r, δLmm δL0i (**)
    };
```

Symmetry factor:

```
DCfacList[i_, j_] := FactorList[DCColumn[[i]] DCRow[[j]]];
DCSymFac[i_, j_] := (If[Length[DCfacList[i, j]] == 2, Return[Factorial[4]]];
    If[Length[DCfacList[i, j]] == 3, If[(DCfacList[i, j])[[2, 2]] == 2 &&
        (DCfacList[i, j])[[3, 2]] == 2, Return[4], Return[Factorial[3]]]];
    If[Length[DCfacList[i, j]] == 4, Return[2]];
    If[Length[DCfacList[i, j]] == 5, Return[1]]);

DCcoeff[i_, j_] := Coefficient[Vtot, DCColumn[[i]] DCRow[[j]]];
DCMatFunc[i_, j_] := DCSymFac[i, j] DCcoeff[i, j];

For[i = 1; DCklist = {}, i ≤ 26, i++,
 For[j = 1; DCjlist = {}, j ≤ 26, j++, AppendTo[DCjlist, {DCMatFunc[i, j]}]];
 AppendTo[DCklist, Flatten[DCjlist]]]
(*DCklist//MatrixForm;*)
(*Eigenvalues[DCklist]*)
```

For triply charged two-particle states

```
TCColumn = { ϕ1p δRpp, ϕ1p δLpp , ϕ2p δRpp , ϕ2p δLpp, δRp δRpp, δRp δLpp, δLp δRpp, δLp δLpp};
TCRow = { ϕ1m δRmm, ϕ1m δLmm , ϕ2m δRmm , ϕ2m δLmm, δRm δRmm, δRm δLmm, δLm δRmm, δLm δLmm};
```

Symmetry factor:

```
TCfacList[i_, j_] := FactorList[TCColumn[[i]] TCRow[[j]]];
TCSymFac[i_, j_] := (If[Length[TCfacList[i, j]] == 2, Return[Factorial[4]]];
    If[Length[TCfacList[i, j]] == 3, If[(TCfacList[i, j])[[2, 2]] == 2 &&
        (TCfacList[i, j])[[3, 2]] == 2, Return[4], Return[Factorial[3]]]];
    If[Length[TCfacList[i, j]] == 4, Return[2]];
    If[Length[TCfacList[i, j]] == 5, Return[1]]);

TCcoeff[i_, j_] := Coefficient[Vtot, TCColumn[[i]] TCRow[[j]]];
TCMatFunc[i_, j_] := TCSymFac[i, j] TCcoeff[i, j];

For[i = 1; TCklist = {}, i ≤ 8 , i++,
 For[j = 1; TCjlist = {}, j ≤ 8, j++, AppendTo[TCjlist, {TCMatFunc[i, j]}]];
 AppendTo[TCklist, Flatten[TCjlist]]]
(*TCklist//MatrixForm*)
(*Eigenvalues[TCklist]*)
```

The MATHEMATICA file Eigenvalue_collect.nb

Eigenvalues of the Scattering Matrices and Unitarity:

Eigenvalues of all the scattering matrices of q-charged 2-particle states. Each eigenvalue will have to be less than equal to 8π which is basically the unitarity condition. At the very end we also enlist the vacuum stability criteria.

Eigenvalues from neutral 2-particle scattering matrix:

Total 56 eigenvalues among which 29 (e1neut to e21neut + 8 soln) are independent:

$$\text{e1neut} = \frac{4}{3}(4\lambda_5+\lambda_6-\lambda_7) - \left(2^{1/3}\left(-76\lambda_5^2-80\lambda_5\lambda_6-112\lambda_6^2+68\lambda_5\lambda_7+44\lambda_6\lambda_7-16\lambda_7^2\right)\right)\Big/ \left(3\left(1280\lambda_5^3+2544\lambda_5^2\lambda_6-1344\lambda_5\lambda_6^2-2176\lambda_6^3-1752\lambda_5^2\lambda_7-2352\lambda_5\lambda_6\lambda_7+912\lambda_6^2\lambda_7+816\lambda_5\lambda_7^2+528\lambda_6\lambda_7^2-128\lambda_7^3+\sqrt{\left(4\left(-76\lambda_5^2-80\lambda_5\lambda_6-112\lambda_6^2+68\lambda_5\lambda_7+44\lambda_6\lambda_7-16\lambda_7^2\right)^3+\left(1280\lambda_5^3+2544\lambda_5^2\lambda_6-1344\lambda_5\lambda_6^2-2176\lambda_6^3-1752\lambda_5^2\lambda_7-2352\lambda_5\lambda_6\lambda_7+912\lambda_6^2\lambda_7+816\lambda_5\lambda_7^2+528\lambda_6\lambda_7^2-128\lambda_7^3\right)^2\right)}\right)^{1/3}\right) + \frac{1}{3\times 2^{1/3}}\left(1280\lambda_5^3+2544\lambda_5^2\lambda_6-1344\lambda_5\lambda_6^2-2176\lambda_6^3-1752\lambda_5^2\lambda_7-2352\lambda_5\lambda_6\lambda_7+912\lambda_6^2\lambda_7+816\lambda_5\lambda_7^2+528\lambda_6\lambda_7^2-128\lambda_7^3+\sqrt{\left(4\left(-76\lambda_5^2-80\lambda_5\lambda_6-112\lambda_6^2+68\lambda_5\lambda_7+44\lambda_6\lambda_7-16\lambda_7^2\right)^3+\left(1280\lambda_5^3+2544\lambda_5^2\lambda_6-1344\lambda_5\lambda_6^2-2176\lambda_6^3-1752\lambda_5^2\lambda_7-2352\lambda_5\lambda_6\lambda_7+912\lambda_6^2\lambda_7+816\lambda_5\lambda_7^2+528\lambda_6\lambda_7^2-128\lambda_7^3\right)^2\right)}\right)^{1/3};$$

$$\text{e2neut} = \frac{4}{3}(4\lambda_5+\lambda_6-\lambda_7) + \left(\left(1+i\sqrt{3}\right)\left(-76\lambda_5^2-80\lambda_5\lambda_6-112\lambda_6^2+68\lambda_5\lambda_7+44\lambda_6\lambda_7-16\lambda_7^2\right)\right)\Big/\left(3\times 2^{2/3}\left(1280\lambda_5^3+2544\lambda_5^2\lambda_6-1344\lambda_5\lambda_6^2-2176\lambda_6^3-1752\lambda_5^2\lambda_7-2352\lambda_5\lambda_6\lambda_7+912\lambda_6^2\lambda_7+816\lambda_5\lambda_7^2+528\lambda_6\lambda_7^2-128\lambda_7^3+\sqrt{\left(4\left(-76\lambda_5^2-80\lambda_5\lambda_6-112\lambda_6^2+68\lambda_5\lambda_7+44\lambda_6\lambda_7-16\lambda_7^2\right)^3+\left(1280\lambda_5^3+2544\lambda_5^2\lambda_6-1344\lambda_5\lambda_6^2-2176\lambda_6^3-1752\lambda_5^2\lambda_7-2352\lambda_5\lambda_6\lambda_7+912\lambda_6^2\lambda_7+816\lambda_5\lambda_7^2+528\lambda_6\lambda_7^2-128\lambda_7^3\right)^2\right)}\right)^{1/3}\right) - \frac{1}{6\times 2^{1/3}}\left(1-i\sqrt{3}\right)\left(1280\lambda_5^3+2544\lambda_5^2\lambda_6-1344\lambda_5\lambda_6^2-2176\lambda_6^3-1752\lambda_5^2\lambda_7-2352\lambda_5\lambda_6\lambda_7+912\lambda_6^2\lambda_7+816\lambda_5\lambda_7^2+528\lambda_6\lambda_7^2-128\lambda_7^3+\sqrt{\left(4\left(-76\lambda_5^2-80\lambda_5\lambda_6-112\lambda_6^2+68\lambda_5\lambda_7+44\lambda_6\lambda_7-16\lambda_7^2\right)^3+\left(1280\lambda_5^3+2544\lambda_5^2\lambda_6-1344\lambda_5\lambda_6^2-2176\lambda_6^3-1752\lambda_5^2\lambda_7-2352\lambda_5\lambda_6\lambda_7+912\lambda_6^2\lambda_7+816\lambda_5\lambda_7^2+528\lambda_6\lambda_7^2-128\lambda_7^3\right)^2\right)}\right)^{1/3};$$

$$\text{e3neut} = \frac{4}{3}(4\lambda_5+\lambda_6-\lambda_7) + \left(\left(1-i\sqrt{3}\right)\left(-76\lambda_5^2-80\lambda_5\lambda_6-112\lambda_6^2+68\lambda_5\lambda_7+44\lambda_6\lambda_7-16\lambda_7^2\right)\right)\Big/\left(3\times 2^{2/3}\left(1280\lambda_5^3+2544\lambda_5^2\lambda_6-1344\lambda_5\lambda_6^2-2176\lambda_6^3-1752\lambda_5^2\lambda_7-2352\lambda_5\lambda_6\lambda_7+912\lambda_6^2\lambda_7+816\lambda_5\lambda_7^2+528\lambda_6\lambda_7^2-128\lambda_7^3+\sqrt{\left(4\left(-76\lambda_5^2-80\lambda_5\lambda_6-112\lambda_6^2+68\lambda_5\lambda_7+44\lambda_6\lambda_7-16\lambda_7^2\right)^3+\left(1280\lambda_5^3+2544\lambda_5^2\lambda_6-1344\lambda_5\lambda_6^2-2176\lambda_6^3-1752\lambda_5^2\lambda_7-2352\lambda_5\lambda_6\lambda_7+912\lambda_6^2\lambda_7+816\lambda_5\lambda_7^2+\right.}\right.\right.$$

$$528\,\lambda_6\,\lambda_7^2-128\,\lambda_7^3\big)^2\Big)\Big)^{1/3}\Big)-\frac{1}{6\times 2^{1/3}}\left(1+i\sqrt{3}\right)$$
$$\Big(1280\,\lambda_5^3+2544\,\lambda_5^2\,\lambda_6-1344\,\lambda_5\,\lambda_6^2-2176\,\lambda_6^3-1752\,\lambda_5^2\,\lambda_7-2352\,\lambda_5\,\lambda_6\,\lambda_7+912\,\lambda_6^2\,\lambda_7+$$
$$816\,\lambda_5\,\lambda_7^2+528\,\lambda_6\,\lambda_7^2-128\,\lambda_7^3+\sqrt{\Big(4\left(-76\,\lambda_5^2-80\,\lambda_5\,\lambda_6-112\,\lambda_6^2+68\,\lambda_5\,\lambda_7+44\,\lambda_6\,\lambda_7-16\,\lambda_7^2\right)^3+}$$
$$\big(1280\,\lambda_5^3+2544\,\lambda_5^2\,\lambda_6-1344\,\lambda_5\,\lambda_6^2-2176\,\lambda_6^3-1752\,\lambda_5^2\,\lambda_7-2352$$
$$\lambda_5\,\lambda_6\,\lambda_7+912\,\lambda_6^2\,\lambda_7+816\,\lambda_5\,\lambda_7^2+528\,\lambda_6\,\lambda_7^2-128\,\lambda_7^3\big)^2\Big)\Big)^{1/3};$$

$$\text{e4neut}=\frac{\lambda_{12}}{2}-\left(-48\,\lambda_{10}^2-9\,\lambda_{12}^2\right)\Big/\left(3\times 2^{2/3}\left(54\,\lambda_{12}^3+\sqrt{2916\,\lambda_{12}^6+4\left(-48\,\lambda_{10}^2-9\,\lambda_{12}^2\right)^3}\right)^{1/3}\right)+\frac{\left(54\,\lambda_{12}^3+\sqrt{2916\,\lambda_{12}^6+4\left(-48\,\lambda_{10}^2-9\,\lambda_{12}^2\right)^3}\right)^{1/3}}{6\times 2^{1/3}};\text{(* Appeared 4 times *)}$$

$$\text{e5neut}=\frac{\lambda_{12}}{2}+\left(\left(1+i\sqrt{3}\right)\left(-48\,\lambda_{10}^2-9\,\lambda_{12}^2\right)\right)\Big/\left(6\times 2^{2/3}\left(54\,\lambda_{12}^3+\sqrt{2916\,\lambda_{12}^6+4\left(-48\,\lambda_{10}^2-9\,\lambda_{12}^2\right)^3}\right)^{1/3}\right)-\frac{1}{12\times 2^{1/3}}\left(1-i\sqrt{3}\right)\left(54\,\lambda_{12}^3+\sqrt{2916\,\lambda_{12}^6+4\left(-48\,\lambda_{10}^2-9\,\lambda_{12}^2\right)^3}\right)^{1/3};\text{(* Appeared 4 times *)}$$

$$\text{e6neut}=\frac{\lambda_{12}}{2}+\left(\left(1-i\sqrt{3}\right)\left(-48\,\lambda_{10}^2-9\,\lambda_{12}^2\right)\right)\Big/\left(6\times 2^{2/3}\left(54\,\lambda_{12}^3+\sqrt{2916\,\lambda_{12}^6+4\left(-48\,\lambda_{10}^2-9\,\lambda_{12}^2\right)^3}\right)^{1/3}\right)-\frac{1}{12\times 2^{1/3}}\left(1+i\sqrt{3}\right)\left(54\,\lambda_{12}^3+\sqrt{2916\,\lambda_{12}^6+4\left(-48\,\lambda_{10}^2-9\,\lambda_{12}^2\right)^3}\right)^{1/3};\text{(* Appeared 4 times *)}$$

$$\text{e7neut}=\frac{\lambda_{12}}{2}-\left(-48\,\lambda_{10}^2-9\,\lambda_{12}^2\right)\Big/\left(3\times 2^{2/3}\left(-54\,\lambda_{12}^3+\sqrt{2916\,\lambda_{12}^6+4\left(-48\,\lambda_{10}^2-9\,\lambda_{12}^2\right)^3}\right)^{1/3}\right)+\frac{\left(-54\,\lambda_{12}^3+\sqrt{2916\,\lambda_{12}^6+4\left(-48\,\lambda_{10}^2-9\,\lambda_{12}^2\right)^3}\right)^{1/3}}{6\times 2^{1/3}};\text{(* Appeared 4 times *)}$$

$$\text{e8neut}=\frac{\lambda_{12}}{2}+\left(\left(1+i\sqrt{3}\right)\left(-48\,\lambda_{10}^2-9\,\lambda_{12}^2\right)\right)\Big/\left(6\times 2^{2/3}\left(-54\,\lambda_{12}^3+\sqrt{2916\,\lambda_{12}^6+4\left(-48\,\lambda_{10}^2-9\,\lambda_{12}^2\right)^3}\right)^{1/3}\right)-\frac{1}{12\times 2^{1/3}}\left(1-i\sqrt{3}\right)\left(-54\,\lambda_{12}^3+\sqrt{2916\,\lambda_{12}^6+4\left(-48\,\lambda_{10}^2-9\,\lambda_{12}^2\right)^3}\right)^{1/3};\text{(* Appeared 4 times *)}$$

$$\text{e9neut}=\frac{\lambda_{12}}{2}+\left(\left(1-i\sqrt{3}\right)\left(-48\,\lambda_{10}^2-9\,\lambda_{12}^2\right)\right)\Big/\left(6\times 2^{2/3}\left(-54\,\lambda_{12}^3+\sqrt{2916\,\lambda_{12}^6+4\left(-48\,\lambda_{10}^2-9\,\lambda_{12}^2\right)^3}\right)^{1/3}\right)-$$

$$\frac{1}{12\times 2^{1/3}}\left(1+i\sqrt{3}\right)\left(-54\,\lambda_{12}^3+\sqrt{2916\,\lambda_{12}^6+4\left(-48\,\lambda_{10}^2-9\,\lambda_{12}^2\right)^3}\right)^{1/3}$$; (* Appeared 4 times *)

e10neut = $2\,(\lambda_1 - 2\,\lambda_2 - \lambda_3)$; (* Appeared twice *)
e11neut = $4\,(\lambda_1 - 2\,\lambda_2 - \lambda_3)$;
e12neut = $2\,(\lambda_1 + 2\,\lambda_2 + \lambda_3)$; (* Appeared twice *)
e13neut = $2\,(\lambda_1 + 2\,\lambda_2 + \lambda_3 - 2\,\lambda_4)$;
e14neut = $2\,(\lambda_1 + 2\,\lambda_2 + \lambda_3 + 2\,\lambda_4)$;
e15neut = $3\,\lambda_1 + 6\,\lambda_2 + 3\,\lambda_3 - \sqrt{\lambda_1^2 + 4\,\lambda_1\,\lambda_2 + 4\,\lambda_2^2 + 2\,\lambda_1\,\lambda_3 + 4\,\lambda_2\,\lambda_3 + \lambda_3^2 + 32\,\lambda_4^2}$;
e16neut = $3\,\lambda_1 + 6\,\lambda_2 + 3\,\lambda_3 + \sqrt{\lambda_1^2 + 4\,\lambda_1\,\lambda_2 + 4\,\lambda_2^2 + 2\,\lambda_1\,\lambda_3 + 4\,\lambda_2\,\lambda_3 + \lambda_3^2 + 32\,\lambda_4^2}$;
e17neut = $2\,\lambda_5$; (* Appeared twice *)
e18neut = $4\,\lambda_5$; (* Appeared twice *)
e19neut = λ_7; (* Appeared twice *)
e20neut = $\lambda_7 - 4\,\lambda_8$; (* Appeared 3 times *)
e21neut = $\lambda_7 + 4\,\lambda_8$; (* Appeared 3 times *)

The Equation:

Remaining 8 eigenvalues are the solution of x of the following eqn of the following form. Please check the original notebook file for the coefficients ($\sharp_x$). We omitted the exact expression here because the coeffients are lengthy.

$$x^8 + \sharp_7\,x^7 + \sharp_6\,x^6 + \sharp_5\,x^5 + \sharp_4\,x^4 + \sharp_3\,x^3 + \sharp_2\,x^2 + \sharp_1\,x + \sharp\,\text{Constant} == 0;$$

Eigenvalues from singly charged 2-particle scattering matrix:

Total 40 eigenvalues among which 14 (e1sing - e14sing) are independent.

(*e1sing-e3sing appeared once,e4sing-e9sing appeared twice and four zero eigenvalues.*)

$$\begin{aligned}\text{e1sing} = {} & \frac{2}{3}\,(2\,\lambda_1+\lambda_5) - \\ & \left(2^{1/3}\left(-4\,\lambda_1^2-12\,\lambda_4^2+8\,\lambda_1\,\lambda_5-4\,\lambda_5^2-6\,\lambda_{12}^2\right)\right)\Big/\Bigg(3\,\Big(-16\,\lambda_1^3+144\,\lambda_1\,\lambda_4^2+48\,\lambda_1^2\,\lambda_5-144\,\lambda_4^2\,\lambda_5- \\ & \quad 48\,\lambda_1\,\lambda_5^2+16\,\lambda_5^3-36\,\lambda_1\,\lambda_{12}^2+36\,\lambda_5\,\lambda_{12}^2+\sqrt{\Big(4\left(-4\,\lambda_1^2-12\,\lambda_4^2+8\,\lambda_1\,\lambda_5-4\,\lambda_5^2-6\,\lambda_{12}^2\right)^3+} \\ & \quad\quad \overline{\left(-16\,\lambda_1^3+144\,\lambda_1\,\lambda_4^2+48\,\lambda_1^2\,\lambda_5-144\,\lambda_4^2\,\lambda_5-48\,\lambda_1\,\lambda_5^2+16\,\lambda_5^3-36\,\lambda_1\,\lambda_{12}^2+36\,\lambda_5\,\lambda_{12}^2\right)^2\Big)}\Big)^{1/3}\Bigg)+ \\ & \frac{1}{3\times 2^{1/3}}\Big(-16\,\lambda_1^3+144\,\lambda_1\,\lambda_4^2+48\,\lambda_1^2\,\lambda_5-144\,\lambda_4^2\,\lambda_5-48\,\lambda_1\,\lambda_5^2+16\,\lambda_5^3-36\,\lambda_1\,\lambda_{12}^2+ \\ & \quad 36\,\lambda_5\,\lambda_{12}^2+\sqrt{\Big(4\left(-4\,\lambda_1^2-12\,\lambda_4^2+8\,\lambda_1\,\lambda_5-4\,\lambda_5^2-6\,\lambda_{12}^2\right)^3+} \\ & \quad\quad \overline{\left(-16\,\lambda_1^3+144\,\lambda_1\,\lambda_4^2+48\,\lambda_1^2\,\lambda_5-144\,\lambda_4^2\,\lambda_5-48\,\lambda_1\,\lambda_5^2+16\,\lambda_5^3-36\,\lambda_1\,\lambda_{12}^2+36\,\lambda_5\,\lambda_{12}^2\right)^2\Big)}\Big)^{1/3};\end{aligned}$$

$$\begin{aligned}\text{e2sing} = {} & \frac{2}{3}\,(2\,\lambda_1+\lambda_5) + \\ & \left(\left(1+i\sqrt{3}\right)\left(-4\,\lambda_1^2-12\,\lambda_4^2+8\,\lambda_1\,\lambda_5-4\,\lambda_5^2-6\,\lambda_{12}^2\right)\right)\Big/\Big(3\times 2^{2/3}\Big(-16\,\lambda_1^3+144\,\lambda_1\,\lambda_4^2+48\,\lambda_1^2\,\lambda_5- \\ & \quad 144\,\lambda_4^2\,\lambda_5-48\,\lambda_1\,\lambda_5^2+16\,\lambda_5^3-36\,\lambda_1\,\lambda_{12}^2+36\,\lambda_5\,\lambda_{12}^2+\sqrt{\Big(4\left(-4\,\lambda_1^2-12\,\lambda_4^2+8\,\lambda_1\,\lambda_5-4\,\lambda_5^2-6\,\lambda_{12}^2\right)^3+}\end{aligned}$$

$$\left(-16\lambda_1^3+144\lambda_1\lambda_4^2+48\lambda_1^2\lambda_5-144\lambda_4^2\lambda_5-48\lambda_1\lambda_5^2+16\lambda_5^3-36\lambda_1\lambda_{12}^2+36\lambda_5\lambda_{12}^2\right)^2\Big)\Big)^{1/3}\Big)-$$
$$\frac{1}{6\times 2^{1/3}}\left(1-\mathrm{i}\sqrt{3}\right)\Big(-16\lambda_1^3+144\lambda_1\lambda_4^2+48\lambda_1^2\lambda_5-144\lambda_4^2\lambda_5-48\lambda_1\lambda_5^2+16\lambda_5^3-36\lambda_1\lambda_{12}^2+36\lambda_5\lambda_{12}^2+\sqrt{\Big(4\left(-4\lambda_1^2-12\lambda_4^2+8\lambda_1\lambda_5-4\lambda_5^2-6\lambda_{12}^2\right)^3+\left(-16\lambda_1^3+144\lambda_1\lambda_4^2+48\lambda_1^2\lambda_5-144\lambda_4^2\lambda_5-48\lambda_1\lambda_5^2+16\lambda_5^3-36\lambda_1\lambda_{12}^2+36\lambda_5\lambda_{12}^2\right)^2\Big)}\Big)^{1/3};$$

$$\mathrm{e3sing}=\frac{2}{3}(2\lambda_1+\lambda_5)+\Big(\left(1-\mathrm{i}\sqrt{3}\right)\left(-4\lambda_1^2-12\lambda_4^2+8\lambda_1\lambda_5-4\lambda_5^2-6\lambda_{12}^2\right)\Big)\Big/\Big(3\times 2^{2/3}\Big(-16\lambda_1^3+144\lambda_1\lambda_4^2+48\lambda_1^2\lambda_5-144\lambda_4^2\lambda_5-48\lambda_1\lambda_5^2+16\lambda_5^3-36\lambda_1\lambda_{12}^2+36\lambda_5\lambda_{12}^2+\sqrt{\Big(4\left(-4\lambda_1^2-12\lambda_4^2+8\lambda_1\lambda_5-4\lambda_5^2-6\lambda_{12}^2\right)^3+\left(-16\lambda_1^3+144\lambda_1\lambda_4^2+48\lambda_1^2\lambda_5-144\lambda_4^2\lambda_5-48\lambda_1\lambda_5^2+16\lambda_5^3-36\lambda_1\lambda_{12}^2+36\lambda_5\lambda_{12}^2\right)^2\Big)}\Big)^{1/3}\Big)-\frac{1}{6\times 2^{1/3}}\left(1+\mathrm{i}\sqrt{3}\right)\Big(-16\lambda_1^3+144\lambda_1\lambda_4^2+48\lambda_1^2\lambda_5-144\lambda_4^2\lambda_5-48\lambda_1\lambda_5^2+16\lambda_5^3-36\lambda_1\lambda_{12}^2+36\lambda_5\lambda_{12}^2+\sqrt{\Big(4\left(-4\lambda_1^2-12\lambda_4^2+8\lambda_1\lambda_5-4\lambda_5^2-6\lambda_{12}^2\right)^3+\left(-16\lambda_1^3+144\lambda_1\lambda_4^2+48\lambda_1^2\lambda_5-144\lambda_4^2\lambda_5-48\lambda_1\lambda_5^2+16\lambda_5^3-36\lambda_1\lambda_{12}^2+36\lambda_5\lambda_{12}^2\right)^2\Big)}\Big)^{1/3};$$

$$\mathrm{e4sing}=\frac{\lambda_{12}}{3}-\left(-192\lambda_{10}^2-28\lambda_{12}^2\right)\Big/\Big(24\Big(144\lambda_{10}^2\lambda_{12}-10\lambda_{12}^3+3\sqrt{3}\sqrt{\left(-4096\lambda_{10}^6-1024\lambda_{10}^4\lambda_{12}^2-368\lambda_{10}^2\lambda_{12}^4-9\lambda_{12}^6\right)}\Big)^{1/3}\Big)+\frac{1}{6}\Big(144\lambda_{10}^2\lambda_{12}-10\lambda_{12}^3+3\sqrt{3}\sqrt{\left(-4096\lambda_{10}^6-1024\lambda_{10}^4\lambda_{12}^2-368\lambda_{10}^2\lambda_{12}^4-9\lambda_{12}^6\right)}\Big)^{1/3};$$

$$\mathrm{e5sing}=\frac{\lambda_{12}}{3}+\Big(\left(1+\mathrm{i}\sqrt{3}\right)\left(-192\lambda_{10}^2-28\lambda_{12}^2\right)\Big)\Big/\Big(48\Big(144\lambda_{10}^2\lambda_{12}-10\lambda_{12}^3+3\sqrt{3}\sqrt{\left(-4096\lambda_{10}^6-1024\lambda_{10}^4\lambda_{12}^2-368\lambda_{10}^2\lambda_{12}^4-9\lambda_{12}^6\right)}\Big)^{1/3}\Big)-\frac{1}{12}\left(1-\mathrm{i}\sqrt{3}\right)\Big(144\lambda_{10}^2\lambda_{12}-10\lambda_{12}^3+3\sqrt{3}\sqrt{\left(-4096\lambda_{10}^6-1024\lambda_{10}^4\lambda_{12}^2-368\lambda_{10}^2\lambda_{12}^4-9\lambda_{12}^6\right)}\Big)^{1/3};$$

$$\mathrm{e6sing}=\frac{\lambda_{12}}{3}+\Big(\left(1-\mathrm{i}\sqrt{3}\right)\left(-192\lambda_{10}^2-28\lambda_{12}^2\right)\Big)\Big/\Big(48\Big(144\lambda_{10}^2\lambda_{12}-10\lambda_{12}^3+3\sqrt{3}\sqrt{\left(-4096\lambda_{10}^6-1024\lambda_{10}^4\lambda_{12}^2-368\lambda_{10}^2\lambda_{12}^4-9\lambda_{12}^6\right)}\Big)^{1/3}\Big)-\frac{1}{12}\left(1+\mathrm{i}\sqrt{3}\right)\Big(144\lambda_{10}^2\lambda_{12}-10\lambda_{12}^3+3\sqrt{3}\sqrt{\left(-4096\lambda_{10}^6-1024\lambda_{10}^4\lambda_{12}^2-368\lambda_{10}^2\lambda_{12}^4-9\lambda_{12}^6\right)}\Big)^{1/3};$$

$$\mathrm{e7sing}=\frac{2\lambda_{12}}{3}-\left(-192\lambda_{10}^2-28\lambda_{12}^2\right)\Big/\Big(24\Big(-144\lambda_{10}^2\lambda_{12}+10\lambda_{12}^3+3\sqrt{3}\sqrt{\left(-4096\lambda_{10}^6-1024\lambda_{10}^4\lambda_{12}^2-368\lambda_{10}^2\lambda_{12}^4-9\lambda_{12}^6\right)}\Big)^{1/3}\Big)+\frac{1}{6}\Big(-144\lambda_{10}^2\lambda_{12}+10\lambda_{12}^3+3\sqrt{3}\sqrt{\left(-4096\lambda_{10}^6-1024\lambda_{10}^4\lambda_{12}^2-368\lambda_{10}^2\lambda_{12}^4-9\lambda_{12}^6\right)}\Big)^{1/3};$$

$$\mathrm{e8sing}=\frac{2\lambda_{12}}{3}+\Big(\left(1+\mathrm{i}\sqrt{3}\right)\left(-192\lambda_{10}^2-28\lambda_{12}^2\right)\Big)\Big/\Big(48\Big(-144\lambda_{10}^2\lambda_{12}+10\lambda_{12}^3+3\sqrt{3}\sqrt{\left(-4096\lambda_{10}^6-1024\lambda_{10}^4\lambda_{12}^2-368\lambda_{10}^2\lambda_{12}^4-9\lambda_{12}^6\right)}\Big)^{1/3}\Big)-\frac{1}{12}\left(1-\mathrm{i}\sqrt{3}\right)\Big(-144\lambda_{10}^2\lambda_{12}+10\lambda_{12}^3+3\sqrt{3}\sqrt{\left(-4096\lambda_{10}^6-1024\lambda_{10}^4\lambda_{12}^2-368\lambda_{10}^2\lambda_{12}^4-9\lambda_{12}^6\right)}\Big)^{1/3};$$

$$\mathrm{e9sing}=\frac{2\lambda_{12}}{3}+\Big(\left(1-\mathrm{i}\sqrt{3}\right)\left(-192\lambda_{10}^2-28\lambda_{12}^2\right)\Big)\Big/$$

$$\left(48\left(-144\lambda_{10}^2\lambda_{12}+10\lambda_{12}^3+3\sqrt{3}\sqrt{\left(-4096\lambda_{10}^6-1024\lambda_{10}^4\lambda_{12}^2-368\lambda_{10}^2\lambda_{12}^4-9\lambda_{12}^6\right)}\right)^{1/3}\right)-$$
$$\frac{1}{12}\left(1+i\sqrt{3}\right)\left(-144\lambda_{10}^2\lambda_{12}+10\lambda_{12}^3+3\sqrt{3}\sqrt{\left(-4096\lambda_{10}^6-1024\lambda_{10}^4\lambda_{12}^2-368\lambda_{10}^2\lambda_{12}^4-9\lambda_{12}^6\right)}\right)^{1/3};$$

```
e10sing = 2 (λ1 - λ4); (* Appeared 3 times *)
e11sing = 2 (λ1 + λ4); (* Appeared 3 times *)
e12sing = 2 λ5; (* Appeared 5 times *)
e13sing = λ7; (* Appeared 6 times *)
e14sing = λ12; (* Appeared 4 times *)
(* Total 3+(6*2)+4+3+3+5+6+4=40 *)
```

Eigenvalues from doubly charged 2-particle scattering matrix:

Total 26 eigenvalues among which 16 (e1doub - e16doub) are independent.

$$\text{e1doub}=\frac{\lambda_{12}}{2}-\left(-48\lambda_{10}^2-9\lambda_{12}^2\right)\Big/\left(3\times 2^{2/3}\left(54\lambda_{12}^3+\sqrt{2916\lambda_{12}^6+4\left(-48\lambda_{10}^2-9\lambda_{12}^2\right)^3}\right)^{1/3}\right)+$$
$$\frac{\left(54\lambda_{12}^3+\sqrt{2916\lambda_{12}^6+4\left(-48\lambda_{10}^2-9\lambda_{12}^2\right)^3}\right)^{1/3}}{6\times 2^{1/3}};\ \texttt{(* Appeared twice *)}$$

$$\text{e2doub}=\frac{\lambda_{12}}{2}+\left(\left(1+i\sqrt{3}\right)\left(-48\lambda_{10}^2-9\lambda_{12}^2\right)\right)\Big/$$
$$\left(6\times 2^{2/3}\left(54\lambda_{12}^3+\sqrt{2916\lambda_{12}^6+4\left(-48\lambda_{10}^2-9\lambda_{12}^2\right)^3}\right)^{1/3}\right)-$$
$$\frac{1}{12\times 2^{1/3}}\left(1-i\sqrt{3}\right)\left(54\lambda_{12}^3+\sqrt{2916\lambda_{12}^6+4\left(-48\lambda_{10}^2-9\lambda_{12}^2\right)^3}\right)^{1/3};\ \texttt{(* Appeared twice *)}$$

$$\text{e3doub}=\frac{\lambda_{12}}{2}+\left(\left(1-i\sqrt{3}\right)\left(-48\lambda_{10}^2-9\lambda_{12}^2\right)\right)\Big/$$
$$\left(6\times 2^{2/3}\left(54\lambda_{12}^3+\sqrt{2916\lambda_{12}^6+4\left(-48\lambda_{10}^2-9\lambda_{12}^2\right)^3}\right)^{1/3}\right)-$$
$$\frac{1}{12\times 2^{1/3}}\left(1+i\sqrt{3}\right)\left(54\lambda_{12}^3+\sqrt{2916\lambda_{12}^6+4\left(-48\lambda_{10}^2-9\lambda_{12}^2\right)^3}\right)^{1/3};\ \texttt{(* Appeared twice *)}$$

$$\text{e4doub}=\frac{\lambda_{12}}{2}-\left(-48\lambda_{10}^2-9\lambda_{12}^2\right)\Big/\left(3\times 2^{2/3}\left(-54\lambda_{12}^3+\sqrt{2916\lambda_{12}^6+4\left(-48\lambda_{10}^2-9\lambda_{12}^2\right)^3}\right)^{1/3}\right)+$$
$$\frac{\left(-54\lambda_{12}^3+\sqrt{2916\lambda_{12}^6+4\left(-48\lambda_{10}^2-9\lambda_{12}^2\right)^3}\right)^{1/3}}{6\times 2^{1/3}};\ \texttt{(* Appeared twice *)}$$

$$\text{e5doub}=\frac{\lambda_{12}}{2}+\left(\left(1+i\sqrt{3}\right)\left(-48\lambda_{10}^2-9\lambda_{12}^2\right)\right)\Big/$$
$$\left(6\times 2^{2/3}\left(-54\lambda_{12}^3+\sqrt{2916\lambda_{12}^6+4\left(-48\lambda_{10}^2-9\lambda_{12}^2\right)^3}\right)^{1/3}\right)-$$

$$\frac{1}{12\times 2^{1/3}}\left(1-\mathrm{i}\sqrt{3}\right)\left(-54\,\lambda_{12}^3+\sqrt{2916\,\lambda_{12}^6+4\left(-48\,\lambda_{10}^2-9\,\lambda_{12}^2\right)^3}\right)^{1/3}\text{; (* Appeared twice *)}$$

$$\text{e6doub} = \frac{\lambda_{12}}{2}+\left(\left(1-\mathrm{i}\sqrt{3}\right)\left(-48\,\lambda_{10}^2-9\,\lambda_{12}^2\right)\right)\Big/\left(6\times 2^{2/3}\left(-54\,\lambda_{12}^3+\sqrt{2916\,\lambda_{12}^6+4\left(-48\,\lambda_{10}^2-9\,\lambda_{12}^2\right)^3}\right)^{1/3}\right)-$$

$$\frac{1}{12\times 2^{1/3}}\left(1+\mathrm{i}\sqrt{3}\right)\left(-54\,\lambda_{12}^3+\sqrt{2916\,\lambda_{12}^6+4\left(-48\,\lambda_{10}^2-9\,\lambda_{12}^2\right)^3}\right)^{1/3}\text{; (* Appeared twice *)}$$

e7doub = $4\,\lambda_1$; (* Appeared twice *)

e8doub = $2\,\lambda_1+4\,\lambda_2+2\,\lambda_3$;

e9doub = $2\,(\lambda_5+2\,\lambda_6)$; (* Appeared twice *)

e10doub = λ_7; (* Appeared 3 times *)

e11doub = $\lambda_7-4\,\lambda_8$;

e12doub = $\lambda_7+4\,\lambda_8$;

e13doub = $3\,\lambda_5+4\,\lambda_6-4\,\lambda_8-\sqrt{\lambda_5^2+16\,\lambda_6^2-32\,\lambda_6\,\lambda_8+16\,\lambda_8^2}$;

e14doub = $3\,\lambda_5+4\,\lambda_6-4\,\lambda_8+\sqrt{\lambda_5^2+16\,\lambda_6^2-32\,\lambda_6\,\lambda_8+16\,\lambda_8^2}$;

e15doub = $3\,\lambda_5+4\,\lambda_6+4\,\lambda_8-\sqrt{\lambda_5^2+16\,\lambda_6^2+32\,\lambda_6\,\lambda_8+16\,\lambda_8^2}$;

e16doub = $3\,\lambda_5+4\,\lambda_6+4\,\lambda_8+\sqrt{\lambda_5^2+16\,\lambda_6^2+32\,\lambda_6\,\lambda_8+16\,\lambda_8^2}$;

(*Total (7*2)+1+2+3+6=26 eigenvalues.*)

Eigenvalues from triply charged 2-particle scattering matrix:

e1trip = λ_{12};(*Appeared twice*)

e2trip = $2\,\lambda_5$;(*Appeared twice*)

e3trip = λ_7;(*Appeared twice*)(*Total (3*2)+2=8 eigenvalues.Two of them are zero*)

Eigenvalues from quartically charged 2-particle scattering matrix:

e1quart = $4\,\lambda_5$; (* Appeared twice *)

e2quart = λ_7;

(* Total 3 eigenvalues *)

Vacuum stability criteria of left-right model from copositivity [Phys.Rev. D89 (2014) 9, 095008]

$\lambda_1 > 0$;

$\lambda_5 > 0$;

$\lambda_5+\lambda_6 > 0$;

$16\,\lambda_1\,\lambda_5-\lambda_{12}^2 > 0$;

Bibliography

[1] H. Fritzsch, Murray Gell-Mann, and H. Leutwyler. Advantages of the Color Octet Gluon Picture. *Phys. Lett.*, B47:365–368, 1973.

[2] S. L. Glashow. Partial Symmetries of Weak Interactions. *Nucl. Phys.*, 22:579–588, 1961.

[3] Abdus Salam and John Clive Ward. Electromagnetic and weak interactions. *Phys. Lett.*, 13:168–171, 1964.

[4] Steven Weinberg. A Model of Leptons. *Phys. Rev. Lett.*, 19:1264–1266, 1967.

[5] Georges Aad et al. Observation of a new particle in the search for the Standard Model Higgs boson with the ATLAS detector at the LHC. *Phys.Lett.*, B716:1–29, 2012.

[6] Serguei Chatrchyan et al. Observation of a new boson at a mass of 125 GeV with the CMS experiment at the LHC. *Phys.Lett.*, B716:30–61, 2012.

[7] Benjamin W. Lee, C. Quigg, and H.B. Thacker. Weak Interactions at Very High-Energies: The Role of the Higgs Boson Mass. *Phys.Rev.*, D16:1519, 1977.

[8] Andrew G. Akeroyd, Abdesslam Arhrib, and El-Mokhtar Naimi. Note on tree level unitarity in the general two Higgs doublet model. *Phys.Lett.*, B490:119–124, 2000.

[9] Lorenzo Basso, Stefano Moretti, and Giovanni Marco Pruna. A Renormalisation Group Equation Study of the Scalar Sector of the Minimal B-L Extension of the Standard Model. *Phys.Rev.*, D82:055018, 2010.

[10] Joydeep Chakrabortty, Partha Konar, and Tanmoy Mondal. Constraining a class of $B-L$ extended models from vacuum stability and perturbativity. *Phys.Rev.*, D89(5):056014, 2014.

[11] Kaushik Bhattacharya, Joydeep Chakrabortty, Suratna Das, and Tanmoy Mondal. Higgs vacuum stability and inflationary dynamics after BICEP2 and PLANCK dust polarisation data. *JCAP*, 1412(12):001, 2014.

[12] Jogesh C. Pati and Abdus Salam. Lepton Number as the Fourth Color. *Phys.Rev.*, D10:275–289, 1974.

[13] Rabindra N. Mohapatra and Jogesh C. Pati. Left-Right Gauge Symmetry and an Isoconjugate Model of CP Violation. *Phys.Rev.*, D11:566–571, 1975.

[14] R.N. Mohapatra and Jogesh C. Pati. A Natural Left-Right Symmetry. *Phys.Rev.*, D11:2558, 1975.

[15] G. Senjanovic and Rabindra N. Mohapatra. Exact Left-Right Symmetry and Spontaneous Violation of Parity. *Phys.Rev.*, D12:1502, 1975.

[16] Carolina Arbeláez, Martin Hirsch, Michal Malinský, and Jorge C. Romão. LHC-scale left-right symmetry and unification. *Phys.Rev.*, D89(3):035002, 2014.

[17] Joydeep Chakrabortty, Partha Konar, and Tanmoy Mondal. Copositive Criteria and Boundedness of the Scalar Potential. *Phys.Rev.*, D89(9):095008, 2014.

[18] Gulab Bambhaniya, Subrata Khan, Partha Konar, and Tanmoy Mondal. Constraints on a seesaw model leading to quasidegenerate neutrinos and signatures at the LHC. *Phys. Rev.*, D91(9):095007, 2015.

[19] Martin Holthausen, Kher Sham Lim, and Manfred Lindner. Planck scale Boundary Conditions and the Higgs Mass. *JHEP*, 1202:037, 2012.

[20] Giuseppe Degrassi, Stefano Di Vita, Joan Elias-Miro, Jose R. Espinosa, Gian F. Giudice, et al. Higgs mass and vacuum stability in the Standard Model at NNLO. *JHEP*, 1208:098, 2012.

[21] T. S. Motzkin. Copositive quadratic forms. *National Bureau of Standards Report*, 1818(0):11 – 22, 1952.

[22] K.P. Hadeler. On copositive matrices. *Linear Algebra and its Applications*, 49(0):79 – 89, 1983.

[23] Hannu Väliaho. Criteria for copositive matrices. *Linear Algebra and its Applications*, 81(0):19 – 34, 1986.

[24] Li Ping and Feng Yu Yu. Criteria for copositive matrices of order four. *Linear Algebra and its Applications*, 194(0):109 – 124, 1993.

[25] Wilfred Kaplan. A test for copositive matrices. *Linear Algebra and its Applications*, 313(1–3):203 – 206, 2000.

[26] Wilfred Kaplan. A copositivity probe. *Linear Algebra and its Applications*, 337(1–3):237 – 251, 2001.

[27] Stefan Bundfuss. *Copositive matrices, copositive programming, and applications*. Der Andere Verlag, 2009.

[28] L.E. Andersson, G.Chang, and T.Elfving. Criteria for copositive matrices using simplices and barycentric coordinates. *Linear Algebra and its Applications*, 220(0 9), 1995.

[29] R.W. Cottle, G.J. Habetler, and C.E. Lemke. On classes of copositive matrices. *Linear Algebra and its Applications*, 3(3):295 – 310, 1970.

[30] A. Arhrib, R. Benbrik, M. Chabab, G. Moultaka, M.C. Peyranere, et al. The Higgs Potential in the Type II Seesaw Model. *Phys.Rev.*, D84:095005, 2011.

[31] J. Horejsi and M. Kladiva. Tree-unitarity bounds for THDM Higgs masses revisited. *Eur.Phys.J.*, C46:81–91, 2006.

[32] Shinya Kanemura, Takahiro Kubota, and Eiichi Takasugi. Lee-Quigg-Thacker bounds for Higgs boson masses in a two doublet model. *Phys.Lett.*, B313:155–160, 1993.

[33] Dipankar Das and Ujjal Kumar Dey. Analysis of an extended scalar sector with S_3 symmetry. *Phys.Rev.*, D89(9):095025, 2014.

[34] L. Basso, A. Belyaev, S. Moretti, and G. M. Pruna. Tree-level unitarity bounds for the minimal $b-l$ model. *Phys. Rev. D*, 81:095018, May 2010.

[35] Shaaban Khalil. TeV-scale gauged B-L symmetry with inverse seesaw mechanism. *Phys.Rev.*, D82:077702, 2010.

[36] R.E. Marshak and Rabindra N. Mohapatra. Quark - Lepton Symmetry and B-L as the U(1) Generator of the Electroweak Symmetry Group. *Phys.Lett.*, B91:222–224, 1980.

[37] Satoshi Iso, Nobuchika Okada, and Yuta Orikasa. The minimal B-L model naturally realized at TeV scale. *Phys.Rev.*, D80:115007, 2009.

[38] F. del Aguila, M. Masip, and M. Perez-Victoria. Physical parameters and renormalization of U(1)-a x U(1)-b models. *Nucl. Phys.*, B456:531–549, 1995.

[39] Piotr H. Chankowski, Stefan Pokorski, and Jakub Wagner. Z-prime and the Appelquist-Carrazzone decoupling. *Eur. Phys. J.*, C47:187–205, 2006.

[40] Lorenzo Basso. *Phenomenology of the minimal B-L extension of the Standard Model at the LHC.* PhD thesis, Southampton U., 2011.

[41] Bob Holdom. Two U(1)'s and Epsilon Charge Shifts. *Phys.Lett.*, B166:196, 1986.

[42] F. del Aguila, G.D. Coughlan, and M. Quiros. GAUGE COUPLING RENORMALIZATION WITH SEVERAL U(1) FACTORS. *Nucl.Phys.*, B307:633, 1988.

[43] Georges Aad et al. Search for dilepton resonances in pp collisions at $\sqrt{s} = 7$ TeV with the ATLAS detector. *Phys.Rev.Lett.*, 107:272002, 2011.

[44] Nobuchika Okada, Mansoor Ur Rehman, and Qaisar Shafi. Non-Minimal B-L Inflation with Observable Gravity Waves. *Phys. Lett.*, B701:520–525, 2011.

[45] Nobuchika Okada and Qaisar Shafi. Observable Gravity Waves From $U(1)_{B-L}$ Higgs and Coleman-Weinberg Inflation. 2013.

[46] Joan Elias-Miro, Jose R. Espinosa, Gian F. Giudice, Hyun Min Lee, and Alessandro Strumia. Stabilization of the Electroweak Vacuum by a Scalar Threshold Effect. *JHEP*, 06:031, 2012.

[47] P.A.R. Ade et al. Planck 2013 results. XVI. Cosmological parameters. 2013.

[48] P.A.R. Ade et al. BICEP2 I: Detection Of B-mode Polarization at Degree Angular Scales. 2014.

[49] R. Adam et al. Planck intermediate results. XXX. The angular power spectrum of polarized dust emission at intermediate and high Galactic latitudes. 2014.

[50] P.A.R. Ade et al. Planck 2013 results. XXII. Constraints on inflation. 2013.

[51] Vedat Nefer Senoguz and Qaisar Shafi. Chaotic inflation, radiative corrections and precision cosmology. *Phys.Lett.*, B668:6–10, 2008.

[52] C.S. Wu, E. Ambler, R.W. Hayward, D.D. Hoppes, and R.P. Hudson. EXPERIMENTAL TEST OF PARITY CONSERVATION IN BETA DECAY. *Phys.Rev.*, 105:1413–1414, 1957.

[53] Goran Senjanovic. Spontaneous Breakdown of Parity in a Class of Gauge Theories. *Nucl.Phys.*, B153:334, 1979.

[54] Biswajoy Brahmachari, Ernest Ma, and Utpal Sarkar. Truly minimal left right model of quark and lepton masses. *Phys.Rev.Lett.*, 91:011801, 2003.

[55] Utpal Sarkar. Parity in left-right symmetric models. *Phys.Lett.*, B594:308–314, 2004.

[56] Rabindra N. Mohapatra and Goran Senjanovic. Neutrino Masses and Mixings in Gauge Models with Spontaneous Parity Violation. *Phys. Rev.*, D23:165, 1981.

[57] J. Basecq and D. Wyler. Mass limits on scalar bosons in left-right-symmetric models. *Phys. Rev. D*, 39:870–872, Feb 1989.

[58] N.G. Deshpande, J.F. Gunion, Boris Kayser, and Fredrick I. Olness. Left-right symmetric electroweak models with triplet Higgs. *Phys.Rev.*, D44:837–858, 1991.

[59] P. Duka, J. Gluza, and M. Zralek. Quantization and renormalization of the manifest left-right symmetric model of electroweak interactions. *Annals Phys.*, 280:336–408, 2000.

[60] M. Czakon, M. Zralek, and J. Gluza. Left-right symmetry and heavy particle quantum effects. *Nucl.Phys.*, B573:57–74, 2000.

[61] Martin Holthausen, Manfred Lindner, and Michael A. Schmidt. Radiative Symmetry Breaking of the Minimal Left-Right Symmetric Model. *Phys.Rev.*, D82:055002, 2010.

[62] Kristjan Kannike. Vacuum Stability Conditions From Copositivity Criteria. *Eur.Phys.J.*, C72:2093, 2012.

[63] M. Maniatis, A. von Manteuffel, O. Nachtmann, and F. Nagel. Stability and symmetry breaking in the general two-Higgs-doublet model. *Eur.Phys.J.*, C48:805–823, 2006.

[64] I.P. Ivanov. Minkowski space structure of the Higgs potential in 2HDM. *Phys.Rev.*, D75:035001, 2007.

[65] I.Z. Rothstein. Renormalization group analysis of the minimal left-right symmetric model. *Nucl.Phys.*, B358:181–194, 1991.

[66] N.G. Deshpande, J.F. Gunion, Boris Kayser, and Fredrick I. Olness. Left-right symmetric electroweak models with triplet Higgs. *Phys.Rev.*, D44:837–858, 1991.

[67] G. Beall, Myron Bander, and A. Soni. Constraint on the Mass Scale of a Left-Right Symmetric Electroweak Theory from the K(L) K(S) Mass Difference. *Phys.Rev.Lett.*, 48:848, 1982.

[68] Paul Langacker and S. Uma Sankar. Bounds on the Mass of W(R) and the W(L)-W(R) Mixing Angle xi in General SU(2)-L x SU(2)-R x U(1) Models. *Phys.Rev.*, D40:1569–1585, 1989.

[69] M. Czakon, J. Gluza, and J. Hejczyk. Muon decay to one loop order in the left-right symmetric model. *Nucl.Phys.*, B642:157–172, 2002.

[70] J. Chakrabortty, J. Gluza, R. Sevillano, and R. Szafron. Left-Right Symmetry at LHC and Precise 1-Loop Low Energy Data. *JHEP*, 1207:038, 2012.

[71] Miha Nemevsek, Fabrizio Nesti, Goran Senjanovic, and Yue Zhang. First Limits on Left-Right Symmetry Scale from LHC Data. *Phys.Rev.*, D83:115014, 2011.

[72] A. Ferrari, Johann Collot, M-L. Andrieux, B. Belhorma, P. de Saintignon, et al. Sensitivity study for new gauge bosons and right-handed Majorana neutrinos in pp collisions at $s = 14$-TeV. *Phys.Rev.*, D62:013001, 2000.

[73] Serguei Chatrchyan et al. Search for heavy narrow dilepton resonances in pp collisions at $\sqrt{s} = 7$ TeV and $\sqrt{s} = 8$ TeV. *Phys.Lett.*, B720:63–82, 2013.

[74] Georges Aad et al. Search for high-mass resonances decaying to dilepton final states in pp collisions at s**(1/2) $=$ 7-TeV with the ATLAS detector. *JHEP*, 1211:138, 2012.

[75] Tanmoy Mondal, Ujjal Kumar Dey, and Partha Konar. Implications of unitarity and charge breaking minima in a left-right symmetric model. *Phys. Rev.*, D92(9):096005, 2015.

[76] G. Ecker, W. Grimus, and H. Neufeld. Higgs Induced Flavor Changing Neutral Interactions in SU(2)-l X SU(2)-r X U(1). *Phys. Lett.*, B127:365, 1983. [Erratum: Phys. Lett.B132,467(1983)].

[77] Rabindra N. Mohapatra, Goran Senjanovic, and Minh D. Tran. Strangeness Changing Processes and the Limit on the Right-handed Gauge Boson Mass. *Phys. Rev.*, D28:546, 1983.

[78] M. E. Pospelov. FCNC in left-right symmetric theories and constraints on the right-handed scale. *Phys. Rev.*, D56:259–264, 1997.

[79] Diego Guadagnoli and Rabindra N. Mohapatra. TeV Scale Left Right Symmetry and Flavor Changing Neutral Higgs Effects. *Phys. Lett.*, B694:386–392, 2011.

[80] Anindya Datta and Amitava Raychaudhuri. Mass bounds for triplet scalars of the left-right symmetric model and their future detection prospects. *Phys. Rev.*, D62:055002, 2000.

[81] P.A.R. Ade et al. Planck 2013 results. XVI. Cosmological parameters. 2013.

[82] Steven Weinberg. Baryon and Lepton Nonconserving Processes. *Phys.Rev.Lett.*, 43:1566–1570, 1979.

[83] Peter Minkowski. mu $\to$ e gamma at a Rate of One Out of 1-Billion Muon Decays? *Phys.Lett.*, B67:421, 1977.

[84] Tsutomu Yanagida. HORIZONTAL SYMMETRY AND MASSES OF NEUTRINOS. *Conf.Proc.*, C7902131:95–99, 1979.

[85] Murray Gell-Mann, Pierre Ramond, and Richard Slansky. COMPLEX SPINORS AND UNIFIED THEORIES. *Conf.Proc.*, C790927:315–321, 1979.

[86] S.L. Glashow. THE FUTURE OF ELEMENTARY PARTICLE PHYSICS. *NATO Adv.Study Inst.Ser.B Phys.*, 59:687, 1980.

[87] Rabindra N. Mohapatra and Goran Senjanovic. Neutrino Mass and Spontaneous Parity Violation. *Phys. Rev. Lett.*, 44:912, 1980.

[88] J.A. Casas, V. Di Clemente, A. Ibarra, and M. Quiros. Massive neutrinos and the Higgs mass window. *Phys.Rev.*, D62:053005, 2000.

[89] Ilia Gogoladze, Nobuchika Okada, and Qaisar Shafi. Higgs Boson Mass Bounds in the Standard Model with Type III and Type I Seesaw. *Phys.Lett.*, B668:121–125, 2008.

[90] Werner Rodejohann and He Zhang. Impact of massive neutrinos on the Higgs self-coupling and electroweak vacuum stability. *JHEP*, 1206:022, 2012.

[91] Joydeep Chakrabortty, Moumita Das, and Subhendra Mohanty. Constraints on TeV scale Majorana neutrino phenomenology from the Vacuum Stability of the Higgs. 2012.

[92] Chian-Shu Chen and Yong Tang. Vacuum stability, neutrinos, and dark matter. *JHEP*, 1204:019, 2012.

[93] Subrata Khan, Srubabati Goswami, and Sourov Roy. Vacuum Stability constraints on the minimal singlet TeV Seesaw Model. *Phys.Rev.*, D89:073021, 2014.

[94] Dario Buttazzo, Giuseppe Degrassi, Pier Paolo Giardino, Gian F. Giudice, Filippo Sala, et al. Investigating the near-criticality of the Higgs boson. *JHEP*, 1312:089, 2013.

[95] Vincenzo Branchina and Emanuele Messina. Stability, Higgs Boson Mass and New Physics. *Phys.Rev.Lett.*, 111:241801, 2013.

[96] Vincenzo Branchina, Emanuele Messina, and Alessia Platania. Top mass determination, Higgs inflation, and vacuum stability. *JHEP*, 1409:182, 2014.

[97] Vincenzo Branchina, Emanuele Messina, and Marc Sher. Lifetime of the electroweak vacuum and sensitivity to Planck scale physics. *Phys.Rev.*, D91(1):013003, 2015.

[98] S.T. Petcov, W. Rodejohann, T. Shindou, and Y. Takanishi. The See-saw mechanism, neutrino Yukawa couplings, LFV decays $l(i) \to l(j) + \gamma$ and leptogenesis. *Nucl.Phys.*, B739:208–233, 2006.

[99] D.N. Dinh, A. Ibarra, E. Molinaro, and S.T. Petcov. The mu - e Conversion in Nuclei, mu → e gamma, mu → 3e Decays and TeV Scale See-Saw Scenarios of Neutrino Mass Generation. *JHEP*, 1208:125, 2012.

[100] A. Abada, Manuel E. Krauss, W. Porod, F. Staub, A. Vicente, et al. Lepton flavor violation in low-scale seesaw models: SUSY and non-SUSY contributions. *JHEP*, 1411:048, 2014.

[101] K. Huitu, J. Maalampi, A. Pietila, and M. Raidal. Doubly charged Higgs at LHC. *Nucl.Phys.*, B487:27–42, 1997.

[102] A.G. Akeroyd and Mayumi Aoki. Single and pair production of doubly charged Higgs bosons at hadron colliders. *Phys.Rev.*, D72:035011, 2005.

[103] Tao Han and Bin Zhang. Signatures for Majorana neutrinos at hadron colliders. *Phys.Rev.Lett.*, 97:171804, 2006.

[104] F. del Aguila, J.A. Aguilar-Saavedra, and R. Pittau. Heavy neutrino signals at large hadron colliders. *JHEP*, 0710:047, 2007.

[105] Tao Han, Biswarup Mukhopadhyaya, Zongguo Si, and Kai Wang. Pair production of doubly-charged scalars: Neutrino mass constraints and signals at the LHC. *Phys.Rev.*, D76:075013, 2007.

[106] A.G. Akeroyd, Mayumi Aoki, and Hiroaki Sugiyama. Probing Majorana Phases and Neutrino Mass Spectrum in the Higgs Triplet Model at the CERN LHC. *Phys.Rev.*, D77:075010, 2008.

[107] Simon Bray, Jae Sik Lee, and Apostolos Pilaftsis. Resonant CP violation due to heavy neutrinos at the LHC. *Nucl.Phys.*, B786:95–118, 2007.

[108] Pavel Fileviez Perez, Tao Han, Gui-yu Huang, Tong Li, and Kai Wang. Neutrino Masses and the CERN LHC: Testing Type II Seesaw. *Phys.Rev.*, D78:015018, 2008.

[109] F. del Aguila and J.A. Aguilar-Saavedra. Distinguishing seesaw models at LHC with multi-lepton signals. *Nucl.Phys.*, B813:22–90, 2009.

[110] Roberto Franceschini, Thomas Hambye, and Alessandro Strumia. Type-III see-saw at LHC. *Phys.Rev.*, D78:033002, 2008.

[111] Zhi-Zhong Xing. Tev Neutrino Physics at the Large Hadron Collider. *Int.J.Mod.Phys.*, A24:3286–3296, 2009.

[112] Anupama Atre, Tao Han, Silvia Pascoli, and Bin Zhang. The Search for Heavy Majorana Neutrinos. *JHEP*, 0905:030, 2009.

[113] Alejandra Melfo, Miha Nemevsek, Fabrizio Nesti, Goran Senjanovic, and Yue Zhang. Type II Seesaw at LHC: The Roadmap. *Phys.Rev.*, D85:055018, 2012.

[114] Mu-Chun Chen and Jinrui Huang. TeV Scale Models of Neutrino Masses and Their Phenomenology. *Mod.Phys.Lett.*, A26:1147–1167, 2011.

[115] O.J.P. Eboli, J. Gonzalez-Fraile, and M.C. Gonzalez-Garcia. Neutrino Masses at LHC: Minimal Lepton Flavour Violation in Type-III See-saw. *JHEP*, 1112:009, 2011.

[116] Sara Vanini. Search for Seesaw type III Signals in 2011 LHC CMS Data. 2012.

[117] Arindam Das and Nobuchika Okada. Inverse Seesaw Neutrino Signatures at LHC and ILC. 2012.

[118] Gulab Bambhaniya, Joydeep Chakrabortty, Srubabati Goswami, and Partha Konar. Generation of Neutrino mass from new physics at TeV scale and Multi-lepton Signatures at the LHC. *Phys.Rev.*, D88:075006, 2013.

[119] P. S. Bhupal Dev, Apostolos Pilaftsis, and Un-ki Yang. New Production Mechanism for Heavy Neutrinos at the LHC. *Phys.Rev.Lett.*, 112:081801, 2014.

[120] J.A. Aguilar-Saavedra, P.M. Boavida, and F.R. Joaquim. Flavoured searches for type-III seesaw at the LHC. *Phys.Rev.*, D88:113008, 2013.

[121] Arindam Das, P.S. Bhupal Dev, and Nobuchika Okada. Direct Bounds on Electroweak Scale Pseudo-Dirac Neutrinos from $\sqrt{s} = 8$ TeV LHC Data. 2014.

[122] Gulab Bambhaniya, Srubabati Goswami, Subrata Khan, Partha Konar, and Tanmoy Mondal. Looking for hints of a reconstructible seesaw model at the Large Hadron Collider. *Phys.Rev.*, D91:075007, 2015.

[123] J. Schechter and J.W.F. Valle. Neutrino Masses in SU(2) x U(1) Theories. *Phys.Rev.*, D22:2227, 1980.

[124] J.A. Casas and A. Ibarra. Oscillating neutrinos and muon —> e, gamma. *Nucl.Phys.*, B618:171–204, 2001.

[125] A. Ibarra and Graham G. Ross. Neutrino phenomenology: The Case of two right-handed neutrinos. *Phys.Lett.*, B591:285–296, 2004.

[126] S. Pascoli, S.T. Petcov, and C.E. Yaguna. Quasidegenerate neutrino mass spectrum, $\mu \to e + gamma$ decay and leptogenesis. *Phys.Lett.*, B564:241–254, 2003.

[127] Srubabati Goswami, Subrata Khan, and Sasmita Mishra. Threshold effects and renormalization group evolution of neutrino parameters in tev scale seesaw models. *Int.J.Mod.Phys.*, A29:1450114, 2014.

[128] M.B. Einhorn and D.R.T. Jones. The Effective potential and quadratic divergences. *Phys.Rev.*, D46:5206–5208, 1992.

[129] Ming-xing Luo and Yong Xiao. Two loop renormalization group equations in the standard model. *Phys.Rev.Lett.*, 90:011601, 2003.

[130] Marie E. Machacek and Michael T. Vaughn. Two Loop Renormalization Group Equations in a General Quantum Field Theory. 1. Wave Function Renormalization. *Nucl.Phys.*, B222:83, 1983.

[131] Marie E. Machacek and Michael T. Vaughn. Two Loop Renormalization Group Equations in a General Quantum Field Theory. 2. Yukawa Couplings. *Nucl.Phys.*, B236:221, 1984.

[132] Marie E. Machacek and Michael T. Vaughn. Two Loop Renormalization Group Equations in a General Quantum Field Theory. 3. Scalar Quartic Couplings. *Nucl.Phys.*, B249:70, 1985.

[133] Stefan Antusch, Joern Kersten, Manfred Lindner, and Michael Ratz. Neutrino mass matrix running for nondegenerate seesaw scales. *Phys.Lett.*, B538:87–95, 2002.

[134] Luminita N. Mihaila, Jens Salomon, and Matthias Steinhauser. Gauge Coupling Beta Functions in the Standard Model to Three Loops. *Phys.Rev.Lett.*, 108:151602, 2012.

[135] K.G. Chetyrkin and M.F. Zoller. Three-loop β-functions for top-Yukawa and the Higgs self-interaction in the Standard Model. *JHEP*, 1206:033, 2012.

[136] Kirill Melnikov and Timo van Ritbergen. The Three loop relation between the MS-bar and the pole quark masses. *Phys.Lett.*, B482:99–108, 2000.

[137] Ralf Hempfling and Bernd A. Kniehl. On the relation between the fermion pole mass and MS Yukawa coupling in the standard model. *Phys.Rev.*, D51:1386–1394, 1995.

[138] Barbara Schrempp and Michael Wimmer. Top quark and Higgs boson masses: Interplay between infrared and ultraviolet physics. *Prog.Part.Nucl.Phys.*, 37:1–90, 1996.

[139] Fedor Bezrukov, Mikhail Yu. Kalmykov, Bernd A. Kniehl, and Mikhail Shaposhnikov. Higgs Boson Mass and New Physics. *JHEP*, 1210:140, 2012.

[140] F. Jegerlehner and M. Yu. Kalmykov. O(alpha alpha(s)) correction to the pole mass of the t quark within the standard model. *Nucl.Phys.*, B676:365–389, 2004.

[141] Giuseppe Degrassi, Stefano Di Vita, Joan Elias-Miro, Jose R. Espinosa, Gian F. Giudice, et al. Higgs mass and vacuum stability in the Standard Model at NNLO. *JHEP*, 1208:098, 2012.

[142] A. Sirlin and R. Zucchini. DEPENDENCE OF THE QUARTIC COUPLING h(M) ON m(H) AND THE POSSIBLE ONSET OF NEW PHYSICS IN THE HIGGS SECTOR OF THE STANDARD MODEL. *Nucl.Phys.*, B266:389, 1986.

[143] J.A. Casas, J.R. Espinosa, and M. Quiros. Improved Higgs mass stability bound in the standard model and implications for supersymmetry. *Phys.Lett.*, B342:171–179, 1995.

[144] J.A. Casas, J.R. Espinosa, and M. Quiros. Standard model stability bounds for new physics within LHC reach. *Phys.Lett.*, B382:374–382, 1996.

[145] Sidney R. Coleman. The Fate of the False Vacuum. 1. Semiclassical Theory. *Phys.Rev.*, D15:2929–2936, 1977.

[146] Jr. Callan, Curtis G. and Sidney R. Coleman. The Fate of the False Vacuum. 2. First Quantum Corrections. *Phys.Rev.*, D16:1762–1768, 1977.

[147] Gino Isidori, Giovanni Ridolfi, and Alessandro Strumia. On the metastability of the standard model vacuum. *Nucl.Phys.*, B609:387–409, 2001.

[148] J.R. Espinosa, G.F. Giudice, and A. Riotto. Cosmological implications of the Higgs mass measurement. *JCAP*, 0805:002, 2008.

[149] D. Tommasini, G. Barenboim, J. Bernabeu, and C. Jarlskog. Nondecoupling of heavy neutrinos and lepton flavor violation. *Nucl.Phys.*, B444:451–467, 1995.

[150] Combination of CDF and D0 results on the mass of the top quark using up to 5.8 fb-1 of data. 2011.

[151] Siegfried Bethke. The 2009 World Average of alpha(s). *Eur.Phys.J.*, C64:689–703, 2009.

[152] W. Grimus and L. Lavoura. The Seesaw mechanism at arbitrary order: Disentangling the small scale from the large scale. *JHEP*, 0011:042, 2000.

[153] J. Adam et al. New constraint on the existence of the $\mu^+ \to e^+\gamma$ decay. *Phys.Rev.Lett.*, 110(20):201801, 2013.

[154] D.V. Forero, M. Tortola, and J.W.F. Valle. Global status of neutrino oscillation parameters after Neutrino-2012. *Phys.Rev.*, D86:073012, 2012.

[155] Manimala Mitra, Goran Senjanovic, and Francesco Vissani. Neutrinoless Double Beta Decay and Heavy Sterile Neutrinos. *Nucl.Phys.*, B856:26–73, 2012.

[156] Joydeep Chakrabortty, H. Zeen Devi, Srubabati Goswami, and Sudhanwa Patra. Neutrinoless double-β decay in TeV scale Left-Right symmetric models. *JHEP*, 1208:008, 2012.

[157] Vladimir Tello, Miha Nemevsek, Fabrizio Nesti, Goran Senjanovic, and Francesco Vissani. Left-Right Symmetry: from LHC to Neutrinoless Double Beta Decay. *Phys.Rev.Lett.*, 106:151801, 2011.

[158] Werner Rodejohann. Neutrinoless double beta decay and neutrino physics. *J. Phys.*, G39:124008, 2012.

[159] Giuseppe Bozzi, Barbara Jager, Carlo Oleari, and Dieter Zeppenfeld. Next-to-leading order QCD corrections to W+ Z and W- Z production via vector-boson fusion. *Phys.Rev.*, D75:073004, 2007.

[160] Johan Alwall, Michel Herquet, Fabio Maltoni, Olivier Mattelaer, and Tim Stelzer. MadGraph 5 : Going Beyond. *JHEP*, 1106:128, 2011.

[161] J. Pumplin, D.R. Stump, J. Huston, H.L. Lai, Pavel M. Nadolsky, et al. New generation of parton distributions with uncertainties from global QCD analysis. *JHEP*, 0207:012, 2002.

[162] Neil D. Christensen and Claude Duhr. FeynRules - Feynman rules made easy. *Comput.Phys.Commun.*, 180:1614–1641, 2009.

[163] Johan Alwall, A. Ballestrero, P. Bartalini, S. Belov, E. Boos, et al. A Standard format for Les Houches event files. *Comput.Phys.Commun.*, 176:300–304, 2007.

[164] Torbjorn Sjostrand, Stephen Mrenna, and Peter Z. Skands. PYTHIA 6.4 Physics and Manual. *JHEP*, 0605:026, 2006.

[165] Michelangelo L. Mangano, Mauro Moretti, Fulvio Piccinini, Roberto Pittau, and Antonio D. Polosa. ALPGEN, a generator for hard multiparton processes in hadronic collisions. *JHEP*, 0307:001, 2003.

[166] G. Bambhaniya, J. Chakrabortty, J. Gluza, M. Kordiaczyńska, and R. Szafron. Left-Right Symmetry and the Charged Higgs Bosons at the LHC. *JHEP*, 05:033, 2014.